



ScuDo

Scuola di Dottorato ~ Doctoral School

WHAT YOU ARE, TAKES YOU FAR



Doctoral Dissertation
Doctoral Program in Energy Engineering (33rd Cycle)

Optimal Management of Network Integrated EV Batteries by Individual EV Usage Forecasts: Vehicle to Home and Vehicle to Grid Case Studies

Francesco Giordano

* * * * *

Supervisors

Prof. Spertino Filippo

Prof. Tenconi Alberto

Doctoral Examination Committee:

Prof. Angela Russo, Politecnico di Torino

Prof. Diego Alejandro Patiño Guevara, Pontificia Universidad Javeriana

Prof. Giorgio Graditi, Enea Portici Research Centre

Prof. Mario Cacciato, Università degli studi di Catania

Prof. Ozan Erdiñç, Yildiz Technical University

Politecnico di Torino

December 31, 2020

This thesis is licensed under a Creative Commons License, Attribution - Noncommercial - NoDerivative Works 4.0 International: see www.creativecommons.org. The text may be reproduced for non-commercial purposes, provided that credit is given to the original author.

I hereby declare that, the contents and organisation of this dissertation constitute my own original work and does not compromise in any way the rights of third parties, including those relating to the security of personal data.

.....
Francesco Giordano
Turin, December 31, 2020

Summary

Francesco Giordano

Optimal Management of Network Integrated EV Batteries by Individual EV Usage Forecasts: Vehicle to Home and Vehicle to Grid Case Studies

The growing attention in sustainability and environmental problems is driven by deep changes in entire sectors. Among others, the transport and the power sectors will assist to the greater transformation in the next years. As a result, recent lines of research are studying the use of Electric Vehicles (EVs) as sources of grid flexibility as well as their effects on the energy balance of users equipped with charging station and Photovoltaic (PV) generators.

This dissertation presents a novel approach to exploit and control the EV batteries of network integrated vehicles using individual EV forecasts. The approach is based on a bilevel programming where the real-time management is integrated by a preliminary optimization phase. On the other hand, the EV forecasts rely on statistical elaborations of real EVs usages historical data. Moreover, the proposed approach has been declined in two different case studies with different purposes.

The first case study regards the integration of an EV in a PV powered household, thus aims to maximize the obtainable PV self-consumption and self-sufficiency. The second case study considers an entire fleet of 214 EVs connected into the power system and able to supply grid services such as Replacement Reserve and Secondary Regulation. The objective of this latest case is to maximize the economic benefit achievable from the bidirectional power exchanges of the EVs fleet from and toward the grid. In both case studies, the results are presented in comparison with specific logics assumed as reference in order to evaluate the effectiveness of the proposed methodology.

Acknowledgment

First, I would like to acknowledge the engineers Marco Pietrucci and Leonardo Zeni from Terna S.p.A for the support and the tutoring in the developing of the research. Their advices and feedbacks have been needful to maintain the research always in line with industrial future developments on technology and regulations. A great thank you goes also to my supervisors Prof. Filippo Spertino and Prof. Alberto Tenconi. In particular, I would like to express my gratitude to Prof. Spertino who has served as an empathic mentor and an always available teacher. Moreover, I thank Prof. Diego Patiño and Prof. Giorgio Graditi for accepting to be the reviewers of this work.

This journey, and more in general my education, has been also possible thanks to my family: my parents and my sister who have always encouraged me to perceive my objectives and overcomes difficulties. Special thanks and love go to the great woman I am lucky to have beside for the emotional and practical support in these years where some critical moments of course existed.

Finally, big hugs and good luck wishes for all the future ahead to my colleagues and friends at PoliTo: Cesar Diaz Londoño for the humanity and the sincerity of our friendship; Alessandro La Ganga because together we have travelled this path from the origin, from when we were just a bit more than teenager; Francesco Arrigo and Carmelo Mosca for the discussions on electric vehicles, environmental problems and politic issues; one by one to all the others for coffee breaks and all the nice moments together.

Table of Contents

Introduction.....	10
Chapter 1 Research Context	12
1.1 Toward the Green New Deal	12
1.2 The Power System Transformation	14
1.2.1 The Renewables Development.....	14
1.2.2 The Power System Flexibility Enabling	16
Italian Ancillary Services Market Opening.....	17
1.2.3 Batteries Price Decreasing	19
1.3 The Road Transport Sector Transformation	19
Chapter 2 Review on Network EV Integration Models and Proposed Approach..	22
.....	22
2.1 Vehicle-to-Grid Concepts	22
2.1.1 Smart Charging	24
Effect on Battery Life of V2G Operations	25
2.1.2 Different Scales and Adoptions.....	26
2.2 EV and PV Integration: Vehicle to Building	26
2.2.1 Smart Charging Approaches on Vehicle to Building.....	27
Heuristic Approach	27
Optimization Approach	28
Hybrid Approach.....	29
2.3 EVs and Grid Integration: Vehicle to Grid	29
2.3.1 Centralized Architecture	29
2.3.2 Decentralized Architecture.....	31
2.3.3 Smart Charging Approaches on Vehicle to Grid	31
Deterministic Methods	32
Stochastic Methods	32
Forecast Based Methods.....	32

2.4	Proposed Approach and Novelty	33
Chapter 3	Individual EV Usage Forecasts.....	34
3.1	Vehicle Dataset	34
3.1.1	Vehicle Dataset Representation: Daily Usage Scenario	35
3.2	Day-ahead Vehicle Forecasts.....	36
3.2.1	Day-ahead Vehicle Forecasts Methodology	36
	Clusterization of the Departure Times	37
3.2.2	Daily Forecast Errors	39
	Trip Consumptions Error (TCE)	39
	Trip Starting-minutes Error (TSE)	40
	Trip Durations Error (TDE)	41
	Total Error (TE)	41
3.2.3	Day-ahead Forecast Results	41
	EV Forecasted Scenarios.....	42
	Global Performance of the Day-ahead Forecasts.....	47
3.3	Infra-day Vehicle forecasts.....	48
3.3.1	Infra-day Vehicle Forecasts Methodology	48
3.3.2	Infra-day Vehicle Forecast Results	50
3.4	Future Works on EV Forecasts.....	55
Chapter 4	EV and PV Integration: A Vehicle to Home Case Study	56
4.1	Household Model.....	57
4.1.1	Photovoltaic Power Profiles	57
4.1.2	Domestic Load Consumption Profiles	58
4.1.3	Choice of the EV usage Profiles	59
	Definition of the EVs Home Presence	59
	Clusterization of the Dataset	61
	Identifying the Correct Number of Clusters.....	61
	EVs Chosen Usages Profile.....	62
4.1.4	Energy Indexes	64
4.2	EV Battery Control Algorithms.....	66
4.2.1	Simple Rule-based Logic Without Forecasts	66
	Self-consumption Logic	66
	Charge once Home Logic.....	67

4.2.2 Proposed Logic.....	68
Methodology	69
STEP # α : Future EV Usage Profiles	70
STEP # α : Future Load and PV Generation Profiles.....	72
STEP # β : Optimization of charge-discharge pattern based on forecasts	74
STEP # γ : Rule-based Real-Time Management.....	77
4.3 Simulation Results	78
4.3.1 Further Results	82
Effect of the Forecasts Error in the PL Performance	83
Effect of the PV Availability in the PL Performance	83
Different EV User Behaviour: Effect on Reference Logic	84
4.4 Future Works on EV and PV integrations	85
Chapter 5 EVs Grid Integration: A Vehicle to Grid Case Study.....	87
5.1 Model Formulation	88
5.1.1 Physical Model.....	89
EVs and Chargers Definitions.....	89
EVs Allocation on Chargers.....	90
Aggregated State of Charge and Power	91
5.1.2 Participation in the Electricity Market	93
Day Ahead Energy Market: Energy Arbitrage Criterion	94
Reserve Market: Replacement Reserve Availability	96
Reserve Market: Secondary Reserve Availability	98
Definition of Aggregated Cost and Economic Benefit	100
5.2 Aggregator Management: Proposed Methodology.....	101
STEP #1: Forecast of Electric Vehicle Usage Profiles	103
STEP #1: Forecast of Electricity Price.....	103
STEP #2: Optimization of the Power Profile Based on Forecasts.....	104
STEP #3: Rule-based Management for the real-time Dispatching	107
5.3 Simulations and Results.....	110
5.3.1 Case with No Grid Services Activation	110
5.3.2 Case with Replacement Reserve Activation	113
5.3.3 Case with Secondary Reserve Activation	116
Sensitivity to Variation of Available Chargers	119
5.4 Future Works on EVs and Grid Integration.....	121

Conclusion	123
References.....	125

List of Tables

Table 2.1 Examples of commercial BEV: autonomy and battery capacity	23
Table 3.1 Daily Forecasts Errors with respect to last Mondays.....	44
Table 3.2 Daily Forecasts Errors per weekdays.....	45
Table 3.3 Daily Forecasted Errors averaged across all the EVs in the dataset	47
Table 3.4 Normalization on EV Battery Capacity: Effect on Errors	48
Table 3.5 Different weights: Effect on Total Error.....	48
Table 3.6 Daily Forecast Errors for each infra-day forecast iteration.....	54
Table 3.7 Daily Forecast Errors of the Complete Applied Forecast	54
Table 3.8 Day-ahead and Infra-day forecasts results comparison	54
Table 4.1 PV generation and sunlight hours percentage in chosen weeks.....	58
Table 4.2 Domestic energy consumed in chosen weeks.....	59
Table 4.3 EV Usages comparison: energy need and PV contemporaneity	64
Table 4.4 EV Daily Forecast Errors: EV#B - week of January	71
Table 4.5 Daily Forecast Errors: EV#A, EV#B, EV#C - all weeks.....	71
Table 4.6 Daily Load Forecast Errors - all weeks.....	74
Table 4.7 Daily PV Forecast Errors - all weeks	74
Table 4.8 Self Consumption: Proposed and Reference Logic	81
Table 4.9 Self Sufficiency: Proposed and Reference Logic	81
Table 4.10 Proposed Logic percentage deviation from Reference	82
Table 4.11 EV consumption under PV energy in charge.....	82
Table 4.12 Case without EV: energy indexes.....	82
Table 4.13 Exact Prediction percentage deviation from Reference	83
Table 4.14 Energy Indexes: SRL-Reference Logic with $SOC_{ch\ grid}=50\%$	85
Table 4.15 PL Percentage Deviation from SRL with $SOC_{ch\ grid}=50\%$	85
Table 5.1 Technical-economic performance: no services activation	113
Table 5.2 Different priorities adoptions comparison: no services activation	113

Table 5.3 Technical-economic performance: Replacement reserve activation	115
Table 5.4 Different priorities adoptions comparison: Replacement reserve activation	116
Table 5.5 Technical-economic performance: Secondary reserve activation.	118
Table 5.6 Different priorities adoptions comparison: Secondary reserve activation	118
Table 5.7 Effect on averagely connected EVs for different number of available chargers	121
Table 5.8 Technical-economic performance: different number of available chargers	121

List of Figures

Figure 1.1 Greenhouse gases emissions reduction - 1,5 °C scenario, [7]	13
Figure 1.2 Renewables global weighted average LCOE - last decade, [4]	15
Figure 1.3 Annual renewables capacity addition - 2013 to 2022, [10]	15
Figure 1.4 Lithium-ion annual battery price - 2010 to 2030, [15]	19
Figure 1.5 Global electric cars stock - 2010 to 2019, [16]	20
Figure 1.6 Annual car sales per typology - 2010 to 2030, [18]	21
Figure 2.1 Vehicle to Home and Vehicle to Grid concepts	24
Figure 2.2 Smart Charging technologies by level of smartness	25
Figure 2.3 V2G Centralized Architecture	30
Figure 2.4 V2G Decentralized Architecture	31
Figure 3.1 EV usage scenario representation	35
Figure 3.2 Day-ahead EV forecast routine	37
Figure 3.3 Clusterization operation - departure times estimation	39
Figure 3.4-(a to l) Day-ahead EV forecasts: EV#1 - EV#10	43
Figure 3.5 Entire week forecasts: EV#5 (a) - EV#6 (b)	46
Figure 3.6 Infra-day EV forecast working principle	49
Figure 3.7 Infra-day EV forecast routine	50
Figure 3.8-(a to n) Infra-day EV#3 forecasts: iterations 0-11	53
Figure 3.9 Complete Applied Forecast at the end of the day	53
Figure 4.1 Scheme of the household model	57
Figure 4.2 PV production in the four chosen weeks	58
Figure 4.3 Domestic load in the four chosen weeks	59
Figure 4.4 EV presence at home hypothesis	60
Figure 4.5 EVs dataset division in two (a), three (b), and four (c) clusters: Silhouette analysis	62
Figure 4.6 EV#A, EV#B, and EV#C profiles: week of January	63

Figure 4.7 EV and PV contemporaneity: EV#C - week of January.....	64
Figure 4.8 Daily power profiles and energy balance for an EV-PV system ...	65
Figure 4.9 Proposed procedure flowchart (household)	69
Figure 4.10 Estimated and real EV usages: EV#B - week of January	70
Figure 4.11 Time frame used for the domestic load forecasts	72
Figure 4.12 Estimated and real domestic loads (a) and PV generation (b):week of January	73
Figure 4.13 Example of Command Vector: Output of STEP # β	76
Figure 4.14 Household system real time management routine	77
Figure 4.15: Control Algorithms comparison: PV production (a) and SOC evolution (b) - EV#C–Monday of the July week	79
Figure 4.16 Control Algorithms comparison: PV production (a) and SOC evolution (b) - EV#C–week of July	80
Figure 4.17 Self-consumptions for different PV plant sizes: PL and PL with exact predictions - EV#C week of January	84
Figure 4.18 Self-sufficiencies for different PV plant sizes: PL and PL with exact predictions - EV#C week of January	84
Figure 5.1 Scheme of the EVs-grid integration model.....	88
Figure 5.2 EV-to-charger connections: battery availability hypothesis.....	89
Figure 5.3 EVs allocation in chargers	91
Figure 5.4 Market model and services activation	93
Figure 5.5 Energy arbitrage criterion	95
Figure 5.6 Electricity cost/price: Italy - April 6 th 2020.....	95
Figure 5.7 Replacement service energy reservation.....	97
Figure 5.8 Replacement service energy cost/price: Italy – April 6 th 2020.....	98
Figure 5.9 Secondary regulation: control signal and activation.....	99
Figure 5.10 Secondary regulation energy cost/price: Italy – April 6 th 2020...	99
Figure 5.11 Proposed procedure flowchart (EV fleet)	102
Figure 5.12 Forecasted and real electricity price: Italy – April 6 th 2020	104
Figure 5.13 EV fleet real time management working principle.....	109
Figure 5.14 EV SOC's evolutions by charger: no services activation	111
Figure 5.15 CH#1 occupation during the simulated day.....	111
Figure 5.16 Aggregated Power and SOC: no services activation	112
Figure 5.17 EV SOC's evolutions by charger: Replacement reserve activation	114
Figure 5.18 Aggregated Power and SOC: Replacement reserve activation..	115
Figure 5.19 EV SOC's evolutions by charger: Secondary reserve activation	116
Figure 5.20 Aggregated Power and SOC: Secondary reserve activation.....	117

Figure 5.21 EV daily cost/revenue profile: EV#3	118
Figure 5.22 Final net cost/revenue per EVs	119
Figure 5.23 Number of connected EVs among the day: 225 available chargers	119
Figure 5.24 Number of connected EVs by varying the chargers availability	120

Introduction

The worldwide industrialization and the increasing demand for electricity result in problems of energy supply and environmental pollution. As an example, in 2019, the transportation sector was responsible of 24% of direct CO₂ emissions in the world, [1]. Referring only to transportation sector, road vehicles (e.g. cars and trucks) accounted for 75% of both global energy demand and CO₂ emissions. Thus, the renewal of transportation sector is fundamental for an effective fight against climate change. In fact, research and industry are working for the electric conversion of the transportation sector [2][3], that will be more and more supplied by renewable sources.

Moreover, the installation cost of renewable systems, especially Photovoltaic (PV) generators faced a drop in the last years, [4]. Thus, in many countries, the local electricity production is more cost-effective than the absorption from the grid. In addition, the batteries installed in Electric Vehicles (EV) could increase the use of renewable resources and the flexibility of the electric system. As a result, recent lines of research are studying the use of EVs as sources of grid flexibility as well as their effects on the energy balance of users equipped with charging station and PV generators. These kinds of researches are in line with the exploitation of the concept of Vehicle to Grid (V2G), [5].

This dissertation proposes a new methodology to optimal manage batteries of network integrated EVs by making use of individual EV behaviour forecasts. In fact, one of the main issues related to the EV-networks integration regards the high level of uncertainty of the variables related to the system (e.g., timing of the EV connection to the charging infrastructure, energy required for future trips, electricity cost/price, and if present PV and load variation).

Furthermore, the EV battery energy scheduling problem presents an intrinsic interdependency between periods. For example, the energy stored in a battery depends on previous decisions such as charging/discharging power or energy spent in trips.

The individual EV behaviour forecasts here introduced are obtained by a specific proposed logic which is based on statistical elaborations of real EVs usages historical data. The forecasts aim to catch the most probable future behaviour of each single EV; thus, they aspire to the realization of an as much as possible autonomous control system able to operate a reliable management even in absence of future travel information directly provided by EV users.

On the other hand, the EV battery energy control employs a bilevel or hybrid approach. First, an optimization phase uses the forecasts in order to trace a close to the optimum energy scheduling. Then, a second level formulated as a rule-based logic, integrates the information deriving from the optimization phase to operate and ensure the real time management.

More in detail, in the following two case studies are presented: one focuses on the EVs integration with a Photovoltaic (PV) plant in a household system (Vehicle to Home); the other focuses on the integration of a EV fleet with the power system (Vehicle to Grid), thus considers the possibility of grid services providing.

The objective pursued in the first case study is the maximization of the PV self-consumption and self-sufficiency. In fact, a better matching between the PV generation and the local electricity absorption has several advantages both economical (due to the low cost of the PV energy) and technical such as a reduction of losses on power distribution, power quality, and safety of the electrical system, [6].

The second case study, instead, pursues the maximization of the economic benefit, that could derive from bidirectional power exchanges (from and toward the grid) of a 214 EVs fleet; while contextually ensures all its energy needed for mobility. Two grid services are considered: Replacement Reserve and Secondary Regulation and the results are provided for the scenario with no services activation, with only Replacement Reserve activation, and with only Secondary Regulation.

Finally, in both case studies the proposed approach is compared with proper logics assumed as references in order to evaluate the quality of the proposed methodology.

In the following, Chapter 1 provides the context of the research, thus discusses the more recent trends in the transportation and power sectors. Chapter 2 introduces the Vehicle to Grid and Vehicle to Home concepts, presents the scientific literature review on the subject, and highlights the contribution of this work. Chapter 3 illustrates the EV behaviour forecast logics and discusses its reliability using specific error indexes. Chapter 4 discusses the proposed battery energy management for a PV powered household. Chapter 5 argues the EVs integration with the power system, thus the proposed EV fleet management. Finally, the main conclusions are drawn in the last pages of this thesis work.

Chapter 1

Research Context

The climate crisis and the related increase in attention about sustainability and environmental problems, drive deep changes in entire sectors. The objective of this chapter is providing an overview on the recent transformation trends for strongly involved sectors such as electric power and road transportation sectors. This overview aims to compose an as much as possible complete framework for this dissertation, thus making clear its motivations, contextualizing and introducing the next covered topics.

In the following, Section 1.1 presents the principal international agreements and objectives targeted to reduce greenhouse gases emissions. Section 1.2 discusses the main factors which are transforming the power system sector and provides the relative trends. Finally, Section 1.3 discusses the road transport sector transformation.

1.1 Toward the Green New Deal

Starting from the 1990, when the first International Panel on Climate Change (IPCC) report has been published, more and more studies have correlated the global warming with the human activities. The increase of consciousness in the subject, led to the stipulation of international agreements and policies targeted to reduce greenhouse gases emissions. In December 2015 during the 21st Conference of Parties (COP), 196 parties signed the “Paris Agreement” which commits to limit the global warming well below 2°C - preferably below 1,5°C.

The “*Global Energy Perspective 2019*” in [7], analyses the dimension of the changes that need to be implemented to achieve the Paris objectives within the 2050. The study concludes that to limit the global warming below 1,5°C it will be necessary a greenhouse gases emission reduction of about two-third with respect to the expectation at 2050. Figure 1.1 shows the result of this analysis where it is evident the huge contribution that the power and transportation sectors are called to give.

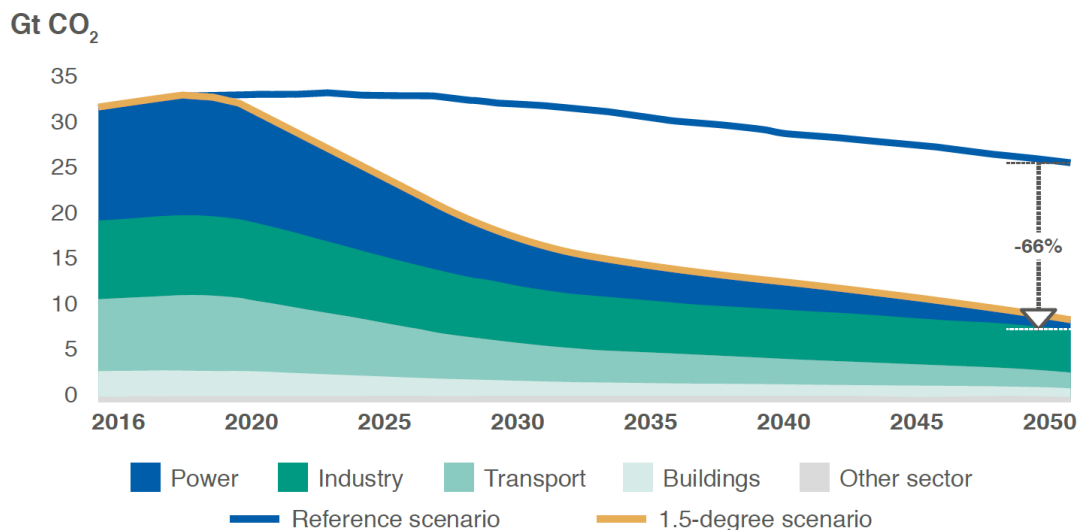


Figure 1.1 Greenhouse gases emissions reduction - 1,5 °C scenario, [7]

In fact, to reach the Paris objective it is needed, on the one hand the disposal of the 90% of the coal powered plant and 80% of the gas-powered plant; on the other hand, the decarbonization of the 100% of the road transports, 80% of the sea transports, and 60% of the air transports by 2050.

The European Union has been the first great power to act to enable a transition process toward a cleaner economy.

In the 2009 was published the “*Climate Energy Package 2020*” document was published which has defined the energetic and climatic European targets for the 2020:

- 20% of renewables quote on gross energy consumption
- 20% of gross energy consumption reduction with respect to the trend
- 20% of greenhouse gases with respect to the level of the 1990.

At the net of the effects caused by the Covid-19 pandemic (2020 data not yet elaborated), the European Union is close to reach two of these objectives, [8]. In particular, the first one with a renewable quote of 19,4 % in 2019 and the third one with a greenhouse gases reduction of 24%. Meanwhile, the gross energy consumption reduction has been achieved only by nine members (Finland, Greece, Italy, Latvia, Netherland, Portugal, Romania, Slovenia, Spain).

In the 2011 the European commission published the “*Roadmap 2050*” throw with Europe committed to reduce of 80-95% the greenhouse gases by 2050.

In the 2016 (after the Paris Agreement) Europe has renewed is commitment with the “*Clean Energy Package for all Europeans*”. Thus, the normative process to achieve a reduction of greenhouse gases of at least 40% by 2030 was started. The principal objectives of the Clean Energy Package can be summarized in:

- 32% of renewables quote on gross energy consumption
- 32,5% of gross energy consumption reduction with respect to the trend
- 40% of greenhouse gases with respect to the level of the 1990.

The Clean Energy Package is also based on other main general principles such as energetic security, innovation and competitiveness and was definitely approved on May 2019. Moreover, it declines itself into the different and more detailed National Plans for Energy and Climate. For example, the “*PNIEC*” (*Piano Integrato per L’energia e il Clima*, [9]) lists the Italian 2030 targets: coal phase-out by 2025, 30% of renewables quote on gross energy consumption (55% renewables in the power sector), 43% of primary energy reduction.

Finally, from December 2019 started the process for an “European Green new Deal” started which aspires to the climatic neutrality within 2050. Moreover, it increases the ambitions also for the target at 2030. In fact, on September 2020 the European commission proposes to raise the reduction objective of greenhouse gases emission from the current 40% to the 55% with respect to the 1990 level. Thus, the actual Energy and Climate Plans will be updated in the next years.

1.2 The Power System Transformation

Power systems around the world are going through a significant change, mostly driven by the increasing availability of low-cost renewable energy, digitalization, and deployment of distributed resources. In the following, three main factors of this change are discussed: the renewable development, the power system flexibility enabling, and the battery price decreasing.

1.2.1 The Renewables Development

The electricity cost from renewables has fallen drastically in the last decade. This was due to an improvement of the technologies, economies of scale and growing developer experience.

According to the latest cost data from the International Renewable Energy Agency (IRENA), the global weighted-average Levelized Cost of Electricity (LCOE) of utility scale photovoltaic (PV) plant fell of the 82% between 2010 and 2019 resulting in the largest price reduction per source in the last decade. However, important reductions in LCOE are observed in the same period also for the other principal renewables: concentrating solar power fell of 47%, onshore wind 39% and offshore wind by 29%.

Figure 1.2 shows the results of the analysis conducted by IRENA, in [4]. The thick lines in figure, are the global weighted average LCOE (in orange) and the auction values (in blue) by year, respectively. The shaded bars that vary by year are the relative cost/price ranges. Finally, the grey band that crosses the entire chart represent the fossil fuel-fired generation cost range.

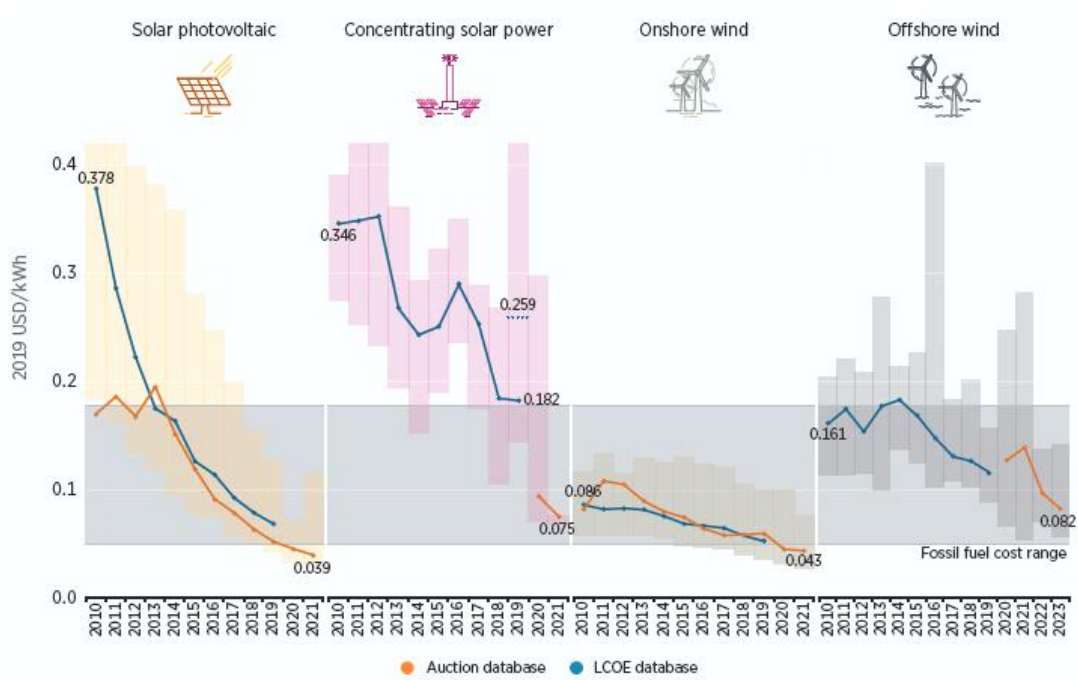


Figure 1.2 Renewables global weighted average LCOE - last decade, [4]

As result of this huge cost reduction, renewables have become the least-cost option for new capacity in many countries over the world, [4]. This has been reflected directly in the new installed capacity quota occupied by renewables worldwide: in 2019 the 72% of new installed capacity was covered by renewables.

Figure 1.3 reports the results of another study, conducted by the International Energy Agency (IEA) in [10], and shows the historical and expected electricity net capacity addition of renewables by technology from 2013 to 2022. In particular, the study presents two expected scenarios: the main case scenario (based on May 2020 updated data) and an accelerated scenario which traces a more optimistic trend based also on the capacity addition of September 2020 (which exceeded the previous forecasts).

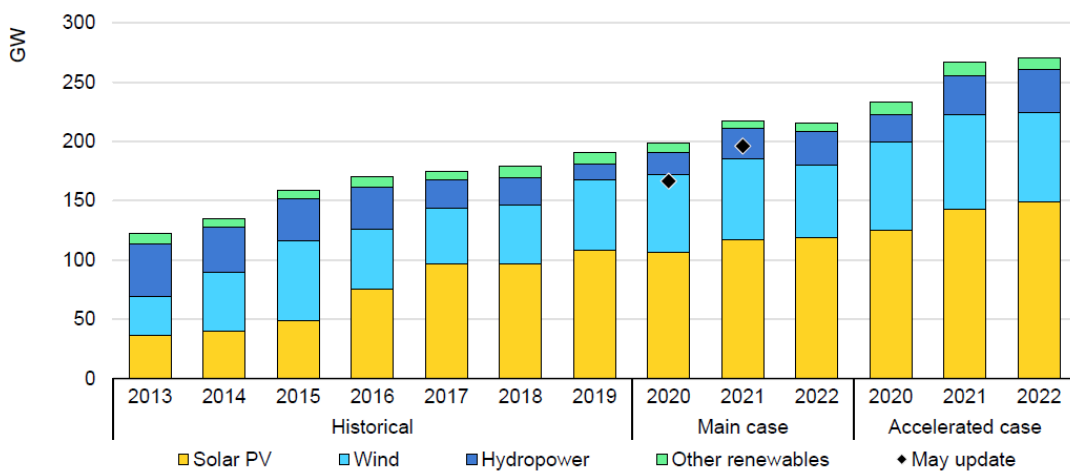


Figure 1.3 Annual renewables capacity addition - 2013 to 2022, [10]

According with the main scenario, despite the Covid-19 crisis, net renewable electricity capacity addition is expected to be almost 4% higher in 2020 than 2019. This is translated in 198 GW of more renewable capacity this year. Higher additions are expected in wind (+8%) and hydropower (+43%), while Photovoltaic (PV) growth remain stable. More in details, the utility scale PV installations are still expected to increase, while distributed PV system growth decreases of about 8% since the reprioritizing of the companies due to the crisis.

In case of accelerated scenario, the new installed renewable capacity in 2020 will account to 234 GW. In both cases, an increasing trend on new renewables capacity addition trained by the photovoltaic technology results evident in the next years. Finally, the same study forecasts a share of renewables in the total electricity generation of 33% by 2025 in increment with respect to the current 27%.

1.2.2 The Power System Flexibility Enabling

The increase of non-programmable renewables such as photovoltaic and wind sources, are characterized by the fact to be not easily predictable. Thus, they add a certain level of uncertainty in the generation side, thus making more complex the managing of the electrical system proportionally to their level of penetration. This brings to the necessity of a corresponding increase in power system flexibility.

The power system flexibility is defined as “the ability of the electrical power system to reliably and cost effectively manage the variability and uncertainty of demand and supply across all relevant timescales, from ensuring instantaneous stability of the power system to supporting long term security of supply”, [11]. Flexibility is already an important characteristic for all power systems, and it is evident that it must assume more and more prominence in order to facilitate the transition toward a more affordable, clean, and reliable energy access.

From a technical point of view, flexibility can be enabled acting on the supply side, demand side, energy storage systems, grid robustness or opportunely integrating all these possibilities.

Supply side flexibility refers to the ability of the generators to follow rapid changes in net load and it depends on the proper technology of the generator. More specifically, a flexible generator can ramp up or down fast, thus it has a low minimum operating level and a fast start-up and shutdown times. For example, hydro generators and open-cycle gas turbine are considered to be among the most flexible conventional generators, while large steam turbines and nuclear generators are on the less flexible, [12].

Demand side flexibility refers to the possibility to act on the demand pattern in order to shift and better match the electricity demand with the supply. Within this category, Demand Response is a specific method that could enable customers to play a role in the operation of the grid by adjusting their electricity consumption (following price signal or throw direct control agreements), [13].

Energy storage systems can be used to shift the timing of electricity supply by storing energy. For example, electricity can be stored when its price is the lowest

and discharged when the price is the highest. This is the case of pumped hydro power. The value of this operation comes from the fact of preventing more expensive generators from generation increases and reductions. Moreover, when associated with non-programmable renewables, storage can be used to mitigate the uncertainty of the supply side. Different scales of variability characterize renewables: from seconds (e.g., when a cloud passes over a PV plant), to years (e.g., seasonal availability of sunlight hours for PV plant, wind speed and air density for wind farm, and water flows for hydro generators). Thus, different storage technologies can be useful to meet the different specific applications.

Finally, grid flexibility refers to the implementation of robust transmission network aiming to balance supply and demand over large balancing areas (i.e., cross border interconnections able to exchange electricity across national borders).

In this frame, the electrical power system can take advantage of the vast diffusion of Information Communication Technologies (ICT) in order to manage at the best all sources of energy and flexibility. Then, the possibility of a new paradigm for the electrical system emerged such as expressed by the concept of smart grid. With smart grid is principally intended a larger or smaller local electrical grid which includes distributed renewable energy sources, measurement systems (e.g., smart meters), and a control system able to maintain the security of the operations and perceive specific objectives such as electricity independency or economic benefit for the locality. Whiting smart grids, the control system is considered able to switch on and off renewable generation, actively acts on the demand side and manage storage systems. Therefore, smart grids and more in general ICT, can represent another important instrument for the flexibility enabling of the power system.

Despite all the possible technical ways, also new power market rules and codes are needful in order to allow an as greater as possible exploitation of all the flexibility sources and better reward flexibility services. In this direction particularly relevance has the possibility to admit distributed energy sources to participates in the ancillary services providing (e.g., flexibility operations) throw reserve and balancing markets (which differ for the time of negotiation, i.e., day ahead and intraday respectively, and together represent the ancillary services market). At this purpose many countries over the word are gradually tracing new power market rules and codes as a key strategy for a liberalised and resilient power system in transition. As an example, in the following is discussed the recent years transformation of the Italian Ancillary Services Market.

Italian Ancillary Services Market Opening

In May 2017 with the approval of the Directive 300/2017, has been laid the basis for the opening of the Italian ancillary services market to aggregated form of distributed energy sources. More in details, after the Directive 300/2017 approval, the Italian energy authority has agreed with the Italian Transmission System Operator (TSO) Terna.S.p.A., the development of pilot projects to admit the

distributed generation at the ancillary services participation. In this context for the first-time different types of Virtual Units have been defined as aggregations of consumption or production entities which are grouped in order to facilitate their participation at the reserve and balancing market. Finally, Aggregators are defined as the subject with the role to manage and control the aggregated Virtual Unit.

The Virtual Units have been differentiated in four main categories based on the nature of the entities aggregated: aggregated virtual units of consumption (UVAC), aggregated virtual units of production (UVAP), mixed aggregated virtual units (UVAM), and nodal virtual units (UVAN). Each category is regulated by proper codes and specific requirements, however UVAM represent the more generic case and it is expected that toward a maturation of the market also the other aggregations will converge on this category, [14].

Before the 2017 only relevant units of production (i.e., with nominal power equal or greater than 10 MW) were enabled at the Italian ancillary service market participation. However, due to the increasing need of flexibility of the power system, currently also virtual units, thus Aggregators are enabled. For sake of completeness, in the following are listed the principal technical requirements are listed for the more generic case of an UVAM enabling.

- The UVAM must be able to change its Power Profile by reducing or increasing its power adsorption of at least of 1 MW. In other words, the Control Power must be at the minimum 1 MW.
- The UVAM must be able to change its Power Profile within 15 min from the reception of the command from the TSO.
- The UVAM must be able to maintain the Power Profile variation for a minimum of two or eight consecutive hours depending on the specific ancillary service provided.
- The UVAM must aggregate energy and flexibility sources within a geographically circumscribed perimeter (regional scale).

Finally, it is worth to mention that in January 2020 the Italian Department of the Economic Development started the process to define the criterion and the actions to encourage electric vehicle integration with the grid. In this context the possibility has emerged to consent at the UVAM consisting of only EV charging infrastructure, to participate in the ancillary service market also with a reduced control power of 0,2 MW. However, this process is still in definition, thus this thesis work bases its analysis on the generic UVAM requirements before discussed.

1.2.3 Batteries Price Decreasing

As discussed above, energy storage systems can be used for power system flexibility. Until now pumped hydro systems are the most widely deployed option for power system storage. However, a rapid decline in technology cost of electrochemical storage systems is creating an important opportunity for batteries to provide power system flexibility. Actually, batteries present a fast and accurate response time to dispatch signals from system operator. Moreover, their modularity enables a wide range of installation from household to utility scale.

Figure 1.4 shows the result of the “2019 Battery Price Survey” conducted by BloombergNEF, in [15]. More in details in figure the observed prices of lithium-ion battery pack are reported from 2010 to 2018, then a forecast on the future behavior of the battery price is provided until 2030, when it is expected to fall to 62\$/kWh. Lithium-ion battery are the most prominent in the market, and their diffusion, thus the correlated price decreasing, is mainly due to the electric vehicles market development.

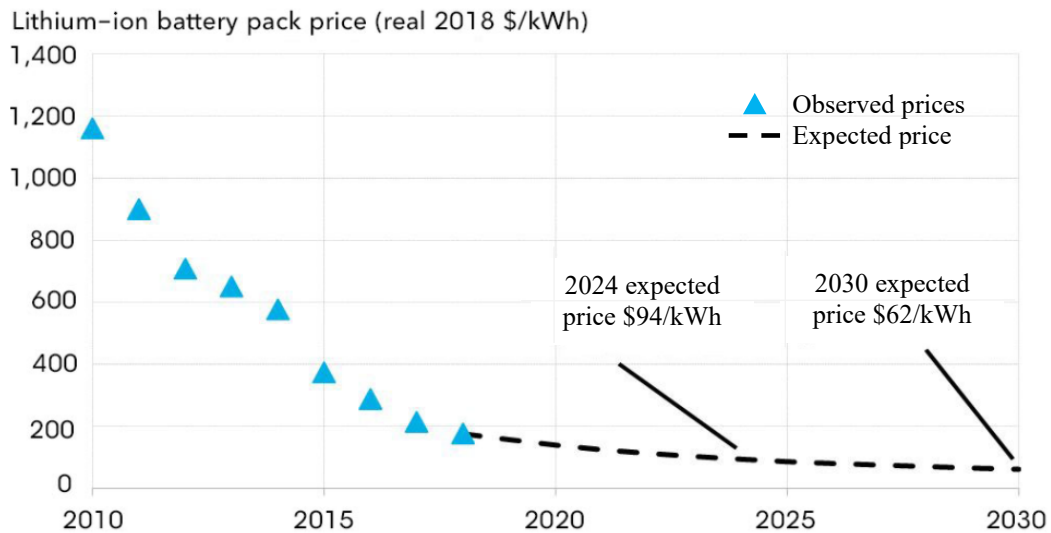


Figure 1.4 Lithium-ion annual battery price - 2010 to 2030, [15]

In the recent years several large grid-scale battery projects have been developed (e.g., in Australia, California, Chile, Italy, Puerto Rico, etc.). However, despite the consistent cost and price decreasing, in most context, stationary batteries for power system flexibility enabling are not yet a fully cost competitive solution, [11]. Another possibility comes from the exploitation of the distributed batteries which constitute electric vehicles (EVs).

1.3 The Road Transport Sector Transformation

The road transport sector is at the beginning of a deep transformation driven by a cross-party willingness of its electrification. In fact, Electric Vehicles including full battery electric vehicles (BEVs) and plug-in hybrid electric vehicles

(PHEVs) can deliver multiple environmental, societal and health benefits. These include:

- Energy efficiency: EVs are three-to-five times more energy efficient than conventional internal combustion engine (ICE) vehicles, [16].
- Energy security: electric mobility reduces oil dependence, thus the oil import for many countries. Indeed, electricity can be produced with a variety of resources and in some case can be generated domestically.
- Greenhouse gas emissions: the increment of electric mobility in association with the progressive increase of low carbon electricity generation can result in a significant reduction in greenhouse gas emission. This role can be expanded by the adoption of EVs for power system flexibility.
- Air pollution and noise reduction: EVs present zero tailpipe emissions and are quieter than ICE vehicles.

All these drivers together with the price decrease of batteries (factor which influences, and it is influenced) led to a consistent development of the electric vehicle global market in the last decade.

Figure 1.5 shows the global electric car stock from the 2010 to 2019 (“*Global EV Outlook*” -IEA, [16]). The global electric car stock expanded by an average of 60% per year from 2014 reaching a total stock of 7.2 million electric cars in 2019, year that has accounted for 2,1 million globally sales (surpassing 2018 already a record year). This amount of sales corresponds to the 2.6% of the global car sales, while the total electric car stock accounts to about 1% of the global car stock. China is the first global market with sales of 1,2 million of new electric cars in 2019 (half of the global). Europe over the year is constantly the second market with 560.000 new electric cars sale in 2019. United States are the third market with 320.000 new electric cars sale in 2019.

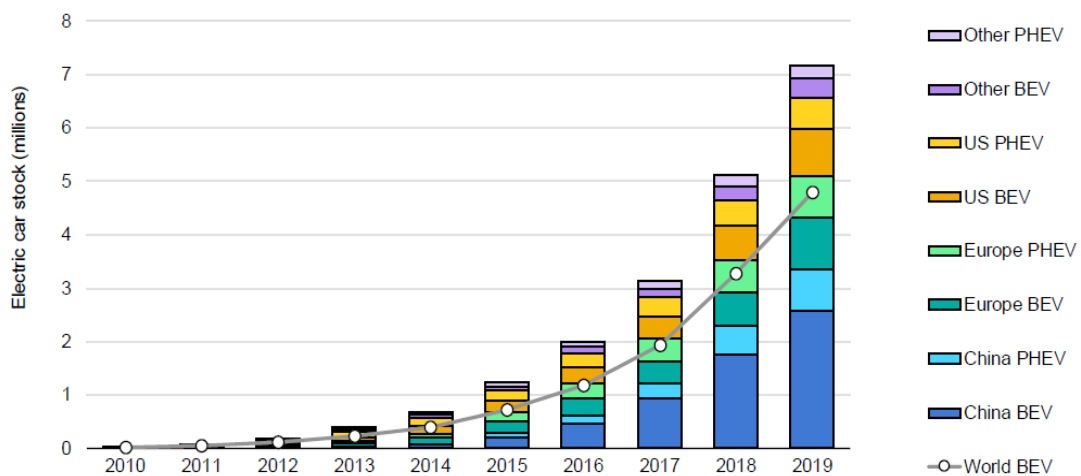


Figure 1.5 Global electric cars stock - 2010 to 2019, [16]

Finally, among other countries, they can be mentioned Japan, Canada, and South Korea, all with a number of electric cars sales in 2019 inferior to 100.000 units.

Within the European market, the first country for electric cars sales is Germany with more than 100.000 electric cars sale in 2019. The second European market is Norway (80.000 electric cars sale), it follows the Great Britain (72.000 sales), Netherland and France (with 67.000 and 61.000 electric cars sale in 2019 respectively). Finally, Italy is the tenth European market with a total electric cars stock of 40.000 units (0.1% of the 2019 total car stock) and 17.000 new electric cars sale in 2019 (0,9% of the total car sales). However, this number of sales represent an increment of about 80% with respect to the 2018, [17].

Regarding the future expectation, the work in [18] (published by Deloitte-Insight) provides a global market forecast scenario for the next ten years also considering the effects of the Covid-19 pandemic. At the end of 2020 the global car market (including both Electric and ICE vehicles) is estimated to decline of about 20% (falling to around 70 million of vehicle sales). This drop is even more severe for Europe and United States where the expectation brings to a decline of around 25%. However, the electric vehicle sales are expected not decrease. In fact, a small increase with respect to the 2019 level, is expected with an absolute number of 2,5 million of EV sales in 2020. Thus, the global stock of EVs is expected to reach around 10 million of units by 2020. Therefore, Deloitte-Insight analysis suggests that EVs will continue to have a positive trajectory during the Covid-19 recovery period, Figure 1.6. In particular, the global annual EVs sale, is forecasted to reach 11,2 million in 2025 and 31,1 million by 2030, thus occupying the 32% of the total market share for new car sales within this decade.

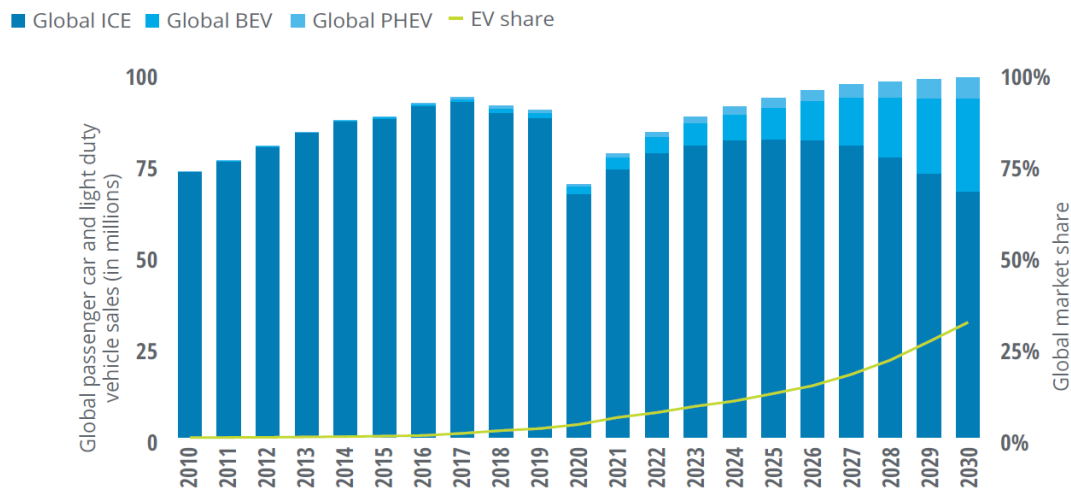


Figure 1.6 Annual car sales per typology - 2010 to 2030, [18]

The EVs European Market was the one that better reacted this year, with an important increase on EV sales of 57% in the first sixth months of the 2020 with respect to the same period of 2019. Following this trend, for Europe a share of EV sales by 2030 can be estimated, sensibly higher than the global average. Finally, for Italy is estimated an EV sales share by 2030 higher than 50%, [17].

Chapter 2

Review on Network EV Integration Models and Proposed Approach

The increasing need of power system flexibility, the battery price decrease, and the road transport sector transformation discussed in Chapter 1, make arise the possibility (and necessity) to opportunely integrate EVs in power systems. Many studies in scientific literature have addressed this issue with different forms, scales and approaches. The objective of this chapter is providing a state of the art on the subject by reviewing the principal concepts, methods, and technologies behind the electric vehicle integration with power systems or more in general with electrical networks. Moreover, the chapter introduces and defines the approach used in this dissertation and aims to highlights its contributions.

In the following, Section 2.1 discusses the Vehicle to Grid (V2G) related concepts. Section 2.2, reviews the works on the integration of EVs with buildings. Section 2.3 reviews the works which considers the integration of EVs with the grid, thus with electricity market participation. Finally, Section 2.4 discusses the proposed approach and highlights the novelties.

2.1 Vehicle-to-Grid Concepts

The Vehicle-to-Grid (V2G) concept traces its origin on the fact that most of vehicles are parked almost 95% of their time [19]. In this way, they can remain connected to the grid and be ready to respond to some grid requirements. These requirements include also delivering part of the energy stored in their batteries, under the concept of V2G earlier introduced by [5]. Moreover, the average daily energy consumption for travelling purpose is in some cases a small portion of the total battery capacity of the vehicle.

Table 2.1 presents the battery capacities and the relative autonomies, in kilometres, of various Battery Electric Vehicle (BEV) manufacturers. For a medium sized car, the most common battery capacity is currently 40kWh. Moreover, the analysis conducted in [20] suggests a medium-high rate of energy consumption per kilometre of 200 Wh. Assuming a battery capacity of 40kWh and an average EV user (travelling 15.000 km per year), the average consumption per day accounts between 20% and 30% of the total capacity.

Depending on the application the EV can be used to provide grid support by giving availability on exploiting part of their battery capacity. This is made more attractive by the fact that Renewable Energy Sources (RES) like wind and photovoltaic (PV) energies are rapidly increasing their penetration into the power system. Renewable energies are intermittent in nature and their behaviour is difficult to be predicted. This will require large energy storage systems able to smooth the power offer, thus meet at all the times the power demand. The works in [21],[22] and [23] review the literature on the interaction between electric vehicle and renewable sources.

Table 2.1 Examples of commercial BEV: autonomy and battery capacity

Car Manufacturer/Model	Declared Autonomy [km]	Capacity [kWh]
Nissan Leaf	175	30
Tesla Model S	500	60-100
Citroën C-Zero	150	15
FCA 500e	320	42
Renault ZOE	300	40
Mercedes-Benz Classe B	250	40
BMW i3	260	40
Volkswagen E-Up	160	18
Volkswagen	330	45
Peugeot iOn	150	16

In this context, two principal concepts emerge from literature: Vehicle to Home (V2H) and Vehicle to Grid (V2G) [24].

The V2H refers to the power exchange between the EV battery and the home power network. In this case, the EV battery can work as energy storage to provide backup energy to the home energy appliances and contextually be recharged from the home renewable energy sources. The works in [25] [26] review the literature on the subject.

The V2G utilizes the energy from relatively local EV fleets and trades them to power grid through the control and management of the Aggregator (an entity appointed for this purpose). In this case, the aggregated battery capacity can be used to dispatch different Ancillary Services. Generally speaking, Ancillary Services are divided in: frequency regulation [27], and reserve services such as Secondary Reserve or Replacement Reserve, [28] [29]. These services differ mainly for their response time scales [30]. However, their purpose is ensuring

safety, security, and reliability of the power grid operations [31]. The works in [32] [33] review the literature on the V2G technology.

Figure 2.1 visually expresses the V2H and V2G concepts. It highlights the capability of the technologies of flattening the curve of the electricity demand by the appropriate exploiting of the battery's capacity, then introduce the concept of smart charging, better discussed in the following.

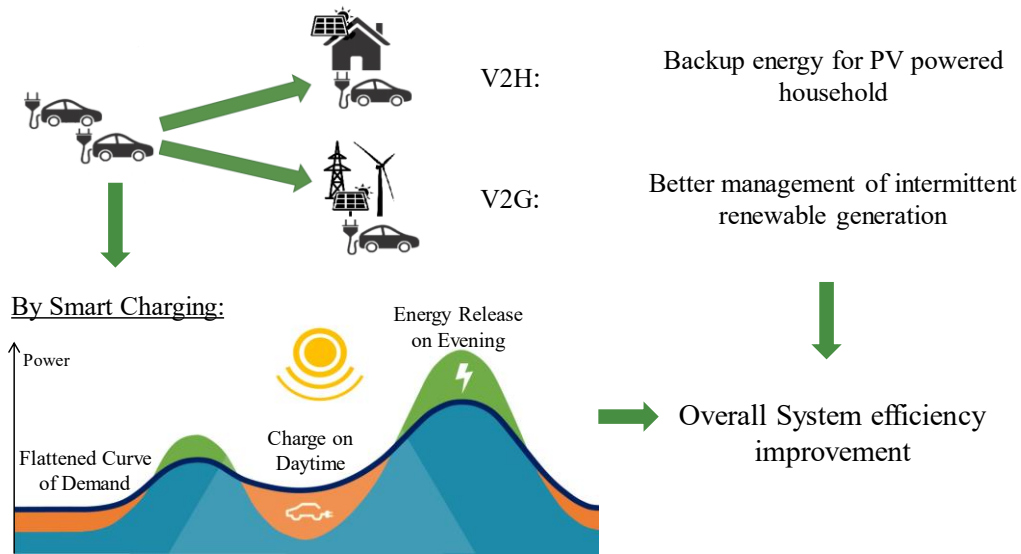


Figure 2.1 Vehicle to Home and Vehicle to Grid concepts

2.1.1 Smart Charging

All the V2G related technologies have as core of their working the possibility to schedule, control and monitor the EV battery power input/output. The set of these active actions is referred in literature as Smart Charging (SC), [34].

The work on [35], divides the smart charging technologies proposed in literature basing on their level of control or “smartness”, thus level of complexity, Figure 2.2. In the case with no active actions the EV is considered a simple electric load, this results in an uncontrolled charging.

The first step toward a full battery control is the off-peak charging or delayed charging [36]. In this case, the EV charge is actively positioned in time periods where no peak of power demand already exists.

A medium level of control is given by the smart charging Valley-filling [37]. In this case, the EV charge is distributed in time in order to flatten the electricity demand curve. However, no bidirectional power exchanges are admitted.

Finally, the ultimate level of control is represented by Smart Charging Peak shaving (Full Smart Charging), [38]. In this case, bidirectional power flows are admitted, thus the electricity demand curve can be fully modified by the EV operated as a storage system. Due to the complexity of this latest case, it has been observed that an optimized algorithm is crucial to effectively schedule and benefits from EV integration into a grid [32].

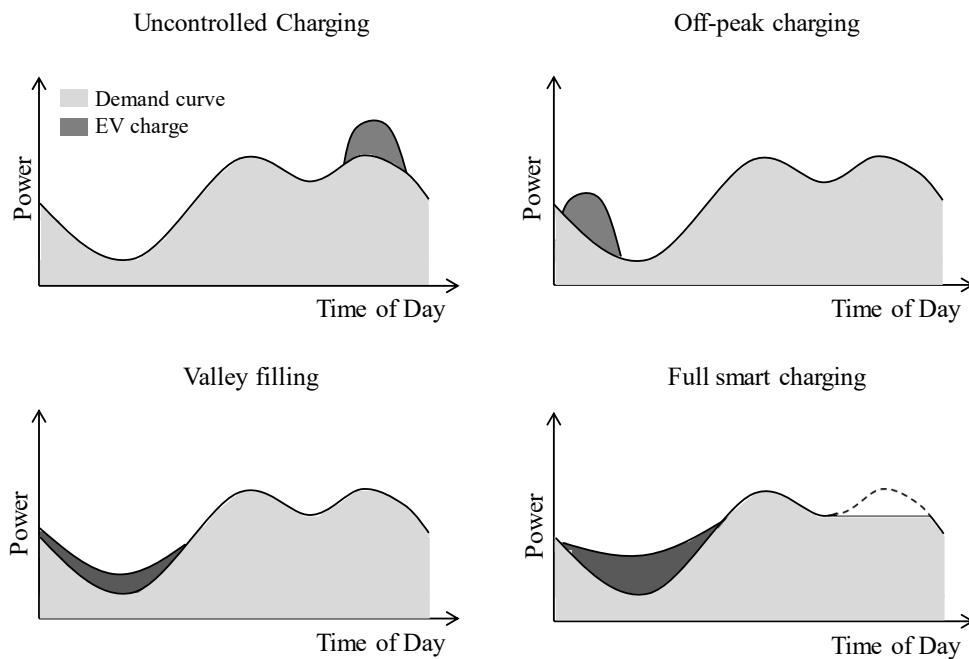


Figure 2.2 Smart Charging technologies by level of smartness

Finally, depending on the application smart charging follows different final purposes. Some works pursue economic criteria such as minimization of charging cost for the electric vehicle or for the entire electricity demand of the building or the grid [39] [40]. On the contrary, other works are more focalized on the optimal fulfilling of technical aspects such as self-consumption improvement for PV powered houses [41], or enlarging flexibility for grid services [42].

Effect on Battery Life of V2G Operations

The main typology of batteries used for the Electric Vehicles are lithium-ion batteries. The rate of degradation is often governed by how battery is used including: magnitude of charging/discharging current, State of Charge (SOC) at which the battery is stored, swing in State of Charge (SOC) and Temperature. For example, storing a battery at progressively higher temperature and SOC will cause higher capacity fade and power fade [43].

The Effect on the battery life (thus both capacity and power fades) of the V2G operation present still some controversial results in literature. For example, the work in [44] conducts an analysis comparing the capacity fade due to driving with the capacity fade due to the V2G cycling. The work concludes that V2G energy incurs in approximately half the capacity loss per unit energy compared to that associated with driving. On a similar direction, the work in [45] concludes that V2G operations are detrimental to cell performance and that it could reduce the lifetime of battery packs to less than five years.

An opposite conclusion was achieved from the work in [46], where it was shown that the V2G could be opportunely exploited by the battery in order to reduce the degradation. For example, by modifying the SOC to one which minimises the degradation when the battery is stored or by using the battery in a

SOC region with a lower internal resistance. In this case, the results, showed a reduced capacity fade up to 9% and a reduced power fade by up to 12% compared with the no V2G operations case.

Finally, due to the apparent contradiction of the results, the Authors of the two above mentioned works ([45] and [46]), have collaborated to provide a synthesis through the work in [47]. In this work, they have conducted critical analysis on their previous works highlighting the imprecisions of the case studies considered and improving the model. They conclude that if V2G is operated without consideration on battery degradation, this results in a not economical viable way, because it adds an additional cycling. However, a smart control algorithm, which considers battery degradation (i.e., avoid too fast charge currents as well as fast discharge currents), could in the worst case have the same impact on battery life as if there was no V2G.

2.1.2 Different Scales and Adoptions

Congruently with the V2H and V2G specifications, proper definitions emerged in literature in order to identify more particular or more generic applications. To refer to the integration of an EV with a generic building (different from a household), Vehicle to Building (V2B) is used. On the other hand, to refer to bidirectional power exchanges among vehicles, Vehicle to Vehicle (V2V) is used. Finally, the generic possibility to operate the vehicles in all the previous applications, is sometimes referred as Vehicle to Everything (V2X), [48].

Furthermore, works in literature differ for the number of vehicles, thus the geographical scale analysed. The work in [49], considers a commercial building equipped with 50kWp capacity of PV. It aims to optimize the charging of 12 EVs by minimizing the total electricity cost. Meanwhile, an university campus microgrid is considered in [50]. A microgrid is defined as a set of loads and microgenerators operating as a single system [51]. The works in [52] and [53] consider a charging station with PV capacity enslaved to a workplace. In [54] a charging station hosting 650 EVs is analysed. Finally, in [55] a large scale Aggregator (controlling up to 600,000 vehicles) is considered in order to estimate the effect of a consistent integration of renewables and EVs.

The next sections review more in detail the subject with respect to Vehicle to Building and Vehicle to Grid applications respectively.

2.2 EV and PV Integration: Vehicle to Building

This section reviews articles that regard the integration of the electric vehicles with PV systems. In fact, due to the rapid growing of PV plants in the power system and the expected increase on EV sales, this topic is getting more and more interest in literature [26]. More in details, this section considers a building or a microgrid scale where the main purpose is a better management or an economic benefit for the considered locality. Thus, works in this section does not aim to

provide any direct services to the grid and does not participate to the electricity market.

Several works focused on PV powered systems aiming to quantifying the potential benefit or the impact, in case of EVs integration. For example, [56] and [57] show two case studies. In both cases stochastic models are used to produce theoretical household load profiles and EV pattern, while PV power is modelled basing on real irradiance data. The results show that, thanks to EVs, an improvement in the matching between PV generation and loads is possible, with consequent energy and economic benefits for the users.

In [58], the energy and the environmental performance of a PV system that satisfies the electric demand of a single EV, as well as space heating and cooling of an office building in Southern Italy, is analysed. Under the assumptions made by the authors, the simulations put into evidence that, in the best case, 59% of the PV production is directly used by local loads and the EV.

A similar work was presented in [59], where the benefit of using PV to charge EV is investigated from the point of view of electric grid management. As a matter of fact, the distribution system operator would reduce the negative effect of high numbers of distributed generators in the grid (such as voltage fluctuations [60], harmonic content increase [61], and the overheating of the power lines). In [59], they concluded that, despite the better matching between loads and PV generation introduced by EVs, system upgrades will be still necessary (e.g., the installation of new transformers with higher sizes and the reduction of impedance of lines).

The main issue of the above cited works is the lack of an advanced control strategy for the optimal management of batteries. In particular, storage is simply discharged when power is required by the car, and batteries are charged when the car is connected to the charging station. A possible improvement consists of the development of a Smart Charging logic (or smart storage management), which optimizes the EV power charge/discharge cycles by pursuing a pre-defined goal. Moreover, the smart management must guarantee the correct work of the storage for traveling, by appropriate constraints. In the following, the principal Smart Charging approaches adopted in literature are described.

2.2.1 Smart Charging Approaches on Vehicle to Building

In order to implement Smart Charging, three possible approaches are proposed in literature: Heuristic, Optimization and Hybrid approaches.

Heuristic Approach

The Heuristic approach operates the management of the charge-discharge cycles of EV batteries taking advantage of a real-time check of PV generation, loads and storage parameters. In such works, algorithms are based on simple logical rules to instantaneously react to new events (e.g. plugging/unplugging of

an EV, increasing/decreasing of PV power). In literature, some energy management logics for EV/PV systems are based on the heuristic approach [62],[63],[64]. However, they use only real-time information, thus it is not possible to optimize the charging pattern for a longer time period. As a conclusion, the need to combine forecasts of future energy flows with an efficient real-time management arises.

Optimization Approach

The Optimization approach, contrarily to the heuristic approach, consists of a procedure, which does not perform a real time management. Thus, the optimal charge-discharge cycles are calculated by elaborating a priori PV production and EV/load profiles. However, this method is useful for scheduling or planning purposes. Basing on the possible data elaboration, optimization algorithms are grouped in three main categories: Deterministic, Stochastic and Forecasting statistical methods.

- In Deterministic methods, the EV-PV-load profiles are inputs of the simulation, and they are fixed a priori. Examples of deterministic method applications for EV-PV-load systems are present in [65] and in [66]. This method is useful in order to test the potential of the optimization phase. In fact, both cases solve a linear optimization problem showing significant improvements compared to the case with uncontrolled charging. In fact, a better match between local PV production and loads is found, and electricity cost reduction is achieved. However, real time management and the relative uncertainty, are not addressed by deterministic methods.
- In Stochastic methods, EV-PV-load profiles are iteratively generated on the basis of opportune criteria. For example, Probability Density Function (PDF) for the PV production is built from historical data [67]. Then, the PDF is used to randomly generate different new profiles (each profile alone can be considered as a deterministic profile). In this case, the objective function of the optimization is the expected sum of the objective functions over the different deterministic scenarios. The works in [68], [69] show that the stochastic methods result in a more realistic analysis, with respect to deterministic methods.
- In Forecasting statistical methods, future EV-PV-load profiles are estimated basing on historical data and trends analysis. In this case, forecasts are used to run the optimization problem. This forecasting method is used in [41] and [53] to predict power flows in a micro-grid, and in office buildings, respectively. Nevertheless, in the two above cited papers, the forecast is used only for PV and loads. Meanwhile, a deterministic approach is used to modelling the Electric Vehicle.

By using the optimization approach alone, in general it is not possible to evaluate the performance of the system in real time. A Heuristic approach is necessary to achieve this aim.

Hybrid Approach

The Hybrid approach combines optimization and heuristic methods. Firstly, an off-line optimization method is used in order to trace the macro trend on battery power flow. Secondly or in parallel, a rule-based decision-making algorithm manages the real time operations. Thus, only Hybrid approach ensures a complete applicability of an optimized scheduling.

In [70], a deterministic optimization approach uses a priori determined data of PV and EV, while a machine learning algorithm is used for the real time decision making. However, this work does not analyse a proper Vehicle to Building application, while a charging station equipped with a PV is considered.

Finally in [71] a forecasting optimization method based on Model Predictive Control is proposed for an household. Model Predictive Control is a control algorithm that utilizes an explicit process to predict the future response of a system. At each control interval an MPC algorithm attempts to optimize future system behaviour basing on the forecasts of the variables in that interval [72]. This work includes both the real time management and the forecast of EV usage. However, aspects related to the maximization of use of local renewable source and the maximization of energy efficiency are not addressed and the work focuses on economic aspects.

2.3 EVs and Grid Integration: Vehicle to Grid

This section reviews articles that regard the integration of the Electric Vehicles with the grid at the purpose of providing grid services. Thus, the participation to the electricity market is considered. To accomplish with this aim in general an Aggregator is needed in order to address the technical management of the EV fleet.

However, it is possible a distinction between the works in literature, basing on the used or proposed Vehicle to Grid system architecture. More in details, the distinction regards the hierarchy on communication and control operations. The most common architectures are: Centralized control architecture and Decentralized control architecture.

2.3.1 Centralized Architecture

In centralized architecture, the Aggregator is responsible for managing directly the power of all the EVs under its region, Figure 2.3. In this case, the Aggregator is not only responsible for the technical management, but also must allow the participation of the EVs at the electricity market. Thus, it must perform daily demand forecasts based on historical data.

Once demand profile forecasts of the EVs is obtained, this profile must be communicated to the Distribution system operator (DSO) for approval. If the profile does not compromise the safe operation of the distribution system, the Aggregator can perform the power purchase bids directly in the day ahead market or through a third entity called Balancing Responsible Party (BRP) – in the following it is assumed that the aggregator directly participates in the day ahead market. In a second phase, the Aggregator can participate also to the Reserve market in order to provide Ancillary services. Thus, the Aggregator will estimate the ability to offer additional services such as Secondary reserve or Replacement reserve. In this instance, the Aggregator assumes the role of a Balancing Service Provider (BSP).

Finally, after market negotiation, the Transmission System Operator (TSO), can in the day of dispatch require changes in the power profile in order to avoid any problem in the electrical system. Thus, the Aggregator will provide the real time charging/discharging set points to each EVs in order to meet all the requirements.

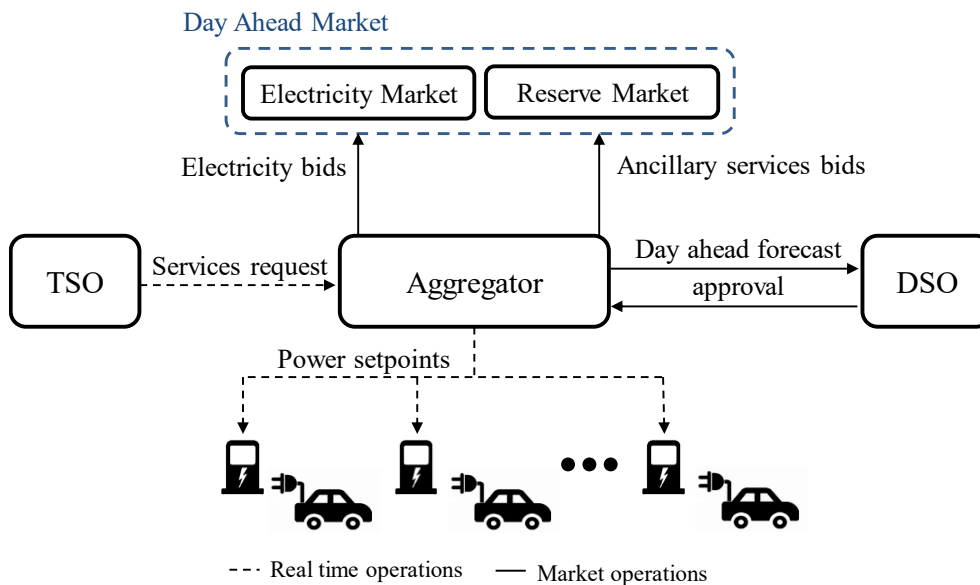


Figure 2.3 V2G Centralized Architecture

Several works in literature consider the Centralized control Architecture. The works in [73] and [74] aim to minimize the operational cost. In particular, the work in [73] focuses on the minimization of the power system cost, thus aims to minimize stationary and ramping operations of the generators. Meanwhile, the work in [74] minimizes the overall system cost including the cost for the charging/discharging operations.

Moreover, other objectives are pursued in literature. The work in [75] aims to avoid overloads of lines and transformers, thus improve the voltage profile through an intelligent charging algorithm. In [76] a minimization of power losses criteria is pursued. Meanwhile, [40] aims to maximize the load factor. Finally, some centralized approaches focus on minimizing the charging cost for the EV users, [77] and [78].

2.3.2 Decentralized Architecture

In a decentralized architecture, the EV users are assumed to have the full control of their EVs, thus interact with the grid individually through control signals or priced-based mechanism, Figure 2.4. This implies that some intelligence must be present on each vehicle. The working principle is similar to that previous discussed, but under certain grid constraint, in this case, each EV can autonomously try to optimize its cost of charge.

Within decentralized architecture, the Aggregator has the role of sending the control or price signals and constraint to each charger, then participate in the electricity market. However, it will not directly provide power set-points to the EVs. This architecture has the advantage of guarantee a higher privacy level for the users. However, its implementation can result complex due to communication overloads. Moreover, the Ancillary services activation can result slow or not efficient due to the absence of a centralized control.

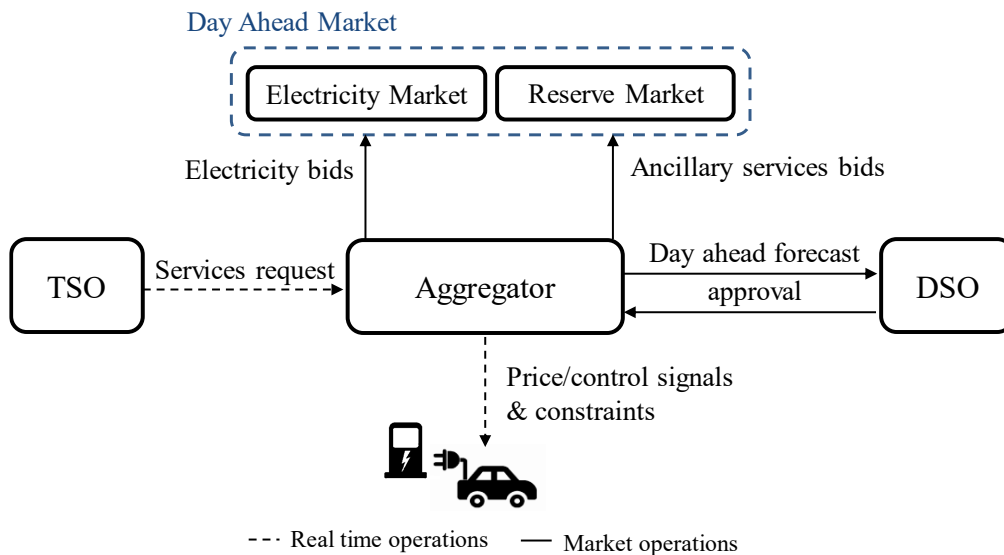


Figure 2.4 V2G Decentralized Architecture

The principal objective of Decentralized control Architecture is minimizing the charging cost for the EVs users. In this context, the work in [79] proposes an iterative algorithm that tries to fill the off peak hours. The EVs update their charging profile according to their own preference but also considering the control signal sent by the Aggregator. The work in [80], uses a decision making approach to encourage the EVs charge when the electricity price is low, thus minimizing the charging cost. Finally, [81] uses a multilevel optimization to achieve valley filling. In particular, at network level the objective is to minimize the overall generating cost, while at user level it is minimizing the charging cost.

2.3.3 Smart Charging Approaches on Vehicle to Grid

The Aggregator must participate in the Day-ahead electricity Market. This means that it must have the ability to schedule in advance the electricity market demand and the capacity availability for grid services. One of the main problems

of the EVs scheduling is its interdependency between periods. For example, the energy stored in the battery in a certain period depends on the decisions applied in previous periods, such as charging/discharging power or energy spent in trips [82]. Due to this complexity of the problem, Optimization or Hybrid Approaches are mostly used in literature. However, similarly to Section 2.2.1, the Optimization approach can be categorized in three principal methods basing on the use of the data and the uncertainty considered: Deterministic, Stochastic and Forecast based methods.

Deterministic Methods

The deterministic method assumes a priori or a fixed knowledge of EVs State of Charge, arrival and departure time. Within this frame, the work in [83] proposes a multi-objective optimization in order to minimize both the total cost of purchasing energy and the grid total losses. In [84] a dynamic programming optimization for a fleet charging is proposed also in order to minimize the overall charging cost. The Authors specify that their proposed method can be used in energy planning studies or integrated with hierarchical algorithms. The Authors of [85] discuss a case study of 25 parking spot used to resolve the grid violation caused by the renewable energy generation.

Finally, the work on [86] presents an hybrid approach, thus combines the optimization phase with a real time logic. Moreover, both centralized and decentralized architectures are compared. However, even in this latest case a deterministic knowledge of the EVs behaviour is considered, thus uncertainty is not addressed.

Stochastic Methods

Stochastic methods introduce a certain level of uncertainty to the problem formulation. The work in [87] introduces random uncertainty in the arrival State of Charge of the EVs basing on the survey on American Behavior in [88]. In particular, [87] integrates an optimization phase, aiming to reduce the total network cost, with a decision making heuristic approach to dispatch the power at real time. An improved EVs characterization can be found in [89] and [90] which use specific Probability Distribution Functions for the EVs trips based on a real survey.

Finally, the work in [91] conducts an optimization strategy aiming to optimize the load factor of an EV parking lot. In this case, uncertainty on State of Charge and arrival time is considered by adding a probability value on the objective function.

Forecast Based Methods

Forecast based method aims to run the optimization phase using estimation of the future behavior of the variables of the problem, such as electricity price, possible renewable energy generation and EVs behavior. The work in [92]

proposes a forecast model for the Day-ahead solar Energy and the electricity price. These forecasts are used to launch a Model Predictive Control optimization. However, regarding the EV behavior, it is assumed that the EV users set the departure time once their vehicle arrives at a parking lot. This can be a reasonable hypothesis for short term parking. However, a full forecast on EV behavior is not addressed.

Differently, the work in [93], in order to simplify the complexity of individual EV behavior forecasts, presents an Aggregated model to forecasts the aggregated charging demand of the EV fleet.

2.4 Proposed Approach and Novelty

This dissertation proposes two case studies, one for a Vehicle to Home application as extension of the work in [94], and the other for a Vehicle to Grid Application as extension of the work in [95]. In both cases the approach is hybrid and integrates the optimization level with a real time management. The method used for the optimization is based on the statistical forecasting of all the variables.

Moreover, a full smart charging is implemented, and battery degradation criteria are considered by adding proper constraints in the problem formulation. More in details, the V2H case study aims to maximize the self-consumption of the household, thus minimize the grid exchanges. Meanwhile, the objective of the V2G case study is to maximize the economic advantage obtainable from the EVs fleet.

The main advancements of the proposed work are:

- The proposal of a procedure to estimate the future behavior of the EVs individually, thus overcome the logic in [92] which depends on direct information provided by the EVs user. In particular the procedure is based on historical data of 214 EV usage patterns available in [96] covering three years (2013-2015). Each EV future behaviour (i.e., trip starting times, trip duration, trip energy consumption) is estimated assuming the statistical based logic discussed in Chapter 3.
- The use of real data in [96] to choose the types of users, thus substituting in this way the survey used as data source in [88].
- The fully use of a forecast statistical method for PV, loads and even EV profiles in coordination with a rule-based logic for the real time operations.
- The development of logics which fully consider real uncertainty, thus providing a reliable simulation of the reality.

Chapter 3

Individual EV Usage Forecasts

As discussed in Chapter 2, in order to assess a full optimal management of an EV battery, estimations of the future behaviours of the EVs are needed. This Chapter focuses on the methodologies proposed in order to achieve usage forecasts of each EV. Two different forecast logics are discussed in the following: Day-ahead and Infra-day forecasts. The forecast logics are based on the historical dataset available in [96]. Both logics have been compared with specific data among the dataset used as reference real scenarios. Thus, opportune errors indexes have been defined and calculated in order to provide a measure of the proposed methodologies performance. All the parts are developed in Matlab.

In the following, Section 3.1 describes the used vehicle dataset and explains the graphical representation of the EV usage scenario. Section 3.2 presents the Day-ahead Forecast logics and provides the relative results. Section 3.3 presents the Infra-day Forecast logic and provides the relative results. Finally, Section 3.4 concludes the chapter and discusses future possible improvements in individual EV usage forecasts.

3.1 Vehicle Dataset

The present work bases its analysis on a dataset of 214 EV usage patterns available in [96] covering three years (2013-2015). In particular, the study was conducted in Great Britain and was addressed by monitoring and measuring real EV travels of different users. The monitoring was possible thanks to Intelligent Control Box at chargers' level and telematic systems vehicle onboard installed. The database includes the departure and the arrival time, the distance, and the energy consumed for every travel occurred during the period of observation of each vehicle.

3.1.1 Vehicle Dataset Representation: Daily Usage Scenario

The data that regard travel information of a vehicle are of different natures. In fact, they include the time at which a certain trip starts and stops (thus provided as set of date and time), energies consumed for each trip, and distance in kilometres travelled for each trip. It follows, that in general the EV behaviour information cannot be represented as a unique continuous variable in time. However, the energy consumed from an Electric Vehicle among the time can be able to already provide a complete idea of the EV usage during a certain day. For example, when the car is parked its consumption is zero, while when the car is travelling a certain energy consumption arises.

In order to have an instrument as clear as possible to visualize the EV behaviour, this work proposes the graphical representation in Figure 3.1. The graph represents the usage during a day of the car j , with a granularity of 1-min (in the x-axis the hours are indicated with 24-hour clock system, in the following text both 24-h and 12-h clocks are used indistinctly). At the beginning of the day, the car is not moving, thus energy is not consumed by the vehicle (a part for neglected car ancillary services such as air conditioning or stereo which can consume energy even if the car is parked). Thus, the y-axis values are zero. At a certain minute the car starts its first trip. In this moment, the y-axis assumes the value of the total consumed energy of its first trip. This value is maintained until the trip ends. Follows, that each trip results represented by a bar. The height of the bar represents the energy consumption of the trip, while the thickness of the bar represents its duration in time.

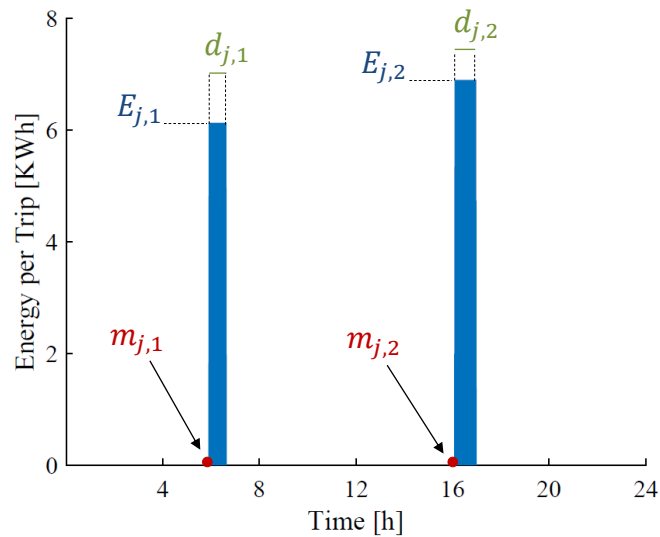


Figure 3.1 EV usage scenario representation

In the specific case of Figure 3.1, the first trip occurs at the minute 354 of the day which correspond at the 5:54 A.M., while the second (last trip) occurs at the minute 965 which correspond at the 4:05 P.M. The trip starting minutes are indicated with the variable $m_{j,z}$, where j identify the car, while z identify the number of trips during a day (i.e., first trip $z=1$, second trip $z=2$, etc.). Similarly,

the energy consumption per trip is indicated with the variables $E_{j,z}$ (in figure equal to 6,12 kWh and 6,9 kWh respectively). Finally, the trip durations are indicated with $d_{j,z}$ (in figure equal to 44 min and 54 min respectively).

3.2 Day-ahead Vehicle Forecasts

The Day-ahead vehicle forecast logic aims to provide a possible usage scenario of the next day. The main idea behind the logic resides in the fact that the days in the dataset may present systematic usages. For example, an EV's user who goes every working day in a certain job site with a precise scheduled time, will have a strong systematic usage during these days. The Day-ahead forecast returns the most probable EV behaviour according to the information in the dataset. Moreover, in order to capture at the best all the possible systematic behaviours, the logic operates a differentiation between the weekdays (e.g. it treats separately Mondays from Tuesdays from Wednesday etc.). The methodology through with the EV forecast behaviour is calculated is explained in detail in Section 3.2.1.

3.2.1 Day-ahead Vehicle Forecasts Methodology

Figure 3.2 shows a flowchart containing the routine used to estimate the use of the generic vehicle j in the next day. The day-ahead forecast routine can be divided in seven different steps indicated with capital letters from "A" to "G" (i.e., STEP#A, STEP#B, STEP#C, etc.).

- In STEP#A, the historical data are ordered and imported for each day of the week, i.e., all Mondays are selected and analysed.
- In STEP#B, all the Mondays included in the database are extracted and the number of trips per each Monday is calculated. For example, considering a 1-year database the total number of Mondays is 52, and therefore 52 numbers of trips are stored in a vector \mathbf{n}_{global} .
- In STEP#C it is defined the estimated future number of trips that will occur in the next Monday (\hat{n}), calculated as the statistical mode of the vector \mathbf{n}_{global} . The number \hat{n} is the first output of the procedure.
- In STEP#D, a subgroup N_{mode} is extracted: it is a matrix containing only the travel information of the Mondays with number of the trips corresponding to the statistical mode \hat{n} .

After the definition of the expected number of trips per day, it is necessary to estimate also the departure time, duration, and energy consumption of each future trip.

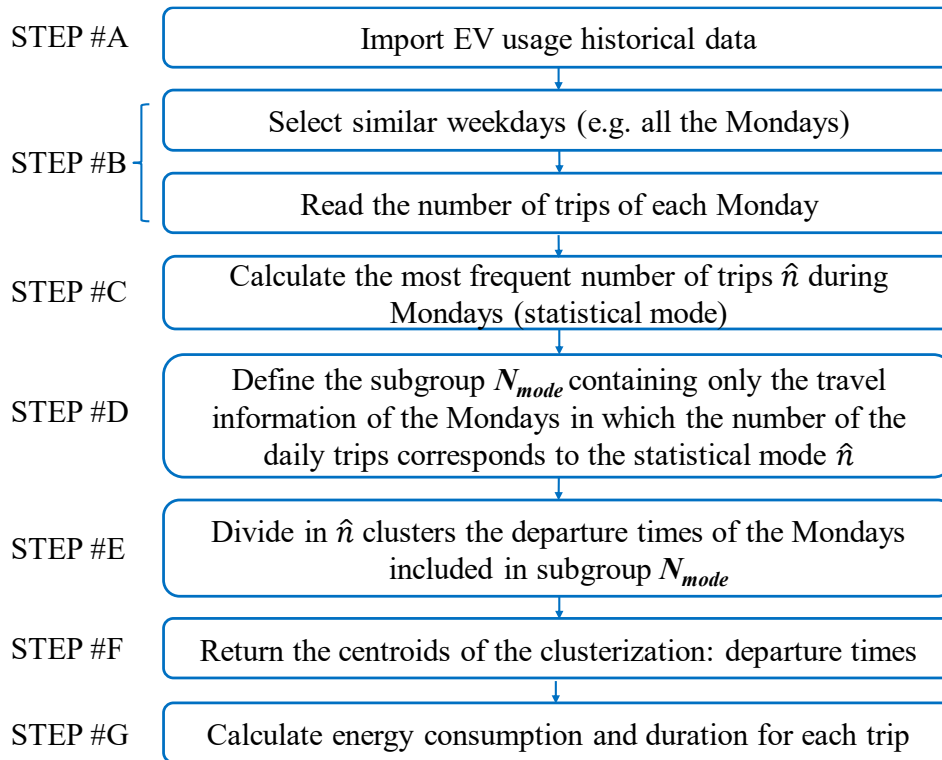


Figure 3.2 Day-ahead EV forecast routine

- STEP#E Identify \hat{n} number of clusters between the departure times in the dataset. Only the departure times m_j of the Mondays in the matrix N_{mode} is used for this operation. The clusterization is operated by k-medoids technique; this action is described more in detail in the next paragraphs.
- STEP#F provides the centroids (data that are centered with respect to the cluster), thus the most probable departure times (\hat{m}_j) for the next Monday as output of the procedure.
- Finally, in STEP#G, forecasted trip duration (\hat{d}_j) and energy consumption (\hat{E}_j) of each trip are calculated as the average values of all the trips occurring in a defined time-frame centered on the centroids \hat{m}_j . For example, $\hat{E}_{j,1}$ is calculated as average of all the energy consumptions of the trips occurred between $\hat{m}_{j,1}$ plus 40 min and $\hat{m}_{j,1}$ minus 40 min. Therefore, STEP#G concludes the scenario.

The same procedure is repeated for all the days of the week.

Clusterization of the Departure Times

Figure 3.3 aims to clarify the clusterization operation, thus the identification of the most probable trip departure times of the next Monday (STEP#E and STEP#F).

Figure 3.3-*a* shows the starting minutes of the trips occurred in the Mondays with 2 trips (Mondays with $\hat{n}=2$ in the subgroup *Nmode*). The trip starting minutes in figure are ordered according to their value (within the day between 0 and 1440). In the example in figure, thirty (30) starting minutes for as many trips are represented by grey circles positioned correspondingly to their values.

Figure 3.3-*b* shows the group (cluster) division of the starting minutes operated by k-medoids (STEP#E). The k-medoids technique is an algorithm which bases its action aiming to minimize the distance between the points labeled to be in a cluster and the point designed as the center of that cluster (centroids), [97][98]. However, k-medoids technique is not able to automatically decide the number of clusters that better represents the dataset; thus, this value must be given as input of the algorithm. More in details, the k-medoids algorithm operates an iteratively process:

- First, a predefined number of points are casually initialized as centroid, thus the distance of each other points is calculated in manner to be associated with the closer centroid (creation of the clusters).
- Second, a cost function of the configuration is calculated through the “Manhattan distance” in Equation (3.1).

$$Cost(p, \tilde{c}) = \sum_k^{nc} \sum_i^{np} |p_i - \tilde{c}_k| \quad (3.1)$$

In Equation (3.1), p_i indicates the generic point belonging to the same cluster of \tilde{c}_k assumed (in this configuration) as centroid, np indicates the number of the points in the considered cluster, while nc is the predefined number of clusters.

- Finally, the next iteration is operated by casually changing the chosen centroids, the costs of the different configuration are compared, thus the algorithm ends when lower configuration costs are not found.

In the example in Figure 3.3-*b* the predefined number of clusters is imposed to be equal to 2 ($\hat{n}=2$). In the first cluster, thirteen (13) starting minutes have been grouped which range in the values included between the 327th and 406th minute of the day (5:27 A.M. to 6:45 A.M.). In the second cluster, seventeen (17) starting minutes have been grouped which range in the values included between the 739th and 1108th minute of the day (12:19A.M. to 6:27 P.M.).

Finally, Figure 3.3-*c* highlights for each cluster the data point that is better centered with respect to its group and thus better represent its cluster. This data point is called centroid or medoid of the cluster. In STEP#F the centroids of the clusters are assumed as the forecasted starting minutes \hat{m}_j of the next Monday. In

the example in figure the centroid of the first cluster is found to correspond with the 398th minute of the day (6:38 A.M.). The centroid of the second cluster is found to correspond with the 987th minute of the day (4:27 P.M.).

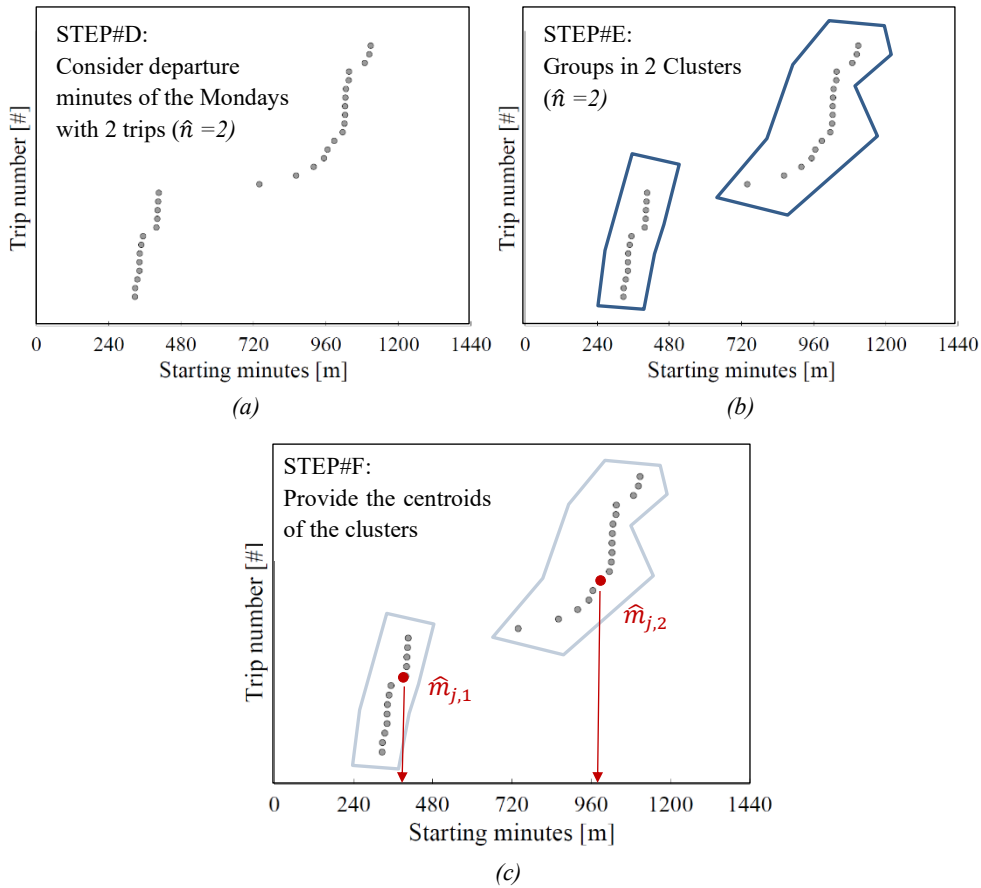


Figure 3.3 Clusterization operation - departure times estimation

3.2.2 Daily Forecast Errors

In order to measure of the performance of the EV usages forecasts, four different errors have been defined: Trip Consumption Error (TCE), Trip Starting-minutes Error (TSE), Trip Duration Error (TDE), and Total Error (TE). As it will be better discussed in Section 3.2.3, the errors are calculated with respect to the EV behaviour in specific days chosen among the dataset as real effective usages. The formulation of each error is discussed in the next paragraphs.

Trip Consumptions Error (TCE)

The Trip Consumption Error (*TCE*), is formulated in order to know how much the effective consumption of an EV at the end of the day differs from the one forecasted. The *TCE* is presented as a percentage error and is calculated by Equation (3.2).

$$TCE = \begin{cases} \frac{|E_j - \hat{E}_j|}{E_j} \cdot 100 = \frac{|\sum_z E_{j,z} - \sum_{\hat{z}} \hat{E}_{j,\hat{z}}|}{\sum_z E_{j,z}} \cdot 100, & \text{for } TCE < 100 \\ 100, & \text{for } TCE \geq 100 \end{cases} \quad (3.2)$$

In Equation (3.2), the variable E_j represents the consumption effectively achieved by the vehicle j at the end of the day. Meanwhile, \hat{E}_j is the forecasted total consumption of the car in that day. Therefore, TCE is the percentage deviation between the forecasted and the effective daily consumption of the car j . However, in order to be more precise, Equation (3.2) presents also another formulation of the error, by making explicit the variables E_j and \hat{E}_j . In fact, $E_{j,z}$ is the energy effectively consumed by the vehicle j during the trip z . The variable z assumes values between 1 and the number of trips (n) effectively occurred during the day. Meanwhile, $\hat{E}_{j,\hat{z}}$ represents the forecasted energy consumption of the forecasted trip \hat{z} . The variable \hat{z} assumes values between 1 and the forecasted number of trips of the day (\hat{n} , in general different from n).

Moreover, the value $|E_j - \hat{E}_j|$ in the numerator, can be in general higher than E_j at the denominator. This case would lead to errors higher than 100%. This happens when the result of the EV forecast is completely out of scale with respect to the effective daily consumption. In order to have an ease to read error, TCE is defined in order to lie always between 0% and 100%. Thus, higher errors are fixed to the maximum value 100% and the forecast, in this case, must be considered completely wrong.

Trip Starting-minutes Error (TSE)

The Starting-minutes Error (TSE), is formulated in order to quantify how much the forecasted scenario differs, in terms of number of trips and their positioning over a day, with respect to the effective scenario. The TSE is presented as a percentage error and is calculated by Equation (3.3).

$$TSE = \begin{cases} \frac{\sum_z |m_{j,z} - \hat{m}_{j,\hat{z}}|}{\sum_z m_{j,z}} \cdot 100, & \text{for } TSE < 100 \\ 100, & \text{for } TSE \geq 100 \end{cases} \quad (3.3)$$

In Equation (3.3), the variable $m_{j,z}$ is the effective starting-minute of the trip z for the j vehicle. Meanwhile, $\hat{m}_{j,\hat{z}}$ is the starting-minute of the forecasted trip which is closer to $m_{j,z}$. The variables $m_{j,z}$ and $\hat{m}_{j,\hat{z}}$ lie between 0 and 1440 (number of minutes in a day). For example, if a car during a day accomplishes two trips one at 6:00A.M. and one at 5:00P.M. the corresponding effective real starting minutes are 360 and 1020. Considering now, that the EV forecast has returned two trips occurring at the minutes 400 and 990; TSE will be the sum of the differences 400-360 min (40 min) and 990-1020 min (30 min) in absolute value, under the total real minutes sum (i.e., 1380 calculated as sum of 360 and 1020).

Moreover, for sake of clarity and simplicity, Equation (3.3) reports the case in which the number of trips effectively travelled n correspond to with the forecasted one \hat{n} . However, if the forecasted number of trips is higher than the real one ($\hat{n} > n$) a fixed error of 1080 min is added to the formulation.

Finally, even in this case, errors can be in general higher than 100%. Thus, *TSE* is defined in order to lie always between 0% and 100%.

Trip Durations Error (TDE)

The Trip Duration error (*TDE*), is formulated in order to quantify the difference between the forecasted time spent for trips and the effective one. The *TDE* is presented as a percentage error and is calculated by Equation (3.4).

$$TDE = \begin{cases} \frac{|\sum_z^n d_{j,z} - \sum_{\hat{z}}^{\hat{n}} \hat{d}_{j,\hat{z}}|}{\sum_z d_{j,z}} \cdot 100, & \text{for } TDE < 100 \\ 100, & \text{for } TDE \geq 100 \end{cases} \quad (3.4)$$

In Equation (3.4), The variable $d_{j,z}$ represents the effective duration of the trip z travelled by the vehicle j . Meanwhile, $\hat{d}_{j,\hat{z}}$ is the duration of the relative forecasted trip \hat{z} . It follows, that *TDE* is the percentage deviation between the forecasted and the effective daily time spent during trips. Finally, *TDE* is defined in order to lie always between 0% and 100%.

Total Error (TE)

The above defined errors (i.e., *TCE*, *TSE*, and *TDE*) are useful to analyse the errors in trip consumption, trip starting-minutes, and trip durations, individually. In order to have an error which synthesizes the Total performance of the EV forecast routine, the Total Error (*TE*) is formulated. The *TE* is presented as weighted average of the three above defined errors. The Total Error is calculated as in Equation (3.5), where the variables α , β , and γ represents the weighted values for *TCE*, *TSE*, and *TDE* respectively. For the calculation of *TE* the weighted values have been fixed equal to 0.3, 0.6, and 0.1 respectively. These values have been chosen by graphically comparing many EV forecasts among the dataset.

$$TE = \frac{\alpha \cdot TCE_j + \beta \cdot TSE_j + \gamma \cdot TDE_j}{(\alpha + \beta + \gamma)} \quad (3.5)$$

3.2.3 Day-ahead Forecast Results

In order to test the logic, during the forecast operations the last day of usage of each vehicle (e.g. remove all last Mondays, remove all last Tuesdays etc) is removed from the dataset. The objective of this operation is of course using the last days as current real use in order to compare the results. In the following, the real uses will be represented in blue, while the forecasted scenarios in red.

EV Forecasted Scenarios

As explained in Section 3.1, the used dataset includes the information of 214 real life EV's uses. This would result in 214 Day-ahead forecasted scenarios for each weekday. Therefore, in order to provide a graphical representation of the results, thus a tangible picture of the forecasts performance, here are treated the forecasted scenarios of the first 10 vehicles of the dataset are treated.

Figure 3.4-(a to d) represents the real uses (in blue) and the forecasted usages (in red) respectively for the vehicles from 1 to 10, respectively. In this phase only Mondays are considered. Table 3.1 lists the daily forecast errors which permit to quantify the goodness of the outputs.

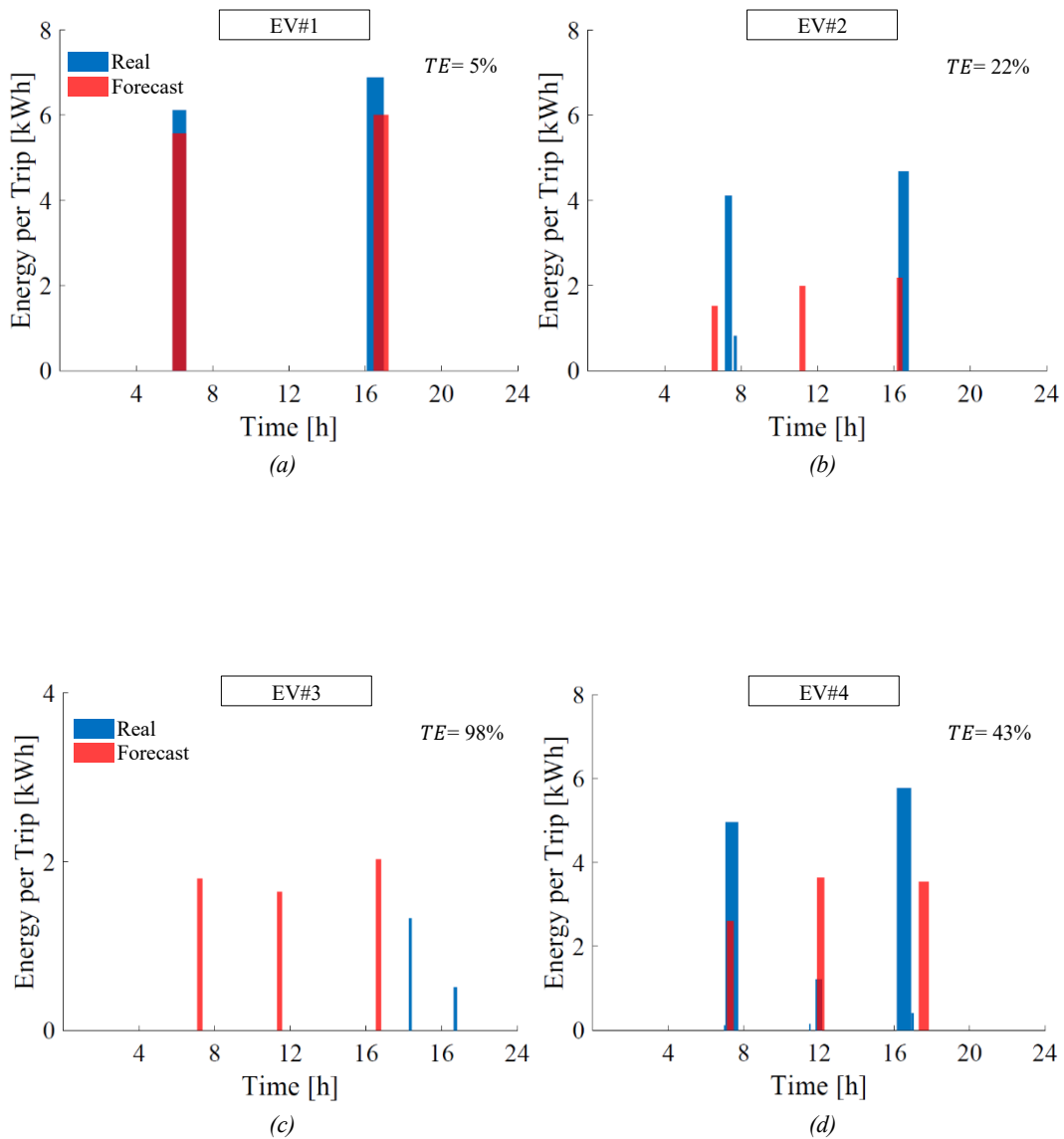


Figure 3.4-(a to d) Day-ahead EV forecasts: EV#1 - EV#4

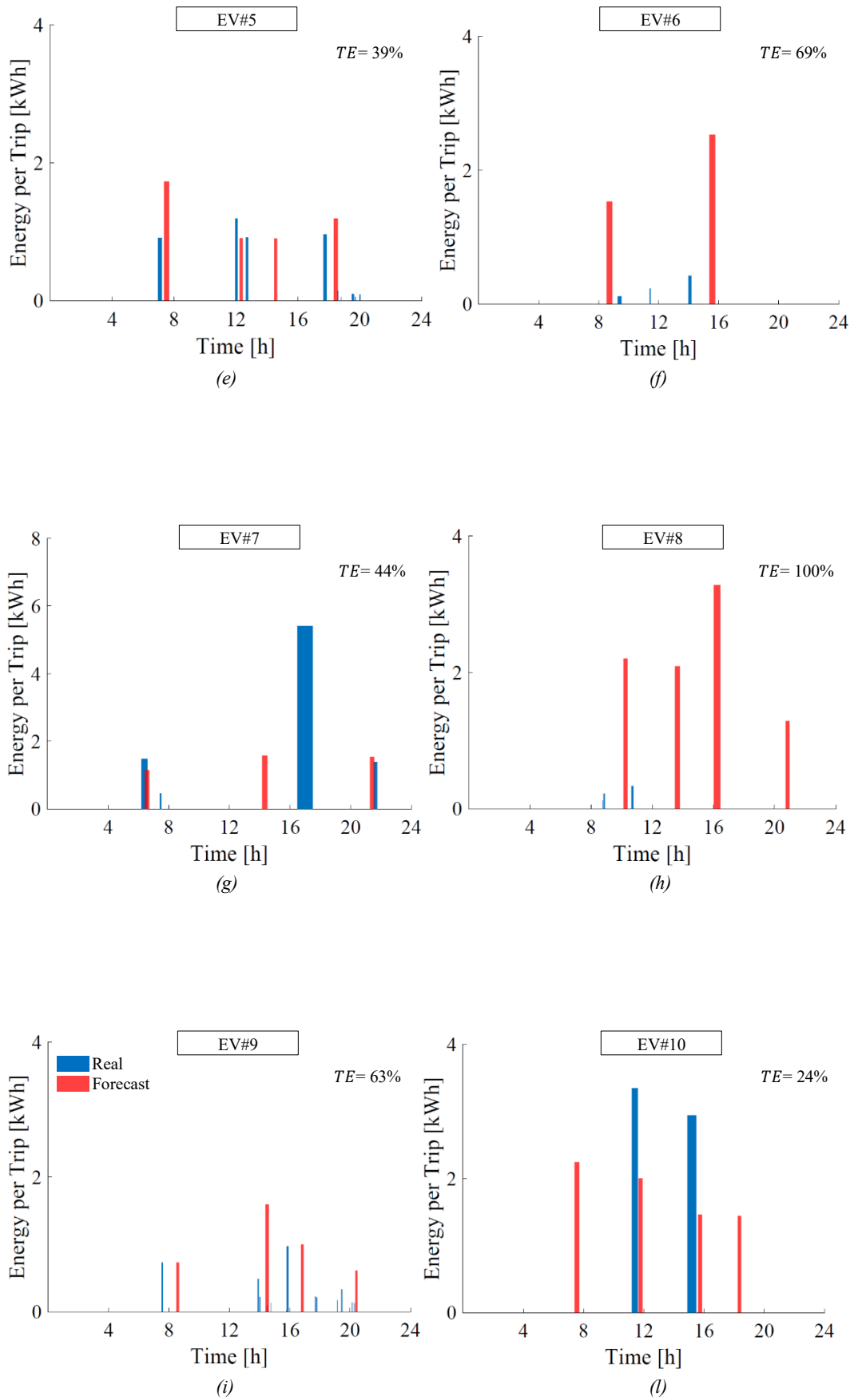


Figure 3.4-(e to l) Day-ahead EV forecasts: EV#5 - EV#10

Table 3.1 Daily Forecasts Errors with respect to last Mondays

	<i>Monday</i>			
	<i>TCE</i> [%]	<i>TSE</i> [%]	<i>TDE</i> [%]	<i>TE</i> [%]
EV#1	11	2	7	5
EV#2	41	14	16	22
EV#3	100	97	100	98
EV#4	13	63	13	43
EV#5	1	62	14	39
EV#6	100	58	44	69
EV#7	51	40	49	44
EV#8	100	100	100	100
EV#9	26	86	32	63
EV#10	14	32	3	24

From Table 3.1 can be seen that the best performance, thus the minor error in the forecasts is achieved for EV#1. In this case in fact, the Total Error TE (given by the weighted average of TCE , TSE , and TDE), is equal to 5 %. A particularly small error is observed for the forecasted trip Starting minutes ($TSE = 2\%$), while forecast Trip Consumptions (TCE) and Trip Durations (TDE) errors values 11% and 7%, respectively. These results are well visible in Figure 3.4-*a*, where it can be seen that the forecasted scenario with its two trips (occurring at the 5:55 A.M. and at the 4:27 P.M. respectively), almost overlaps the current Monday EV's use (5:54 A.M and 16:05 P.M.). Meanwhile energy consumption of the trips presents, in this case, a moderated underestimation (especially for the second trip of the day). These results suggest a strong systematic usage of the EV#1

The worst forecasts have been achieved for EV#3 and EV#8 where errors around or higher the 100% have been found. Even for these cases Figure 3.4-(*c* and *h*) well represents the situation. For EV#3 the forecast has returned a usage scenario with three trips occurring between the 7:05 A.M. and the 4:32 P.M., while the actual scenario presents two trips occurring at the 6:16 P.M. and at the 8:38 P.M. Meanwhile, the energy consumption during the day was estimated to be more than double with respect to the real one. The case of EV#8 is even worst with four trips estimated instead of two and an estimated daily energy consumption much higher than the current Monday's one. The results of EV#3 and EV#8 suggest a strongly irregular usage of these EVs. Finally, the Monday's forecasts of the other vehicles range between 22% (EV#2) and 69% (EV#6) as Total Errors.

Table 3.2 reports the daily Total Errors during a week for the considered 10 vehicles considered (e.g. $TE_{Mon.}$, $TE_{Tue.}$, etc.). Moreover, in order to have an evaluation of the forecasts on a week basis, the average between the seven weekdays errors is listed for each vehicle ($\overline{TE_{week}}$).

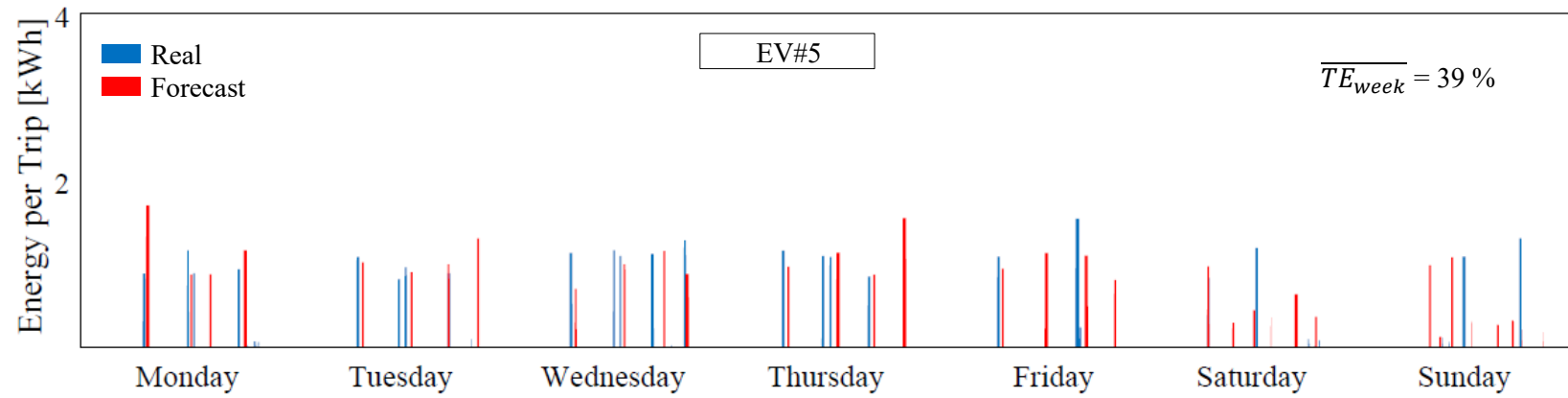
The vehicle with the minimum error on the week basis is EV#5 with an average of 39%. More in detail, EV#5 presents moderate Total Errors for the working days (ranging between 25% and 39 % from Monday to Friday), while a remarkable error of 71 % on Sunday. This result is of course explicable with the typical uncertainty of the feast days.

The vehicle with the maximum error on the week basis is EV#6 with an average of 79%. In two cases (for Wednesday and Saturday) the Total Error was around or higher than 100%, while in the other days the error ranges between 57% and 83%. The other vehicles display an averaged total error in the week between 42% (EV#10) and 75% (EV#9). The best result on a day basis is still the Monday of EV#1 with just 5% as TE . Meanwhile the 100% TE occurs seven times among the presented 70 cases (10% of the considered sample).

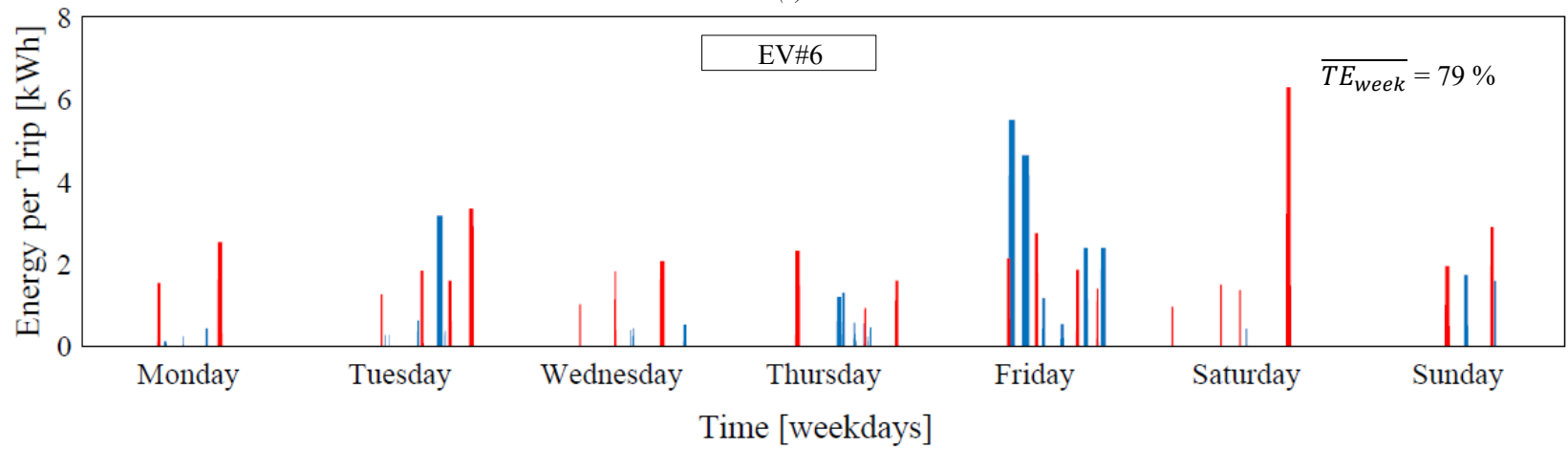
Table 3.2 Daily Forecasts Errors per weekdays

	$TE_{Mon.}$ [%]	$TE_{Tue.}$ [%]	$TE_{Wed.}$ [%]	$TE_{Thu.}$ [%]	$TE_{Fri.}$ [%]	$TE_{Sat.}$ [%]	$TE_{Sun.}$ [%]	$\overline{TE_{week}}$ [%]
EV#1	5	42	85	57	53	64	68	53
EV#2	22	100	53	73	67	87	50	65
EV#3	98	99	59	48	94	23	70	70
EV#4	43	64	31	69	24	39	100	53
EV#5	39	27	38	32	25	42	71	39
EV#6	69	83	100	64	79	100	57	79
EV#7	44	70	58	63	65	78	73	65
EV#8	100	83	66	92	51	26	30	64
EV#9	63	56	63	58	100	81	100	75
EV#10	24	55	31	69	66	43	6	42

Figure 3.5 shows the forecasted scenario and the real EVs use during all the week for the vehicles EV#5 (smaller $\overline{TE_{week}}$) and EV#6 (higher $\overline{TE_{week}}$) respectively. From Figure 3.5-a it is evident a certain regularity of the EV use during the week. In Figure 3.5-b the framework is much more irregular, especially for the day of Friday, characterized by a much different usage scenario with respect to the other days of the week.



(a)



(b)

Figure 3.5 Entire week forecasts: EV#5 (a) - EV#6 (b)

Global Performance of the Day-ahead Forecasts

In order to provide a measurement of the overall performance of the Day-ahead forecasts, the daily forecast errors have been calculated for all the 214 EVs in the dataset, considering for each vehicle its last weekday as current real use.

Table 3.3 lists the averages of these 214 forecasts errors for the different weekdays (e.g. the average of the 214 TCE s is indicated with \overline{TCE}_{EV} , the average on TSE s with \overline{TSE}_{EV} , etc.). According to the defined errors the results show a global reliability of the logic around 50%. As expected, significantly larger Total Errors are obtained in the weekend due to the typical uncertainty of the EVs usages in these days. More in details, it can be observed that the days between Monday and Thursday range between 47% and 50% as \overline{TE}_{EV} , while from Friday to Sunday the Total Error goes to 52%, 54% and 58% respectively. Finally, slightly lower values of \overline{TDE}_{EV} with respect to \overline{TCE}_{EV} and \overline{TSE}_{EV} are revealed from the analysis.

Table 3.3 Daily Forecasted Errors averaged across all the EVs in the dataset

	\overline{TCE}_{EV} [%]	\overline{TSE}_{EV} [%]	\overline{TDE}_{EV} [%]	\overline{TE}_{EV} [%]
Monday	48	50	46	49
Tuesday	47	48	42	47
Wednesday	51	47	46	48
Thursday	49	52	44	50
Friday	50	54	48	52
Saturday	53	56	49	54
Sunday	60	57	56	58

The values reported in Table 3.3 are averages which consider the entire dataset of vehicles. Thus, as already revealed by the analysis on the different weekdays, the forecasts will return better results (minor errors) when the EV user behaviour is more systematic, while worse results are expected when the EV user has irregular habits. Moreover, in order to fully understand the values in Table 3.3, it worth to notice that the Trip Consumption Error TCE is referred to the real daily consumption of a vehicle. However, as discussed in Section 2.1, this amount of energy corresponds, on average, only to the 20-30% of the total battery capacity. Referring the Trip Consumption Error to the total battery capacity can be useful from an Aggregator point of view which needs to schedule in advance the energy required from its fleet for safety and market reasons.

Table 3.4 reports the Trip Consumption Errors referred to the total battery capacity thus the relative impact on the Total Error averaged for the 214 EVs per each weekday. In this case a relevant reduction from an average of 50% to 30% for the \overline{TCE}_{EV} can be seen, while the \overline{TE}_{EV} lies now around 44%. Furthermore, some specific applications may require different choices of the weighed coefficients α , β , and γ defined in Section 3.2.2 ($\alpha=0.3$; $\beta=0.6$; $\gamma=0.1$).

Table 3.4 Normalization on EV Battery Capacity: Effect on Errors

	Mon.	Tue.	Wed.	Thu.	Fri.	Sat.	Sun.
\overline{TCE}_{EV} [%]	26	25	31	31	26	31	36
\overline{TE}_{EV} [%]	42	41	42	45	45	48	51

In this context a higher value of α will lead to a lower Total Error. Table 3.5 presents three others possible combination of the weighted coefficients with a higher value of α , thus shows the relative impact on the Total Error \overline{TE}_{EV} . As expected, the lowest results are found for the last presented combination (highest α) with a \overline{TE}_{EV} which lies around the 34% of Tuesday and 45% of Sunday.

Table 3.5 Different weights: Effect on Total Error

Weights			\overline{TE}_{EV} [%]						
α	β	γ	Mon.	Tue.	Wed.	Thu.	Fri.	Sat.	Sun.
0.4	0.5	0.1	40	39	42	44	42	47	48
0.5	0.4	0.1	38	37	40	42	40	44	46
0.6	0.3	0.1	36	34	38	39	38	42	45

3.3 Infra-day Vehicle forecasts

In order to obtain more accurate estimations of the behaviour of a vehicle in next future hours, it is possible to exploit information coming directly from the usage of the car in the last few hours. This led to a certain number of Infra-day forecasts with the purpose to adjust and possibly improve the precedent day-ahead estimation. The main idea behind Infra-day forecasts resides in the fact that the Mondays in the dataset may present more than one systematic usage.

For example, an EV's user could stock in his dataset a certain number of Mondays in which he moved toward the job site #A, and a certain number of Mondays in which he moved toward the job site #B. Therefore, two systematic scenarios exist in the dataset, each with own typical trip starting-times, energy consumptions and durations. In this latest case, the day-ahead forecast would return just the most probable between scenario #A and scenario #B. Meanwhile, infra-day forecasts may be able to discern the case of the current Monday by "observing" the EV behaviour during the day.

3.3.1 Infra-day Vehicle Forecasts Methodology

The infra-day vehicle forecast logic is based on the methodology described at the Section 3.2.1. However, the forecast is now recalculated at every iteration step p of the logic.

Figure 3.6 shows the working principle at the different p iterations. In particular, the daytime is divided in twelve iterations separated each other by 2h (p assumes the value between 0 and 11). For each iteration the forecast of the

entire day is calculated. For example, at the first iteration ($p=1$), which occurs at the 2:00 A.M. ($t^*=2$) of the current Monday, the forecast of all the day (from h:0:00 to h:24:00) is returned. For the next 2h (from 2:00 to 4:00 A.M.) the result of the first iteration is considered to estimate the EV behaviour. At the 4:00 A.M. ($t^*=4$), the second iteration occurs with another forecast and the previous is substituted. This is repeated for all iterations until $p=11$ which occurs at $t^*=22$. From the above described procedure, follows that the complete effectively applied forecast is given by the union of the considered portions of the respective iterations, as shown in Figure 3.6.

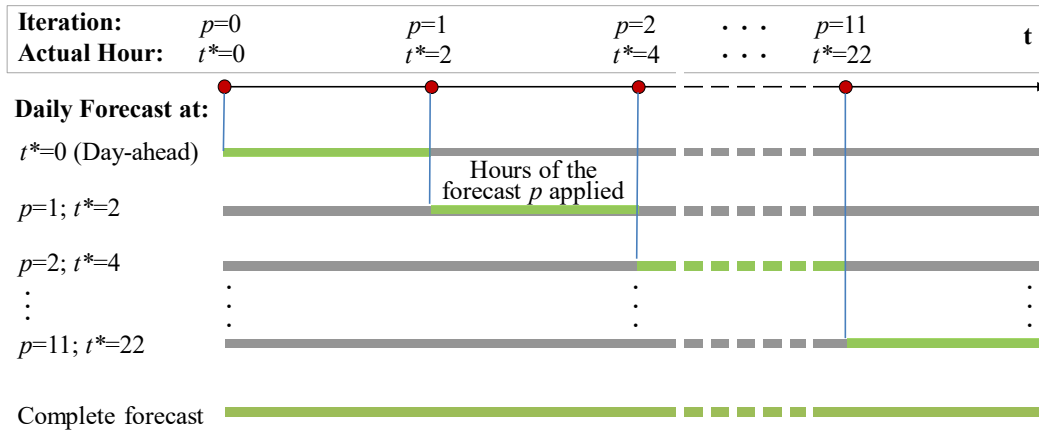


Figure 3.6 Infra-day EV forecast working principle

Figure 3.7 shows the flowchart of the infra-day forecast routine for a fixed iteration p . The Infra-day forecast routine can be divided in six different steps indicated with the lowercase letters from “a” to “f” (i.e., Step #a, Step #b, Step #c, etc.).

- In Step #a, the logic reads the number of trips n_{2p} occurred in the last $2p$ hours of the current day (i.e. Monday). Contemporarily it reads the number of trips. in the last $2p$ hours per each Monday on the dataset of the vehicle to forecast. For example, for $p=1$ the number of trips occurred between midnight and the 2:00 A.M. is read; for $p=2$, the number of trips occurred between midnight and the 4:00 A.M. is read, etc.
- In Step #b, the numbers of trips n_{2p} are compared with the Mondays in the dataset and the subgroup N_{2p} is defined: only the Mondays with the same number of trips in the last $2p$ hours are stored. For example, if in the current Monday one trip is travelled between midnight and 2:00 A.M., N_{2p} will contain all and only the Mondays in which one trip was travelled between midnight and 2:00 A.M.
- In Step #c, the departure times of the Mondays included in the subgroup N_{2p} is clusterized by k-medoids as described in Section

3.2.1. As for the day-ahead forecast, the number of clusters is chosen accordingly with the statistical mode \hat{n} which represents the estimated number of trips during all the day.

- In Step #d, the centroids are provided and assumed as trip starting minutes of the forecast at the iteration p .
- In Step #e, trip duration and energy consumption of each trip are calculated as the average values considering all the trips occurring in a defined timeframe centred on the centroids.
- In Step #f, the number of iterations is updated, and the logic is forced to circle back to Step #a.

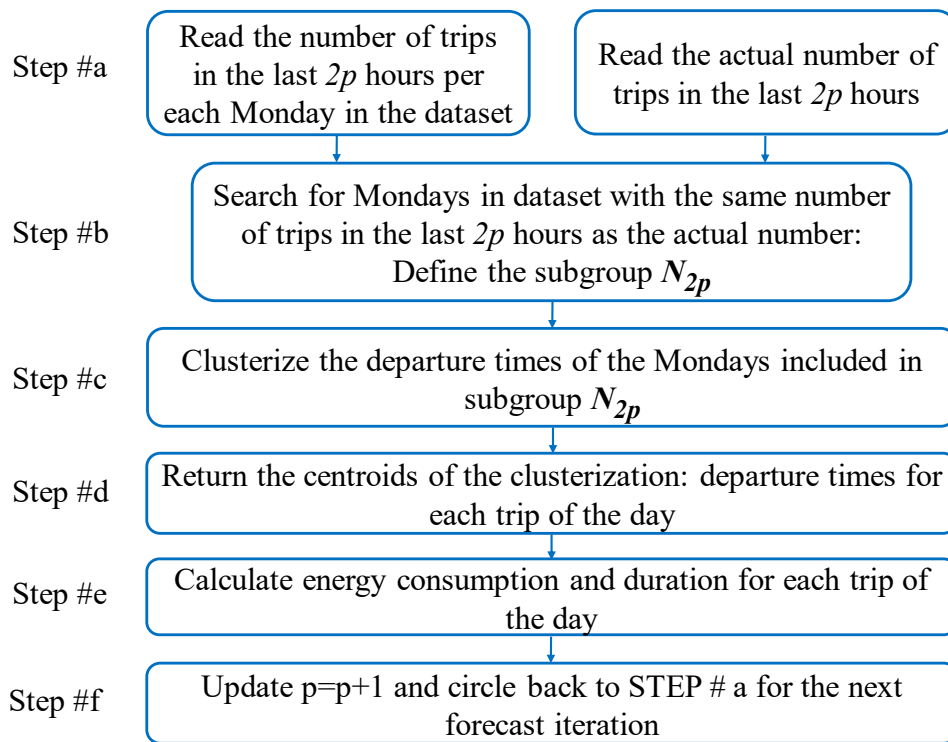


Figure 3.7 Infra-day EV forecast routine

3.3.2 Infra-day Vehicle Forecast Results

Figure 3.8-(a to n) shows iteration by iteration the Infra-day vehicle forecast results during the last Monday of EV#3. As explained in Section 3.3.1, at each iteration the infra-day logic calculates a forecast of the entire day.

At midnight ($t^*=0$) all the Mondays in the vehicle's dataset are used to estimate its future behaviour, thus, as expected, the forecast corresponds to the one calculated from the Day-ahead forecast logic. This forecasted scenario remains the most probable even for the first and second iterations which occur at 2:00 A.M. and 4:00 A.M. respectively, as shown from Figure 3.8-(a to c).

At $t^*=6$, EV#3 has not yet travelled any trip; only the Mondays in the vehicle's dataset with no trips between midnight and 6:00 A.M. are saved in N_{2p} and considered for this iteration. Therefore, some Mondays of the vehicle's dataset are excluded from the calculation and the returned forecasted scenario changes, Figure 3.8-d.

At 12:00 the car was still not moved; the subgroup N_{2p} is again updated to contain, according with the iteration, the Mondays with no trips between midnight to 08:00 A.M. ($p=4$), midnight to 10:00 A.M. ($p=5$), and midnight to 12:00 A.M. ($p=6$). It Follows that the forecasted scenario changes at each iteration for the fourth, fifth and sixth respectively, as shown in Figure 3.8-(e to g).

From the sixth iteration ahead, the forecasted scenario does not change anymore. It consists, in a single forecasted trip occurring at 5:57 P.M. with an energy consumption of almost 3kWh. The real trips of the current Monday will occur at 06:16 P.M. and at 08:38 P.M. with energy consumptions of 1330 Wh and 500 Wh respectively, Figure 3.8-(h to n).

Figure 3.9 shows the complete applied forecast from the infra-day logic. In this specific case it corresponds to the forecasts of the last iterations.

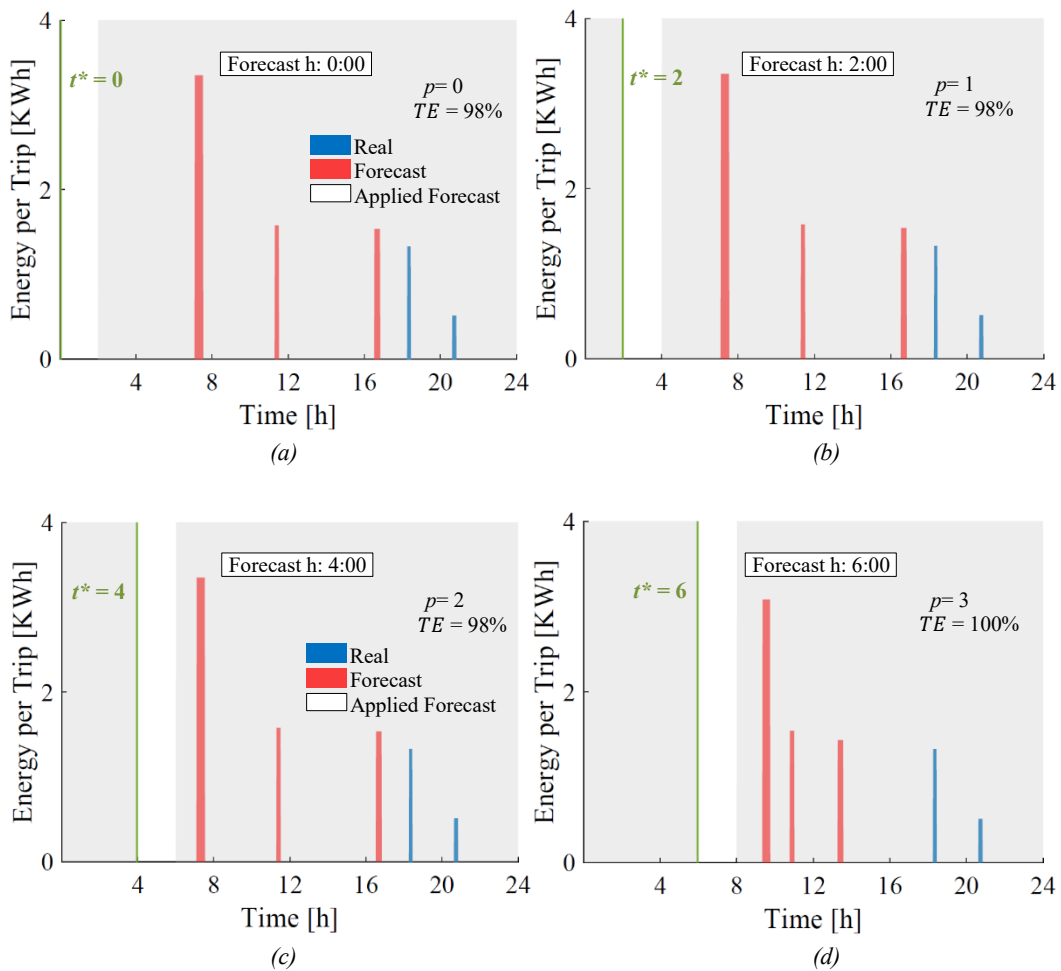


Figure 3.8-(a to d) Infra-day EV#3 forecasts: iterations 0-3

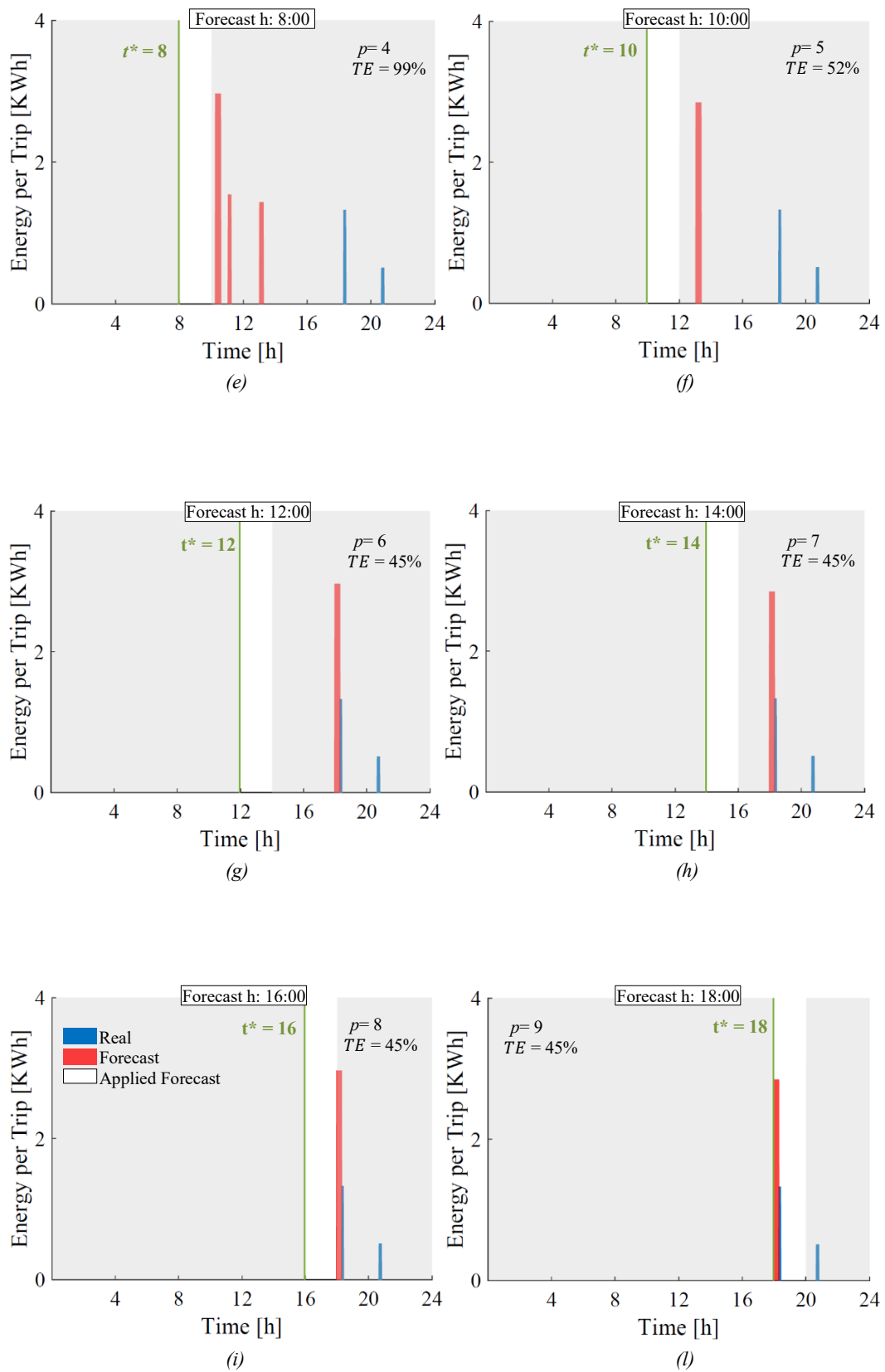


Figure 3.8-(e to l) Infra-day EV#3 forecasts: iterations 4-9

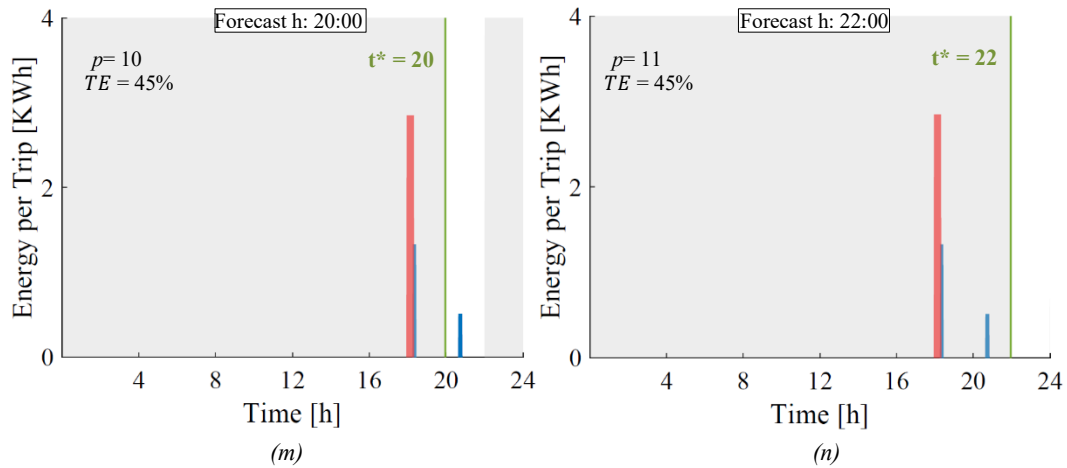


Figure 3.8-(m to n) Infra-day EV#3 forecasts: iterations 10-11

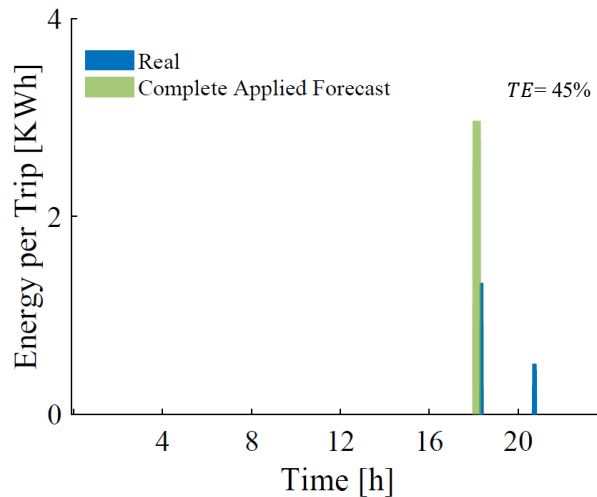


Figure 3.9 Complete Applied Forecast at the end of the day

Table 3.6 reports the Daily Forecast Errors for each iteration of the infra-day forecast. As above mentioned, at each iteration the infra-day forecast logic calculates a forecast of the entire day. Thus, the performance of the forecast at each iteration can be measured by the Daily Forecast Errors with respect to the unique real scenario. From Table 3.6 it can be seen that, a part for iterations $p=3$ and $p=4$ ($t^*=6$ and $t^*=8$), the iterations brings to lower errors values. In particular, TE goes from the 98% of the day ahead forecast ($t^*=0$) to the 45% from $t^*=12$ ahead. Thus, remarkable reduction in all the errors TCE , TSE , and TDE among the day are achieved.

Table 3.6 Daily Forecast Errors for each infra-day forecast iteration

	EV#3											
t^*	0	2	4	6	8	10	12	14	16	18	20	22
<i>TCE</i> [%]	100	100	100	100	100	55	55	55	55	55	55	55
<i>TSE</i> [%]	97	97	97	100	99	60	47	47	47	47	47	47
<i>TDE</i> [%]	100	100	100	100	100	2	2	2	2	2	2	2
<i>TE</i> [%]	98	98	98	100	99	52	45	45	45	45	45	45

It should be noted, that in general the complete final applied forecast is different from all the forecasts of the iterations occurred during the day. This because, the complete final applied forecast is in general created by the different portion of the forecasts at previous iterations. However, in the specific case of EV#3 analysed, it corresponds exactly with the forecasts at the last' iterations. In order to make clear the final effective performance of the infra-day logic for EV#3, Table 3.7 again reports the final daily errors.

Table 3.7 Daily Forecast Errors of the Complete Applied Forecast

	<i>TCE</i> [%]	<i>TSE</i> [%]	<i>TDE</i> [%]	<i>TE</i> [%]
EV3	55	47	2	45

Finally, Table 3.8 compares the final results on the Infra-day logic with the ones achieved by the Day-ahead logic for the considered 10 vehicles considered. The infra-day logic leads to a consistent Forecast error reducing compared to the day-ahead logic for seven case under ten. On the other hand, in the remain three cases, day-ahead and infra-day logics return the same results. The greater error reducing, thus the higher forecast relative improving, is 58% achieved for EV#10 which goes from 24% *TE* using day-ahead forecast to 10% *TE* using infra-day forecasts. Finally, the case of EV#3 above discussed, shows a relative 54% error reducing.

Table 3.8 Day-ahead and Infra-day forecasts results comparison

	<i>TE</i> [%]	<i>TE</i> [%]	Improving [% _{rel}]
Used Logic	Day-ahead	Infra-day	
EV#1	5	5	-
EV#2	22	22	-
EV#3	98	45	54
EV#4	43	43	-
EV#5	39	26	33
EV#6	69	42	39
EV#7	44	27	39
EV#8	100	84	16
EV#9	63	41	35
EV#10	24	10	58

3.4 Future Works on EV Forecasts

This Chapter has discussed the proposed methodologies used to forecast the individual behaviour of an EV. In particular, two logics have been proposed: one for Day-ahead forecasts and the other for infra-day forecasts

The logics rely exclusively on individual EV historical data, however other information could be integrated for future improvements. Such information, can be provided directly from the EV's users (regarding their travels) or provided from internet (e.g., weather data, public transport strikes, viability etc.) in order to implement a more sophisticated algorithm able to better ponder and catch the EV usage systematicities.

Moreover, the here presented logics are not retroactive (even if the infra-day logic implements some comparison with the real scenario). Thus, are not able to adjust themselves basing on an error or a quality index check. In future, this could be another aspect in which to work on. Finally, due to the complexity that would have arisen from the use of infra-day forecasts, the methodologies presented in the next chapters are tested by using only Day-ahead forecasts.

Chapter 4

EV and PV Integration: A Vehicle to Home Case Study

The installation cost of renewable systems, especially Photovoltaic (PV) generators faced a drop in the last years [99]. Thus, in many countries, the local electricity production is more cost-effective than the absorption from the grid [25]. More in details, the economic benefit of local electricity production increases if the PV generation and the local consumption are well matched. In other words, if the self-consumption of a locality is high. Moreover, a good match between local generation and local consumption presents positive effects on the power quality, safety of the distribution system, and as last instance the overall efficiency of the electrical system [6]. As discussed in Section 2.1, the EV batteries can be able to improve this match if a Smart Storage Management is adopted to integrate local renewable generation and loads with Electric vehicles. Finally, this subject becomes even more attractive considering the expected growth of EV sales in the next years.

This Chapter proposes a methodology to integrate an EV with a PV powered Household. It coordinates an optimization phase with a real time management. The main objective of the methodology is to maximize the achievable self-consumption of the household. In this process the Day-ahead EV forecasts, described in Section 3.2, are used to improve the performance of the logic. The results of the proposed methodology are compared with a pure heuristic rule - based logic which does not make use of EV forecasts or optimization. All the simulations are carried out in Matlab.

In the following, Section 4.1 describes in details the used physical model of the household. Section 4.2 describes the battery control algorithms for both the proposed logic and the pure heuristic rule-based logic (in the following simple rule-based Logic). Section 4.3 discusses the results. Finally, Section 4.4 concludes the chapter and discusses possible future improvements the work.

4.1 Household Model

The analysis in this Chapter refers to the model in Figure 4.1. It includes a PV generator, residential loads, and an Electric Vehicle. The EV battery is charged by a charging station, and it can work both as a controllable load (i.e., it can be charged by the PV generator or the grid), or as controllable generator, (i.e., it can discharge to supply local loads). The PV generator is connected to the local AC bus through a DC/AC converter. The model also considers a Smart Storage Management which has the role of monitoring and control the household system in order to optimal dispatch the power flows toward and from the EV battery. Finally, no other storage systems exist, and thus, if the PV production is higher than the load and the car is not at home, the surplus is injected into the grid. In the following is discussed more in details the way through each part of the household system is modelled.

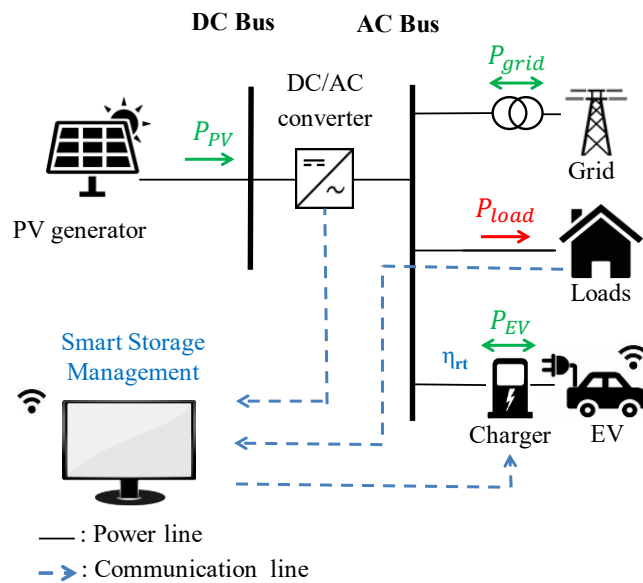


Figure 4.1 Scheme of the household model

4.1.1 Photovoltaic Power Profiles

The photovoltaic power profile represents the operation of the PV plant in the household. It is based on real PV production data (resolution 1-min). The data are related to a roof-mounted 6kWp PV generator located close to Turin - Italy (inclination 15° , azimuth 90° West, latitude $45^\circ 04'$, longitude $7^\circ 41'$). The monitoring was carried out during 2016, therefore it was possible a statistical examination in order to choose the most representing week for each season. In particular, the four weeks chosen from the dataset are: the fourth week of January, the first week of May, the third week of July, and the second week of October. Finally, in order to consider also the effect of the EV integration, the data have been scaled by ϵ_{to} to obtain an equivalent 9 kWp power plant.

Figure 4.2 shows the PV production profiles along the four targeted weeks. Meanwhile, Table 4.1 reports the total generation for each week (indicated with E_{PVweek}), and the percentage of sunlight hours with respect to the total hours ($PV/24h$). This latest parameter represents the percentage of time in which the PV plant is producing, obviously it changes for the different seasons. The week with higher production is the week of July which correspond also to the case with higher sunlight hours percentage. On the other hand, the week with less generation is the week of October even though the poorest light hours percentage is found in the January week.

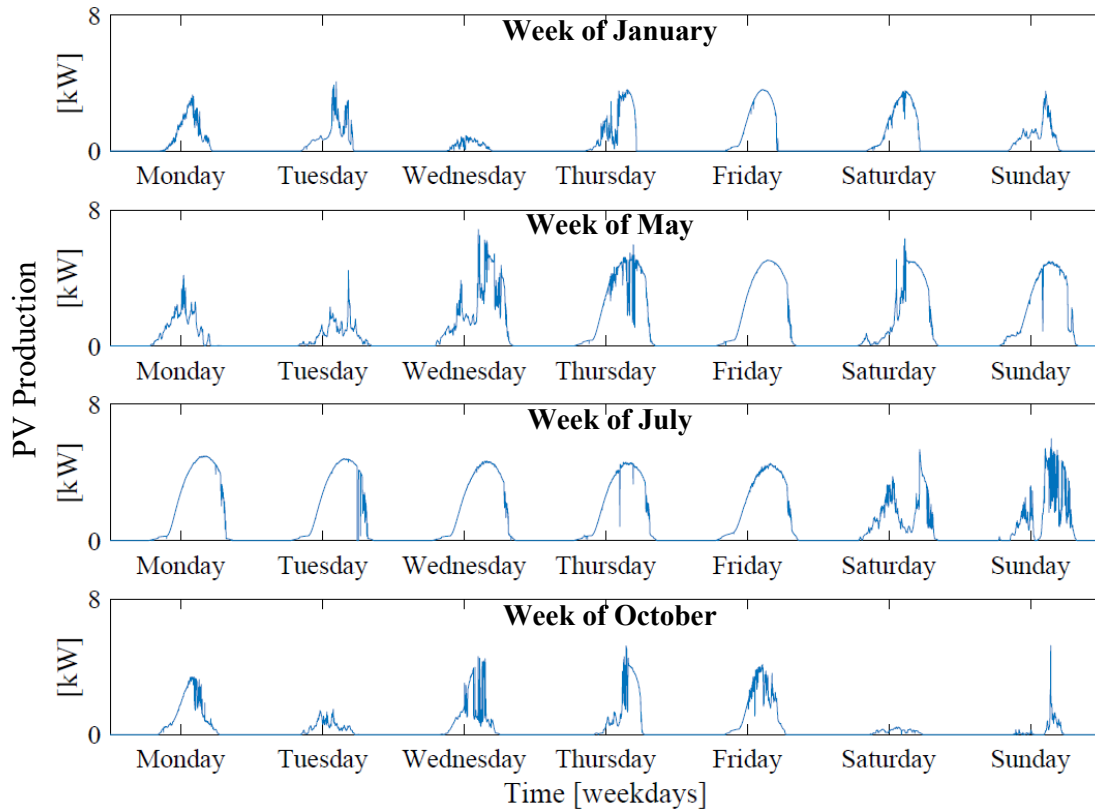


Figure 4.2 PV production in the four chosen weeks

Table 4.1 PV generation and sunlight hours percentage in chosen weeks

Week of:	January	May	July	October
E_{PVweek} [kWh]	79	179	207	65
$PV/24h$ [%]	38	62	63	46

4.1.2 Domestic Load Consumption Profiles

Similarly, to the PV production profiles, also the domestic load consumption profiles refer to a measurement campaign addressed during 2016. The domestic consumption considered is the load truly associated with the PV plant in Section 4.1.1. It refers to a family of two persons, who use the most common appliances and an electric boiler for hot water.

Figure 4.3 shows the load profiles along the four targeted weeks. Table 4.2 reports the total consumption of each week $E_{Load\ week}$. The week with higher consumption is the January week, while in July the lowest consumption is found.

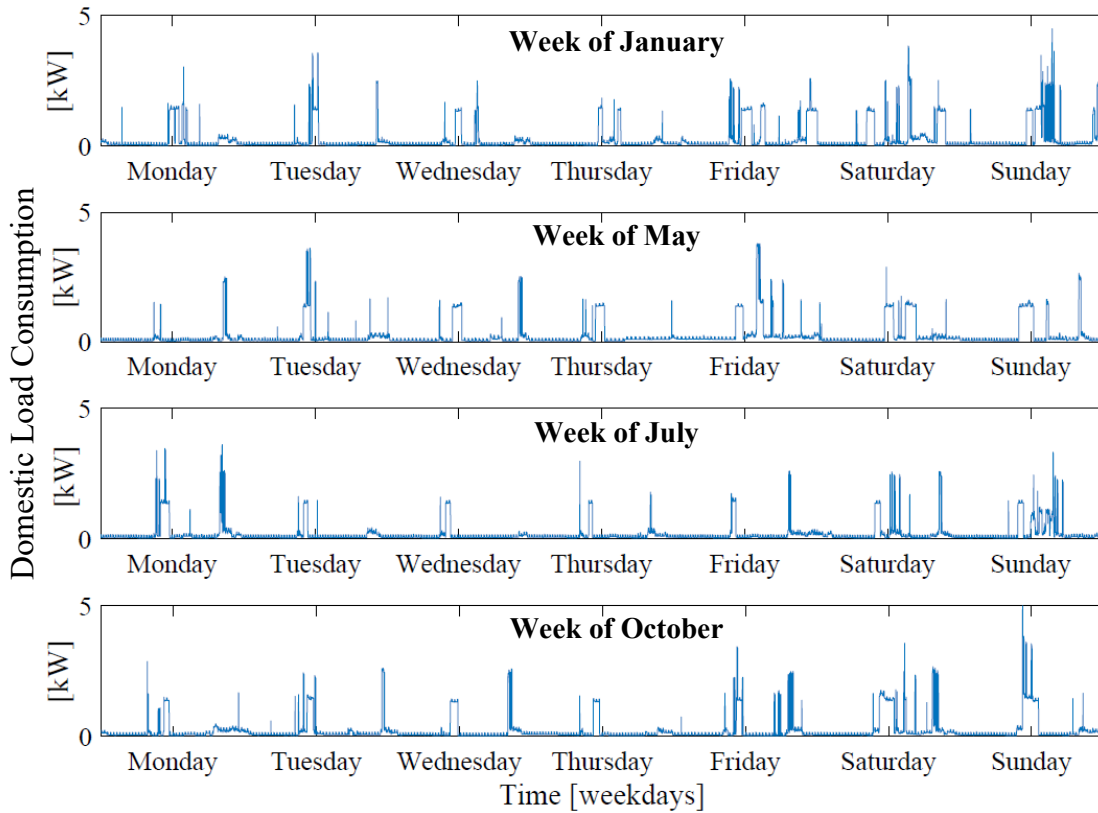


Figure 4.3 Domestic load in the four chosen weeks

Table 4.2 Domestic energy consumed in chosen weeks

Week of:	January	May	July	October
$E_{Load\ week}$ [kWh]	47	42	33	40

4.1.3 Choice of the EV usage Profiles

In order to test various scenarios, different EVs have been chosen from the 214 EVs dataset discussed in Section 3.1. More in detail, the choice is made with respect to the presence at home of the EVs. In fact, this parameter is particularly relevant since it effects the availability of the EV battery for the charging/discharging operations.

Definition of the EVs Home Presence

As already mentioned, the EVs database includes: the departure and the arrival times, the distance and the energy consumed of every trip that occurs during the period of observation of each vehicle. However, it does not include the destination of the trips. Thus, the information related to the presence of the car at

home is missing. Therefore, an assumption is made: each EV is considered parked at home mainly during night (between h:0:00 and the first trip of the day and between last trip of the day and h:24:00). Moreover, it is assumed that if more than two trips are done between the first and the last trip of the day, at least one has as destination the user's home. Figure 4.4 clarifies the assumption made, the presence at home is highlighted by the light grey shaded areas.

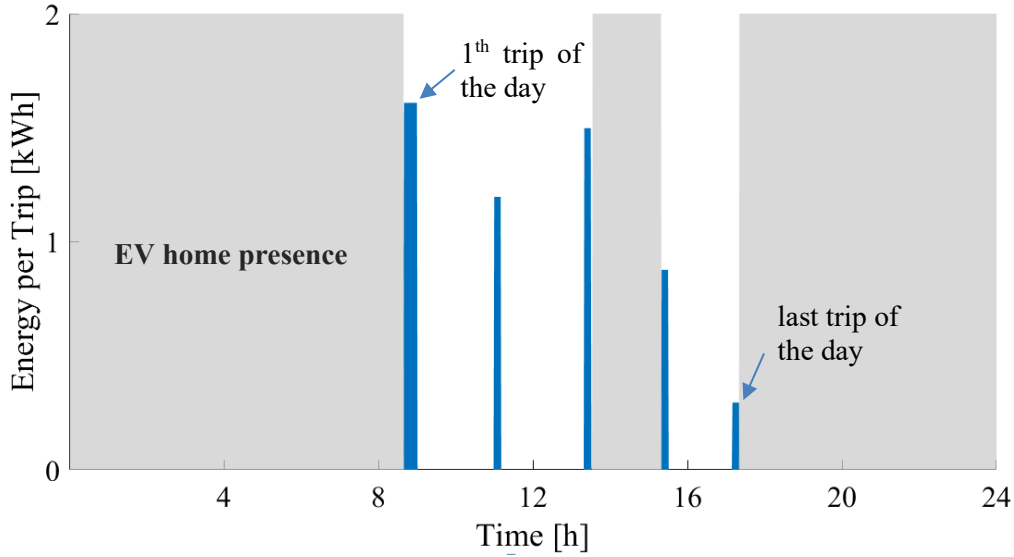


Figure 4.4 EV presence at home hypothesis

Once defined, the EV presence at home is checked for each time step (1-min) and is stored in the Boolean variable $x_{pres,t}$. At time step t , the parameter $x_{pres,t} = 1$, if the car is present at home, or $x_{pres,t} = 0$, if the car is away:

$$x_{pres,t} = \begin{cases} 1, & \text{if EV parked at home} \\ 0, & \text{if away} \end{cases} \quad (4.1)$$

All $x_{pres,t}$ conditions, among the period of observation of the EV, define the Boolean vector \mathbf{x}_{pres} :

$$\mathbf{x}_{pres} = [x_{pres,1}, x_{pres,2}, \dots, x_{pres,T}] \quad (4.2)$$

where, T is the number of minutes in the observed period. Finally, the average \bar{x}_{pres} , is calculated on all the values included in \mathbf{x}_{pres} :

$$\bar{x}_{pres} = \text{mean}(\mathbf{x}_{pres}); \quad (4.3)$$

The average \bar{x}_{pres} represents the fraction of time in which a certain EV is parked at home (i.e. the fraction of time in which the EV battery could be available for charging/discharging operations).

Clusterization of the Dataset

In order to define the different typologies of usage scenarios present in the dataset, a clusterization is made with respect to \bar{x}_{pres} . The aim of the clusterization is to find the most representative vehicles of the dataset to perform simulations. Clustering is performed by the k-medoids algorithm described in Section 3.2.1. This algorithm creates groups of EVs with a similar value of presence at home \bar{x}_{pres} . For each group, the algorithm defines a centroid, which is the EV that better represents the profiles of its group. Finally, the centroids are chosen as the EVs on which to base the simulations and they represent the different typologies of usage scenarios present in the dataset.

Identifying the Correct Number of Clusters

As explained in Section 3.2.1, k-medoids is not able to autonomously decide the number of clusters that better represent the dataset; thus, this value must be assumed a priori (i.e., the number of groups in which clusterize the dataset must be provided as input). The number of clusters is chosen through different iterations which change it at each attempt. A Silhouette Clustering Algorithm (SCA) provides a measure of the quality of each attempt [100]. In particular, the SCA calculates a dimensionless index (ranging between -1 and 1) which measures how close an element (i.e. the presence at home of a certain vehicle) is its own cluster compared to the other existing clusters. In other words, how much an element deserves to be part of its cluster. A mathematical description of the SCA index for a single element of the dataset is provided by Equation (4.4).

$$SCA_{ind} = (b - a) / \max(a, b) \quad (4.4)$$

In Equation (4.4), b is the inter-cluster distance (i.e. the mean distance of the considered element to all points in any other cluster), while a is the intra-cluster distance (i.e. mean distance between the considered element and all the other points in the same cluster).

It follows that the average of the SCA indexes (\overline{SCA}_{ind}) quantifies how much the division in a certain number of clusters well represents the different typologies of scenarios in the dataset (defined through the relative EV presence at home). A high positive SCA index means a good representation of the dataset, while negative values mean a poor representation. Figure 4.5 shows the SCA indexes for a division in two, three and four clusters respectively. The best \overline{SCA}_{ind} (0,56) has been obtained by dividing the whole database in three clusters. Therefore, the three respective centroids are chosen as representative EVs.

The representative EVs chosen are the 12th, 56th and 193rd EV of the dataset. For sake of simplicity, in the following it is referred to them as EV#A, EV#B and EV#C respectively. They present 0.7, 0.8 and 0.9 as \bar{x}_{pres} respectively.

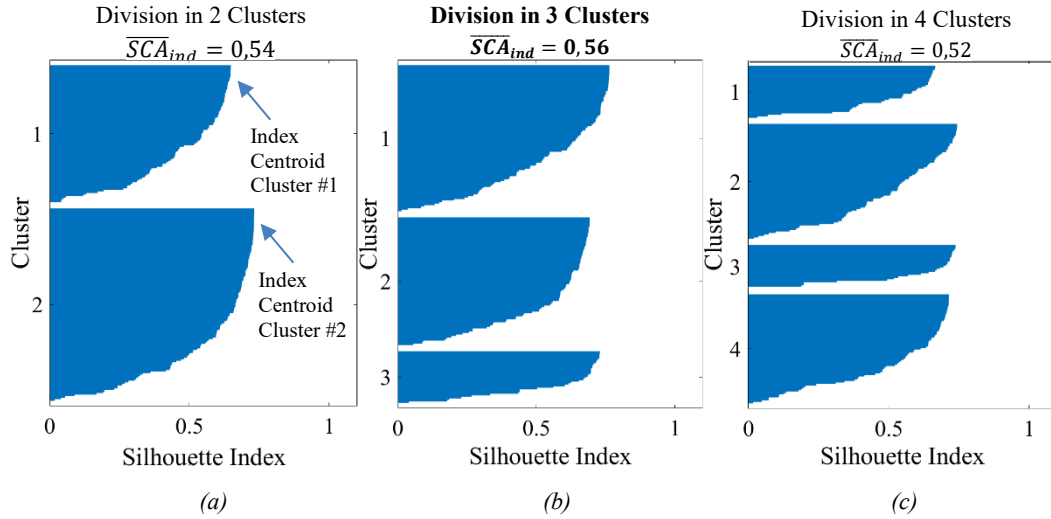


Figure 4.5 EVs dataset division in two (a), three (b), and four (c) clusters: Silhouette analysis

EVs Chosen Usages Profile

In order to compare different EV usages, this work considers alternately the three-representative vehicle EV#A, EV#B and EV#C. The profiles of each vehicle are chosen among the four weeks discussed in Section 4.1.1; i.e., the 4th week of January, the 1st week of May, the 3rd week of July, and the 2nd week of October.

Figure 4.6 shows the comparison between the three chosen EV profiles EV#A, EV#B and EV#C, during the week of January. The x-axis and y-axis show the time-distribution of the trips during the entire week and the relative energy consumptions (in kWh), respectively. The shaded areas indicate the periods of time in which the car is parked at home, i.e. time in which EV storage is available for charging/discharging operations. Although Figure 4.6 represents just a single week of the EVs usage, it is possible to notice that EV#A and EV#B present a relatively systematic behaviour. In fact, in both cases, the car is not available during the working hours, while it is present during the night and often also during weekend.

EV#A is the vehicle with the lowest presence at home during its entire period of observation in the dataset ($\bar{x}_{pres,EV\#1} = 0.70$). Moreover, between the three chosen EVs, EV#A presents the highest energy consumption for trips in the working days as also visible from Figure 4.6. It follows that EV#A may be associated to a typical worker, working relatively far from home.

Among the three chosen vehicles, EV#B has a middle value of presence at home during its entire period of observation ($\bar{x}_{pres,EV\#2} = 0.80$). In this case, the energy consumption of the trips occurring in working days is the lowest among the three vehicles, while higher consumptions are registered during weekends. This vehicle may be associated to a typical worker, working not far from home.

Finally, EV#C is characterized by the highest presence of the car at home during its entire period of observation (with $\bar{x}_{pres,EV\#3} = 0.90$), and a less regular use. In this case, there is not a real difference between working days and EV#C can be considered as a freelance user.

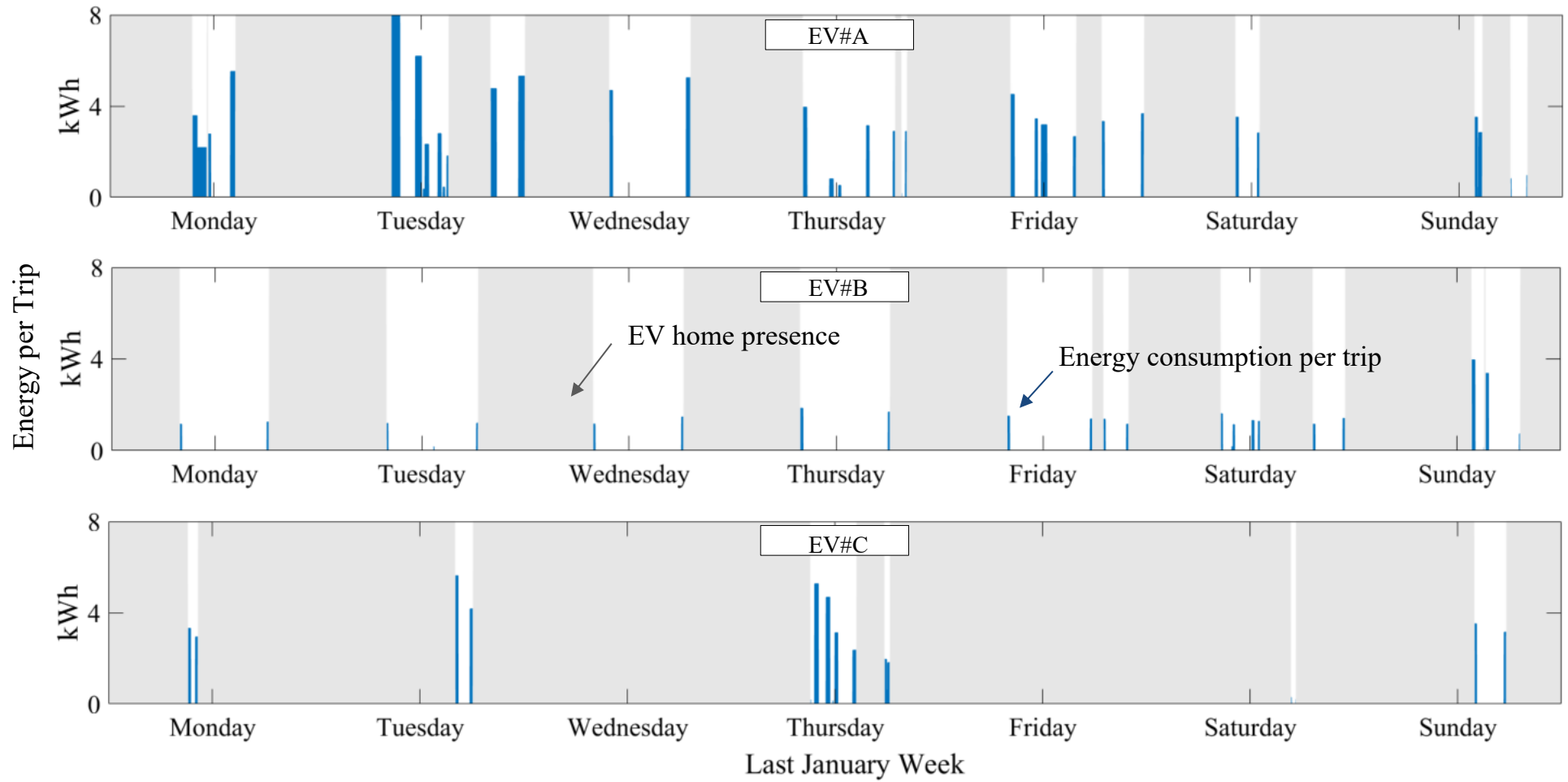


Figure 4.6 EV#A, EV#B, and EV#C profiles: week of January

Table 4.3 reports more details about the three EV profiles in the four considered weeks. The energy consumption during the week is defined by the parameter $E_{EV\ week}$. Meanwhile, \bar{X}_{PV} represents the percentage of time in which the EV is at home and contemporarily the PV is producing, with respect to the total hours of PV production in the week (Table 4.1). Figure 4.7 depicts the EV#C usage in the week of January and the relative PV production; \bar{X}_{PV} is represented from the yellow shaded areas. For sake of clarity this figure reports the PV production in dark yellow instead of the blue used in Figure 4.2.

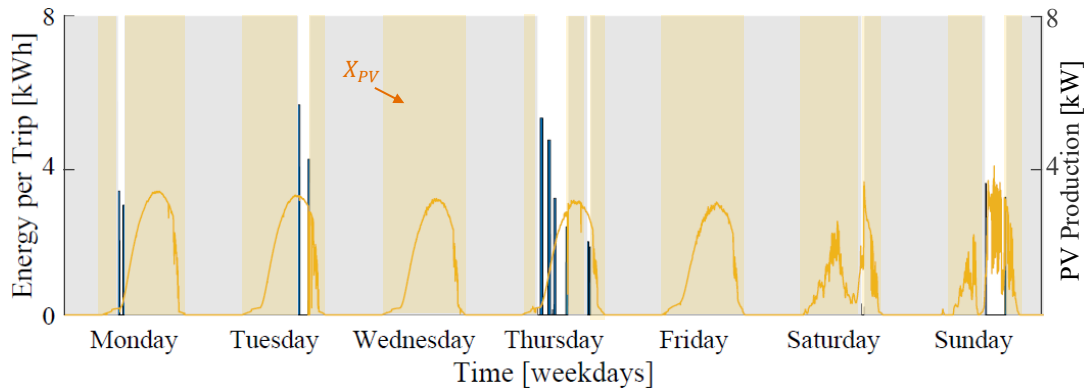


Figure 4.7 EV and PV contemporaneity: EV#C - week of January

As above described the consumption of EV#A is the highest among the four considered weeks with respect to the other vehicles. Moreover, the match with the PV is the poorest. (ranging between 27% and 37%). On the other hand, EV#C presents the best match with the PV production (ranging between 63% and 79%) with a lower energy consumption with respect to EV#A. Finally, EV#B represents an intermediate situation.

Table 4.3 EV Usages comparison: energy need and PV contemporaneity

		Jan	May	Jul	Oct
EV#A	$E_{EV\ week}$ [kWh]	110	65	80	76
	\bar{X}_{PV} [%]	37	27	55	26
EV#B	$E_{EV\ week}$ [kWh]	36	35	30	32
	\bar{X}_{PV} [%]	16	32	52	17
EV#C	$E_{EV\ week}$ [kWh]	45	20	38	50
	\bar{X}_{PV} [%]	79	77	79	63

4.1.4 Energy Indexes

The principal aim of this Chapter is to exploit as much as possible the PV energy for the local consumption. In order to measure this local grid-free ability, two indicators are here formalized: Self-consumption (S_{cons}) and Self-sufficiency (S_{suff}).

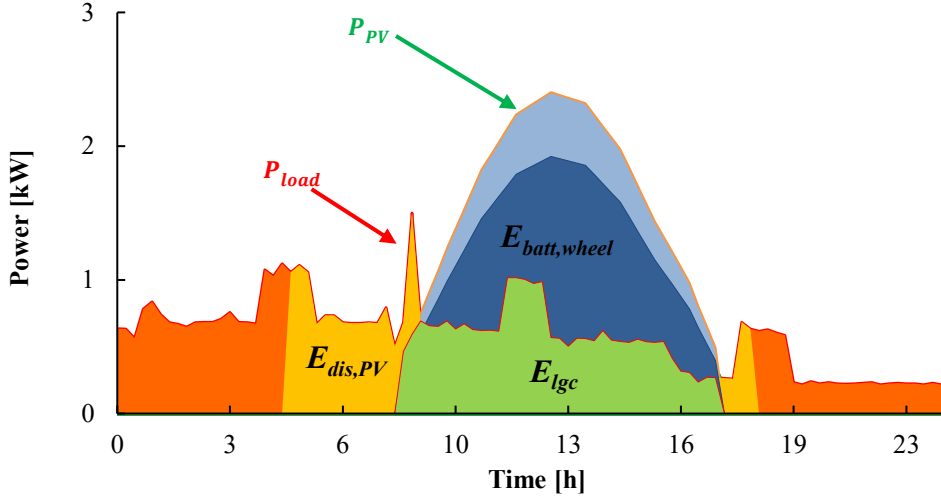


Figure 4.8 Daily power profiles and energy balance for an EV-PV system

Figure 4.8 provides an example of daily power profiles for the household system. For sake of simplicity, in Figure 4.8, the EV is considered at home all day.

The self-consumption index S_{cons} is defined as the ratio between the amount of energy produced by the PV which is directly consumed by the house and the car and the total amount of PV energy produced in a defined time interval:

$$S_{cons} = E_{match}/E_{PV\ Total} \quad (4.5)$$

where $E_{PV\ Total}$ represents the total amount of PV energy produced, and E_{match} represents the portion of energy simultaneously produced and consumed.

Unlikely, the self-sufficiency index S_{suff} is the ratio between the amount of energy produced and directly consumed and the sum of the energy requirements of the house and the car:

$$S_{suff} = E_{match}/E_{L\ Total} \quad (4.6)$$

where $E_{L\ Total}$ represents the local energy demand, thus house and car energy needs.

It is possible to express E_{match} through the following sum:

$$E_{match} = E_{lg} + E_{batt,wheel} + E_{dis,PV} \quad (4.7)$$

where:

- E_{lg} is the energy locally produced by PV generators and immediately consumed by residential loads.
- $E_{batt,wheel}$ is the energy locally produced by PV generators and stored in the EV battery that will be used by the EV.

- $E_{dis,PV}$ is the portion of the energy discharged by EV battery to feed local loads, originally produced by PV.

4.2 EV Battery Control Algorithms

As already mentioned, the Battery Control Algorithm has the role of dispatch the charging/discharging EV battery power in order to accomplish at the best a predetermined objective. In Section 2.2 the principal approaches used in literature for the smart charging were discussed: heuristic approaches, optimization approaches and hybrid approaches.

This section presents two battery control algorithms. Both algorithms aim to maximize the PV self-consumption. The first control algorithm is in the form of a pure heuristic approach, thus only real time information is used by a rule-based decision-making logic. In the following it is referred to this control algorithm as Simple Rule-based Logic (SRL). The SRL is here introduced in order to act as a reference for comparing the results of the proposed approach.

The Proposed Approach (PL) is the second control algorithm presented in this section. It is in the form of a hybrid approach; thus it coordinates an optimization phase with real time management.

4.2.1 Simple Rule-based Logic Without Forecasts

A relatively easy way to control the EV battery charging/discharging pattern resides in a rule-based logic which operates its decisions basing only on real-time data. In the following, an example of rule-based logic which aims to maximize the self-consumption is provided.

Self-consumption Logic

The Rule-based logic uses the differences between PV power and load demand for every current real-time instant indicated with t^* . If there is more PV power than electricity demand, The EV starts charging using the excess of PV power until the battery is full or there is no more excess of PV power. If there is insufficient PV power to cover load demand, energy can be extracted from the EV until the battery State of Charge (SOC) reaches a predefined minimum limit. As hypothesis, it is considered that the EV battery is always connected to the bidirectional charger when at home. The charging power of the EV battery for a time instant t^* is indicated with $P_{batt,t^*}^{ch.}$ and it is defined by the Equation (4.8). Meanwhile, the discharging power of the EV battery is indicated with $P_{batt,t^*}^{dis.}$ and defined in Equation (4.9).

$$P_{batt,t^*}^{ch.} = \begin{cases} P_{PV,t^*} - P_{load,t^*} & \text{if } P_{PV,t^*} > P_{load,t^*} \\ & SOC_{t^*} < SOC_{max} \\ & x_{pres,t^*} = 1 \\ 0, & \text{else} \end{cases} \quad (4.8)$$

$$P_{batt,t^*}^{dis.} = \begin{cases} P_{load,t^*} - P_{PV,t^*} & \text{if } P_{PV,t^*} < P_{load,t^*} \\ & SOC_{t^*} > SOC_{min} \\ & x_{pres,t^*} = 1 \\ 0, & \text{else} \end{cases} \quad (4.9)$$

In Equations (4.8) and (4.9), P_{PV,t^*} and P_{load,t^*} are the photovoltaic power and the household electric consumption at t^* respectively; SOC_{min} and SOC_{max} are the minimum and maximum limits of the State of Charge respectively; x_{pres,t^*} is the Boolean variable described in Section 4.1.3 which indicates if the EV is plugged at home.

Finally, the State of Charge of the battery is step by step updated by the logic through:

$$:= \begin{cases} SOC_{t^*} \\ SOC_{t^*-1} + 100 \cdot \left(\frac{P_{batt,t^*}^{ch.} \cdot \Delta t}{E_{batt,Tot}} - \frac{E_{EV,t^*}}{E_{batt,Tot}} \right) & \text{if } P_{batt,t^*}^{ch.} \neq 0 \\ SOC_{t^*-1} + 100 \cdot \left(\eta_{rt} \frac{P_{batt,t^*}^{dis.} \cdot \Delta t}{E_{batt,Tot}} - \frac{E_{EV,t^*}}{E_{batt,Tot}} \right) & \text{if } P_{batt,t^*}^{dis.} \neq 0 \end{cases} \quad (4.10)$$

In Equation (4.10), η_{rt} is the round-trip efficiency, which indicates the fraction of energy put into the storage that can be retrieved, while $E_{batt,Tot}$ is the total capacity of the EV battery. Finally, $E_{EV,t}$ is the energy among the time associated to the EV trips. In particular $E_{EV,t}$ assumes 0 if no trips occur in t^* , while the energy used for a certain trip z ($E_{trip,z}$) is instantaneously absorbed at the trip starting time $t_{start,z}$. Thus, the SOC is subtracted of the respective trip energy percentage portion at each trip starting minutes.

The above described logic sends a certain level of power in charge or discharge to the battery (if present) basing on the instantaneous values of PV and load. However, it is not able to schedule the EV charging from the main grid in case of PV shortage. The action of the EV's users is necessary for these operations.

Charge once Home Logic

The Charge once Home Logic aims to simulate the charging behaviour of the user. It is assumed that the user decides to recharge his vehicle from the grid every time he/she comes back home if the SOC of the EV is below a certain value $SOC_{ch,grid}$. In these cases, the Self-consumption Logic is bypassed, and the vehicle is charged from the grid of the amount of energy spent during the day (i.e., during his absence from home).

$$\begin{cases} \text{if} & SOC_{thome} < SOC_{ch,grid} \\ \text{then} & P_{batt,t}^{ch.} = P \quad \text{for } t_{home} < t^* < t_{home} + t_c \end{cases} \quad (4.11)$$

In Equation (4.11), t_{home} is the time-step in which the car arrives home, while $SOC_{t_{home}}$ is the corresponding State of Charge. The $SOC_{ch\ grid}$, as above mentioned, is the State of Charge below which the EV user starts a charging from the grid. This value can be in general different from the SOC_{min} used by the Self-consumption Logic. Finally, P is the level of recharge enabled from the main grid, while t_c is the time required to recharge the amount of energy spent during the absence from home at the power P .

It should be noticed that the Charge once Home logic is already a virtuous charging behaviour of the user. In fact, if $SOC_{ch\ grid}$ is chosen to be close to SOC_{min} , the EV user recharges just the amount of energy that he/she has really spent. Another possible behaviour is the Charging Until Full approach. The risk in this latest case, is to nullify the PV power availability. In fact, if the battery is already fully charged it cannot store the PV energy. Moreover, the Charging Until Full approach, unnecessarily stresses the chemistry of the battery which suffers high voltage, thus high SOC rate situations [47].

Despite the above, the Self-consumption and the Charge once Home, as simple rule-based logics, are not able alone to schedule an optimum battery charging/discharging profile. For example, the self-consumption logic it is not able to recognize when is convenient to stop the V2H operations (battery discharging towards the home), thus preserve the energy in the battery, since an imminent trip. Neither, this logic can autonomously position the recharges from the grid in manner to reduce them at the minimum by exploiting at the best the PV production.

4.2.2 Proposed Logic

The EV battery control logic proposed in this work aims to further improve the self-consumption rate compared to that obtained with a simple Rule-based logic. In order to achieve this purpose, the Proposed Logic makes use of PV production, domestic load and EV behaviour future estimations. Moreover, the proposed logic is completely autonomous.

In fact, the EV user is only required to connect his/her vehicle once he/she arrives at home, then all the charging discharging operations, including changings from main grid, will be handled from the battery control algorithm. For example, if an EV user arrives home late in the evening with a relatively low battery level, he/she may want to recharge the battery from the grid (since the PV production is absent) in order to restore the SOC.

However, if in the next day it is forecasted an appropriate PV production and the car charging availability, it is better to not operate the grid charging immediately, thus appropriately exploit the next day PV production. This is properly done by the Proposed Logic. Moreover, during the day, the Proposed Logic can temporarily disable the V2H operations (battery discharging towards the home) if in the next future a relevant trip is forecasted, thus preserving the

energy in the battery for its main purpose and avoiding unnecessary inefficiencies. Finally, PL considers an appropriate level of tolerance in order to guarantee always a reserve of energy, thus overcome forecasts errors and preserve the battery from voltage stress.

Methodology

Figure 4.9 shows the methodology in which the proposed EV battery control logic is built.

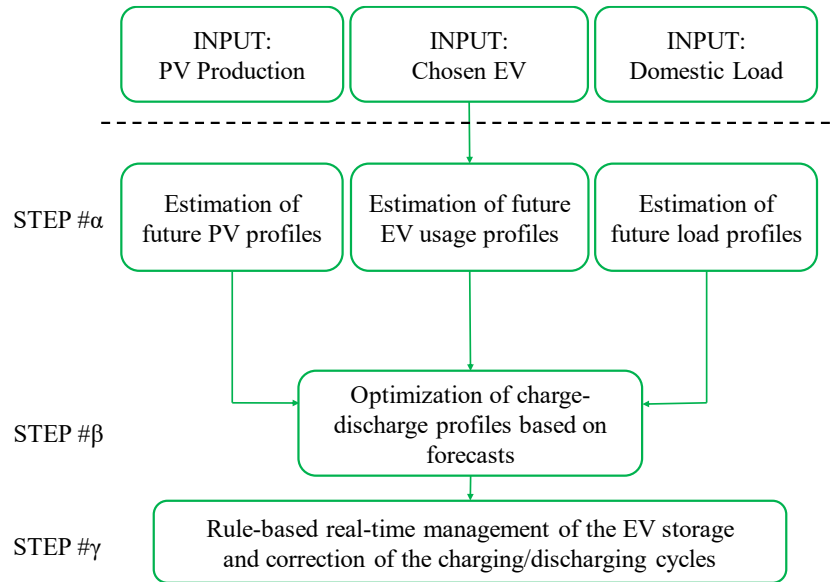


Figure 4.9 Proposed procedure flowchart (household)

The inputs of the Control Algorithm are the all available historical data related to EV usage, PV generation and domestic load. Starting from these inputs the algorithm is then articulated in three steps indicated with Greek letters α , β and γ (i.e., STEP # α , STEP # β , and STEP # γ).

- In STEP # α , each data set is elaborated to estimate the future profiles. For the EV usage profile forecasts the Day-ahead procedure discussed in Section 3.2.1 is used. Meanwhile, for load and PV forecasts, an Autoregressive Moving Average based Algorithms (ARMA) is used. The future estimated profiles are provided on weekly basis with a time-step of 10 min.
- In STEP # β , the future estimated profiles are used to run an optimization problem which aims to find the optimum charging/discharging pattern of the week. Thus, the battery operations that maximize the self-consumption are determined. However, the output of STEP # β is based on estimated profiles which are in general different from the actual behaviour of the EV, the PV generation and the domestic load during the week.
- In STEP # γ a rule-based logic in real time implements the battery operations by considering both the real time data and the outputs of the

optimization of STEP # β . Moreover, the rule-based real time management implements the charging discharging boundaries and tolerances in order to guarantee the safe and correct functionality of the battery.

STEP # α , STEP # β and STEP # γ are in detail presented in the next paragraphs.

STEP # α : Future EV Usage Profiles

For the estimation of the EV behaviour in the week the Day-ahead forecast routine, described in Section 3.2.1 is used. More in details, the routine is run for all the days of the week, leading to the next week most probable future behaviour of the EV. Thus, this forecast is compared with the real EV usage which occurs in the four considered weeks (i.e. week of January, week of May, week of July, week of October).

Figure 4.10 shows an example of comparison between the real EV#B usage profile measured in the week of January and the related EV#B forecast.

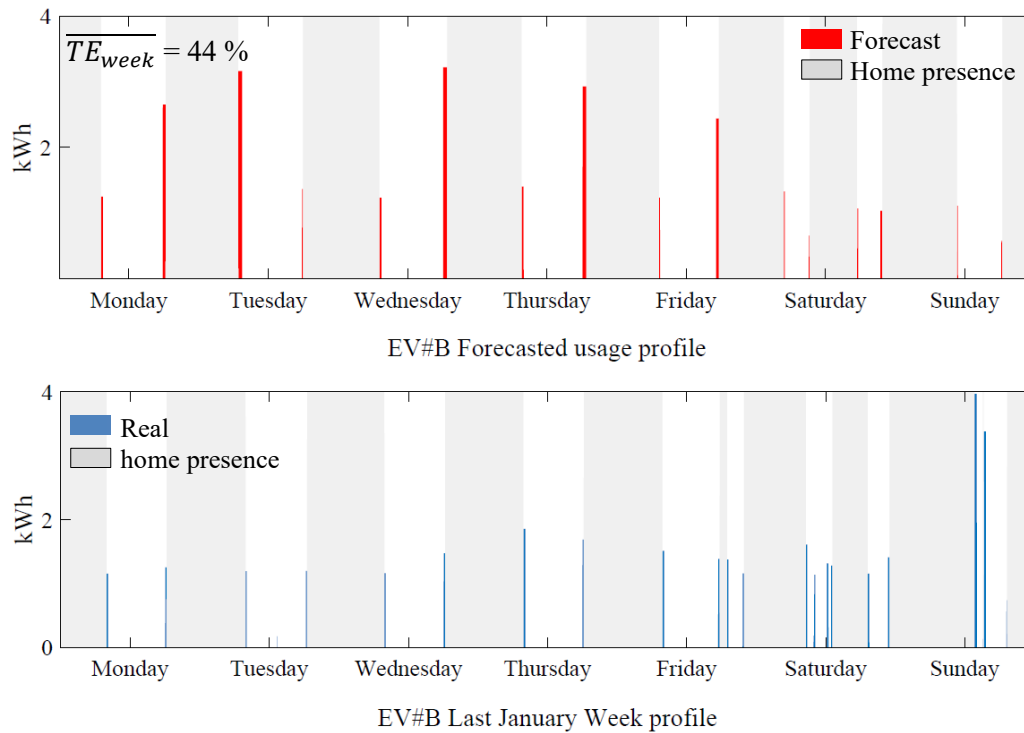


Figure 4.10 Estimated and real EV usages: EV#B - week of January

As in the case of Figure 4.6, Figure 4.10 shows the distribution of the trips during the entire week and the shaded areas indicate the periods of time in which the car is expected to be parked and connected at home. For the real behaviour these areas are identified on the basis of the Boolean vector \mathbf{x}_{pres} defined in Section 4.1.3. Similarly, for the forecast the presence at home is identified through $\hat{\mathbf{x}}_{pres}$ calculated on the basis of the forecasted trips (e.g. the car is assumed at home between h:0:00 and the first forecasted trip of the day and between last forecasted trip of the day and h:24:00).

Table 4.4, reports the Daily forecast Errors (defined in Section 3.2.2) for the case in Figure 4.10. As it can be noticed from the figure, there is a good agreement between the real and the forecasted departure minutes. Thus, the related index Trip Starting-minutes Error (TSE) lies between just the 1% of Thursday and the 66 % of Saturday, with an average value in the week of 34%. However, higher values are obtained for the two other errors: Trip duration Error (TDE) with an average on the week of 66% and the Trip Consumption Error (TCE) with an average on the week of 53%. This led to a Total Error which lies between the 14% of Thursday and the 63% of Tuesday, with an average on the week of 44%.

Table 4.4 EV Daily Forecast Errors: EV#B - week of January

	Mon.	Tue.	Wed.	Thu.	Fri.	Sat.	Sun.	Week
TCE [%]	62	77	69	22	32	53	79	53
TSE [%]	4	49	3	1	56	66	63	34
TDE [%]	81	100	97	61	24	43	58	66
TE [%]	29	63	32	14	46	61	68	44

Finally, Table 4.5 reports the Forecast Daily Total Errors in the four considered weeks for EV#A, EV#B and EV#C respectively. As expected, better results are obtained for the first two vehicles (with a slightly better general behaviour of EV#B compared to EV#A). Meanwhile EV#C is the poorest, since its irregular behaviour presents the highest errors. For many days the EV#C forecast presents error higher than 100%. This is explicable with the fact that for those days EV#C never leaves home while the forecast logic estimates some trips, resulting completely wrong. Finally, the absolute best result is obtained for EV#A in the week of May with an \overline{TE}_{week} of 39%.

Table 4.5 Daily Forecast Errors: EV#A, EV#B, EV#C - all weeks

	Week of:	$TE_{Mon.}$ [%]	$TE_{Tue.}$ [%]	$TE_{Wed.}$ [%]	$TE_{Thu.}$ [%]	$TE_{Fri.}$ [%]	$TE_{Sat.}$ [%]	$TE_{Sun.}$ [%]	\overline{TE}_{week} [%]
EV#A	Jan.	75	75	14	73	77	11	45	53
	May	11	51	10	31	18	78	74	39
	Jul.	77	65	70	61	41	65	67	64
	Oct.	36	36	8	62	28	59	48	40
EV#B	Jan.	29	63	32	14	46	61	68	44
	May	62	47	21	48	31	100	37	49
	Jul.	76	11	61	25	67	38	59	48
	Oct.	78	16	18	47	49	56	100	52
EV#C	Jan.	69	54	100	78	100	49	15	66
	May	46	100	100	100	18	23	78	67
	Jul.	100	69	48	60	48	100	68	71
	Oct.	100	100	18	58	70	55	58	66

STEP #a: Future Load and PV Generation Profiles

In order to optimize the management of the EV battery, it is necessary an estimation of future domestic load and PV generation profiles. For this purpose, an approach based on Auto Regressive Moving Average (ARMA) model is used [101].

ARMA is a mathematical model which uses as inputs a certain number of previous values over time with respect to the current instant t^* . Thus, ARMA provides as forecast output, the average value of these inputs. Once the model arrives at the next time instant, all the inputs are updated and the average recalculated leading to moving average behaviour.

For the specific case of future week estimation, ARMA was performed using the historical data related to the days before and after the week that must be forecasted (or target week). For example, Figure 4.11 shows the data used for the domestic consumption forecasts. The inputs are the historical data related to the 45 days before the target week and the 45 days after, respectively. The values referring to the 45 days after are obtained from the previous year. Moreover, a distinction is done between working days and weekends. The same procedure is used for PV generation, with a different time frame, i.e. 30 days before and after the target week.

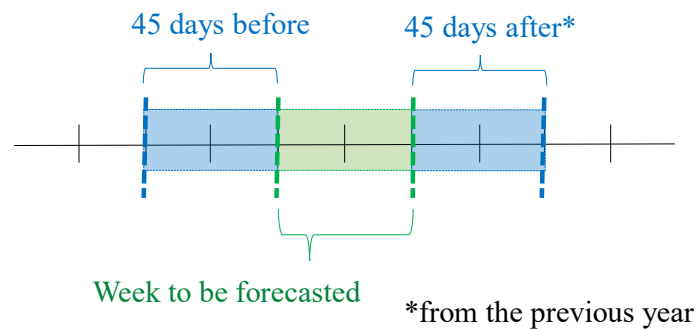


Figure 4.11 Time frame used for the domestic load forecasts

As an example, Figure 4.12 shows the comparison between the real domestic consumption and PV generation (dashed blue line), and the respective estimations (red line) during the week of January. For the specific case, in Figure 4.12-*b* the estimated PV profile well matches the average real production, with the highest variation in case of rainy day (Wednesday). Regarding loads in Figure 4.12-*a*, the variability is higher, since the irregular behaviour of the people in the family.

In order to quantify the quality of the PV and Load forecasts, Daily errors similar to those in Section 3.2.2 are defined. The daily error of the load forecast with respect to the real profile is indicated with Err_{LOAD} and calculated as:

$$Err_{LOAD} = 100 \cdot \left| E_{cons} - \widehat{E}_{cons} \right| / E_{cons} \quad (4.12)$$

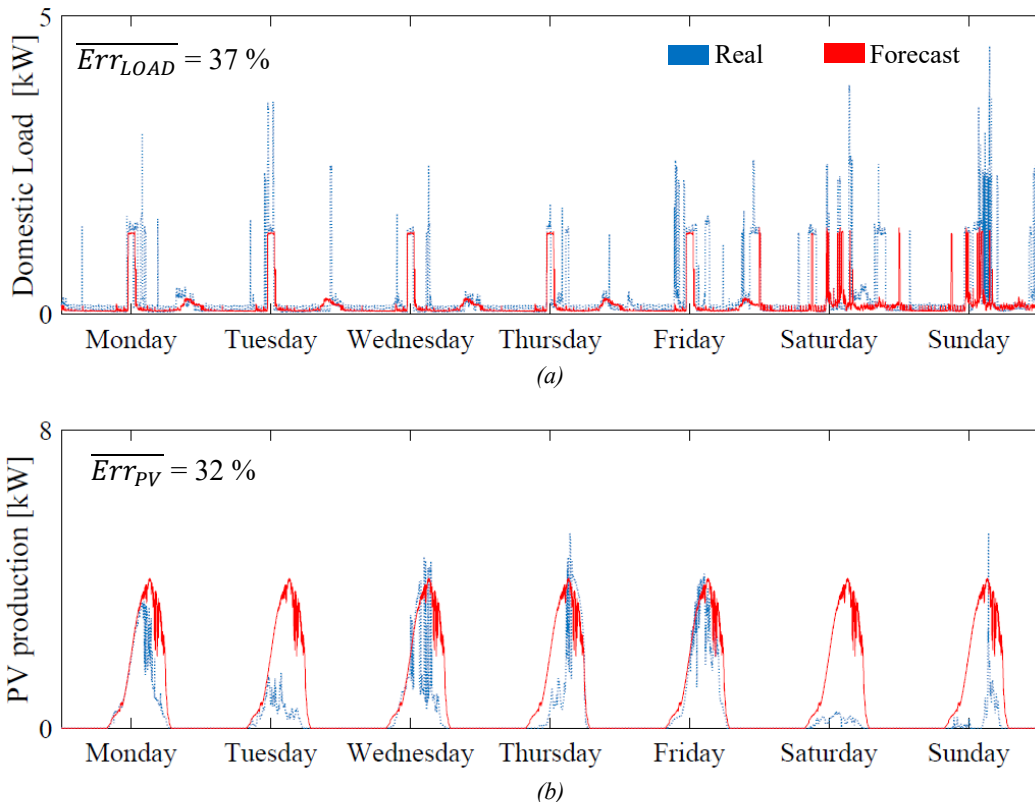


Figure 4.12 Estimated and real domestic loads (a) and PV generation (b):week of January

In Equation (4.12), E_{cons} represents the real amount of energy requested from the house in a day; while \widehat{E}_{cons} the forecasted amount of energy consumed that day. The daily error of the PV generation forecast with respect to the real profile is indicated with Err_{PV} and calculated as:

$$Err_{PV} = 100 \cdot \left| E_{gen} - \widehat{E}_{gen} \right| / E_{gen} \quad (4.13)$$

In Equation (4.13), E_{gen} represents the real amount of energy generated from the PV in a day; while \widehat{E}_{gen} the forecasted amount of energy generated that day.

Similarly, to the errors defined in Section 3.2.2, Err_{LOAD} and Err_{PV} are imposed to range between 0 and 100%. Thus, if errors more than 100% occur, 100% will be considered as the actual value and the forecast will be assumed completely wrong.

Table 4.6 and Table 4.7 report the Daily errors of load consumption and PV generation forecasts respectively; the averages in the week are distinguished by the symbols \overline{Err}_{LOAD} and \overline{Err}_{PV} . The lowest errors have been obtained in the week of July, while the highest error in the week of October. In particular, the \overline{Err}_{LOAD} ranges between the 32% of the July week and 38% of the October week. Meanwhile, \overline{Err}_{PV} ranges between 19% of the July week and 77% of the October week. Finally, it can be noted that several PV forecasts show an error equal or higher than 100%. It occurs for every cloudy day.

Table 4.6 Daily Load Forecast Errors - all weeks

Week of:	$Err_{LOAD} [\%]$							$\overline{Err_{LOAD}} [\%]$
	Mon.	Tue.	Wed.	Thu.	Fri.	Sat.	Sun.	
Jan.	34	28	19	10	64	53	54	37
May	1	34	33	24	63	40	39	34
Jul.	58	10	8	12	31	50	56	32
Oct.	26	43	36	8	46	58	48	38

Table 4.7 Daily PV Forecast Errors - all weeks

Week of:	$Err_{PV} [\%]$							$\overline{Err_{PV}} [\%]$
	Mon.	Tue.	Wed.	Thu.	Fri.	Sat.	Sun.	
Jan.	9	17	100	16	34	30	21	32
May	69	100	27	39	42	23	38	48
Jul.	13	7	6	3	3	55	49	19
Oct.	57	100	87	63	29	100	100	77

STEP # β : Optimization of charge-discharge pattern based on forecasts

The outputs of STEP # α are the forecasts of the EV usage profile, the PV production and the Domestic Consumption. These results are used as inputs of STEP # β . In this further step of the methodology an optimization aiming to minimizing the electricity exchange with the grid is formulated. STEP # β is supposed to be launched before the real time management (i.e., the day before the week starts) and its output will be used as input of STEP # γ .

As specified in the previous sections, the expected presence at home of the EV is defined by the Boolean variable $\hat{x}_{pres,t}$. Due to the presence of this variable, the following problem statement is formulated as a Mixed Integer Linear Programming (MILP) and it is solved by using “Yalmip” Matlab tool.

The optimization consists of the objective function defined in (4.14), which is the minimization of the sum of grid exchanges ($P_{grid,t}$) in the T time steps composing the analysed period (e.g., a week). The output of the optimization problem is the battery power $P_{batt,t}$, assumed positive in case of battery charge and negative in case of battery discharge. The constraints of the optimization problem are defined as follows:

- The first constraint shown in (4.15) imposes a null value for EV battery power ($P_{batt,t}$), when the car is expected not to be at home (i.e., if the Boolean $\hat{x}_{pres,t}$ is equal to 0 in the time-step t).
- The constraint in (4.16) consists of a power adjustment that limits the charge and discharge of the battery in order to do not exceed the Point of Delivery (POD) contractual power P_{contr} . More in details, the difference

between P_{contr} and the expected domestic load \widehat{P}_{load_t} is allowed as maximum power for the battery in a certain t . For example, if the contractual power is 6 kW and the current domestic consumption is 2 kW, the maximum charging power admitted is 4kW. The charging power adjustment is a control logic truly performed by most of the commercial EV chargers, as shown in [102] and [103].

- The constraint in (4.17) is the power balance based on forecasted profiles. This constraint ensures that in case of expected PV power \widehat{P}_{PV_t} shortage and battery absence, the expected domestic load is still powered by the grid $P_{grid,t}$. Vice versa in case of overgeneration, the exceeding \widehat{P}_{PV_t} is injected into the grid.
- The constraint in (4.19) ensures that the charged/discharged energy lies in the State of Charge (SOC) lower and upper boundaries. The upper boundary is indicated with SOC_{max} , while the lower boundary is given by the sum of the SOC_{min} and a tolerance reserve SOC_{TOLL} considered in order to mitigate the forecasts errors.

Finally, the SOC is defined by the Equation (4.19), where \widehat{E}_{EV_t} is the expected energy absorbed for the EV trips, defined similarly to $E_{EV,t}$ in Section 4.2.1; while $E_{batt,Tot}$ is the total battery capacity. The two conditions in Equation (4.19) define the SOC for charging and discharging respectively, and only differ for the round trip efficiency η_{rt} .

$$\min_{P_{batt,t}} \sum_{t=1}^T |P_{grid,t}| \quad (4.14)$$

s.t.

$$|P_{batt,t}| = 0 \quad \forall t | \widehat{x}_t = 0 \quad (4.15)$$

$$P_{batt,t} \leq P_{contr} - \widehat{P}_{load_t} \quad \forall t \quad (4.16)$$

$$P_{grid,t} = \widehat{P}_{PV_t} - \widehat{P}_{load_t} - P_{batt,t} \quad \forall t \quad (4.17)$$

$$SOC_{min} + SOC_{TOLL} \leq SOC_t \leq SOC_{max} \quad \forall t \quad (4.18)$$

Where:

$$SOC_t := \begin{cases} SOC_{t-1} + 100 \cdot \left(\frac{P_{batt,t} \cdot \Delta t}{E_{batt,Tot}} - \frac{\widehat{E}_{EV,t}}{E_{batt,Tot}} \right) & \text{if } P_{batt,t} \geq 0 \\ SOC_{t-1} + 100 \cdot \left(\eta_{rt} \frac{P_{batt,t} \cdot \Delta t}{E_{batt,Tot}} - \frac{\widehat{E}_{EV,t}}{E_{batt,Tot}} \right) & \text{if } P_{batt,t} \leq 0 \end{cases} \quad (4.19)$$

The two SOC limits SOC_{min} and SOC_{max} have been chosen according to battery degradation criterion. In particular, battery degradation can result from over discharge and over charge [104]. Therefore, the minimum and maximum SOC values have been set to 30% and 95% respectively. Meanwhile the tolerance value SOC_{TOLL} that is added to SOC_{min} , has been assigned equal to the 80% of the average trip consumption of the considered EV. In the following, it is referred to the sum $SOC_{min}+SOC_{TOLL}$ with the symbol $SOC_{min,tot}$. Finally, the round-trip efficiency η_{rt} is not easily estimable since it depends on many factors, such as technology of the battery, topology of the charge/discharge regulator, distance from the EV plug-in point to the PV source and the load connection points. However, the main producers of residential systems for the PV energy storage declare for their systems a round-trip efficiency around 80% [102],[103],[105].

As above mentioned, the output of the optimization problem is the variable $P_{batt,t}$. This quantity expresses the power battery profile along the week which permits to minimize the withdrawals from the grid, thus maximize the self-consumption. However, $P_{batt,t}$ is calculated on the basis of the forecasts (STEP # α) which are different from the real PV, Load and EV behaviours. Therefore, $P_{batt,t}$ cannot correspond to the real-time power profile. In order to overcome this issue, the variable $P_{batt,t}$ is discretized in the command vector \mathbf{CV}_{EV} which assumes the unitary values 1 when $P_{batt,t} > 0$, -1 when $P_{batt,t} < 0$, and 0 when $P_{batt,t} = 0$.

$$\mathbf{CV}_{EV} := \begin{cases} 1 & \forall t \mid P_{batt,t} > 0 \\ 0 & \forall t \mid P_{batt,t} = 0 \\ -1 & \forall t \mid P_{batt,t} < 0 \end{cases} \quad (4.20)$$

The command vector \mathbf{CV}_{EV} is the final output of STEP # β . Therefore, once given as input of STEP # γ it is able to suggest an optimized power pattern, leaving the choice of the exact power values to the real-time logic. Figure 4.13 shows the command vector obtained for the optimization of the January week with EV#C.

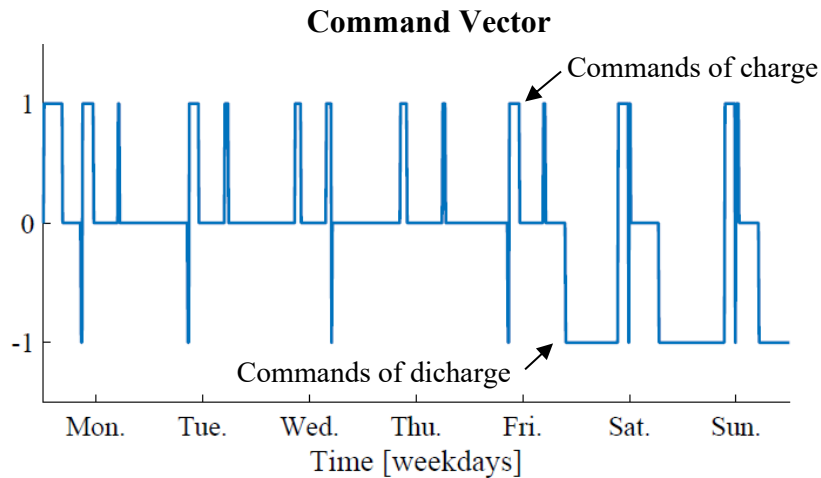


Figure 4.13 Example of Command Vector: Output of STEP # β

STEP # γ : Rule-based Real-Time Management

The Rule-based real-time logic finally applies minute by minute the effective charging/discharging EV battery power. Since here it is referred to a real-time current instant the time steps are indicated with t^* . Therefore, the real time battery power and the relative State of Charge becomes: P_{batt,t^*} and SOC_{t^*} . Figure 4.14 shows the working principle of the real-time management.

First, the logic checks if the car is available at home. If the car is not at home, nothing happens, and the battery power is zero. On the other hand, three different cases are possible depending on the states of the command CV_{EV,t^*} .

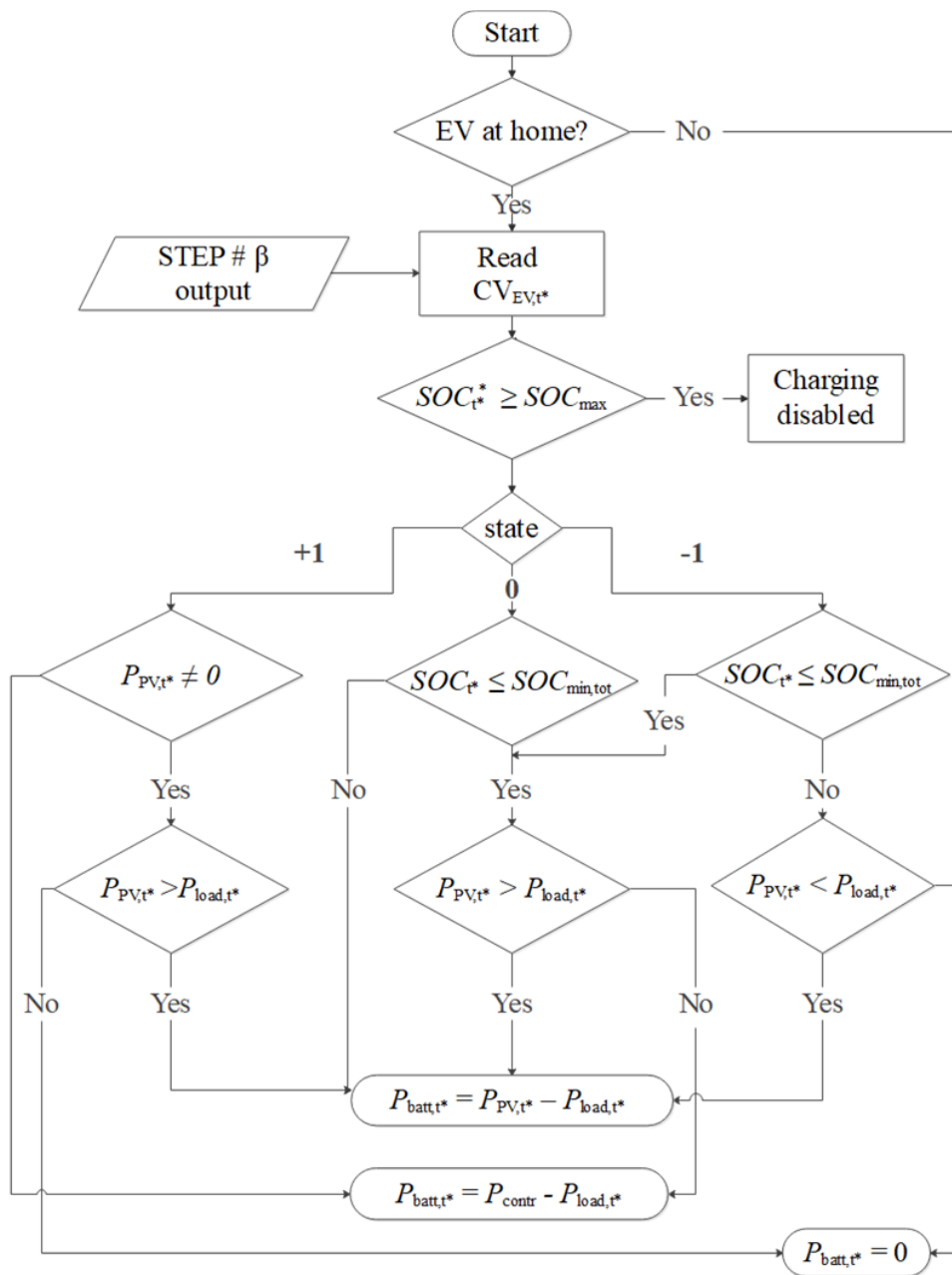


Figure 4.14 Household system real time management routine

The case $CV_{EV} = 1$ means that the command is requiring a charge. The logic checks if there is PV production. A positive answer will result in a charging fed by the PV when its production is greater than the domestic load. Meanwhile in case of negative answer (e.g., during the dark hours), the battery charging power is taken from the grid and dynamically set for not exceeding P_{contr} .

The case $CV_{EV} = -1$, means that the command is requiring a discharge. The logic checks if SOC_{t^*} is less than the lower limit $SOC_{min,tot}$. If the answer is positive, the command vector is changed in the zero state. Otherwise, if the answer is negative, the EV battery will supply the fraction of the load that is not supplied by the PV generator.

The case $CV_{EV} = 0$ means that the command vector is not requiring any specific battery state or was disabled from precedent steps. In this case, the logic behaves as the simple base logic described in Section 4.2.1. If SOC_{t^*} is higher than the lower boundary, P_{batt,t^*} will follow the instantaneous positive or negative difference between PV and load, addressing real-time balancing and maintaining $P_{grid,t}$ equal to zero. On the contrary, only charging will be enabled from the PV or directly from the grid by dynamic charging to not exceed P_{contr} .

Finally, in order to avoid overcharge, in case of $SOC_{t^*} \geq 95\%$, the control will only permit discharge.

4.3 Simulation Results

The proposed methodology is applied to three case studies. For each case study, the residential load and PV generation profiles are identical. On the contrary, the EV Usage profiles are different. As described in Section 4.1.3, the selected EV profiles are the centroids of a database composed of 214 EVs. As a result, EV#A, EV#B and EV#C are different and well represent three typical electric vehicle usage profiles. Regarding the simulated time frame, four weeks are considered to represent the four seasons, as described in Section 4.1.1 and in Section 4.1.2.

The results are compared with respect to the Simple Rule-based Logic (SRL) without forecasts described in Section 4.2.1; which is, thus, chosen as Reference Logic. For both the Simple Rule-based Logic and the Proposed Logic (PL) a SOC_{min} equal to 30% is assumed. Moreover, for the simple Rule-based logic and more specifically for the Charge once Home Logic the $SOC_{ch\ grid}$ was fixed equal to $SOC_{min}=30\%$. However, this leads to two different behaviours between the logics in case of PV shortage.

For the Simple Rule-based, the EV user will starts charging his car from the grid if, once at home, the SOC of the EV is less than 30%. More in details, he/she will recharge the battery of the amount spent during his/her absence from home. Meanwhile, the Proposed Logic will maintain the level of charge constant at 30%

plus SOC_{TOLL} until the PV production is recovered or a charging action is required from the Command Vector CV_{EV} .

The simulations have been run assuming 40 kWh as total EV battery capacity. Finally, the SOC at the beginning of the week is assumed equal to 25%. Thus, the corresponding amount of energy is assumed charged from an external source or coming from the previous week.

Figure 4.15-*b* shows, as an example, the State of Charge evolution of EV#C (Monday of the week of July) for both battery control algorithms: Simple Rule-based Logic (black) and Proposed Logic (green). In the background the contextual EV#C usage profile and the presence at home during the week of July are reported. Finally, Figure 4.15-*a* shows the PV production for the considered day.

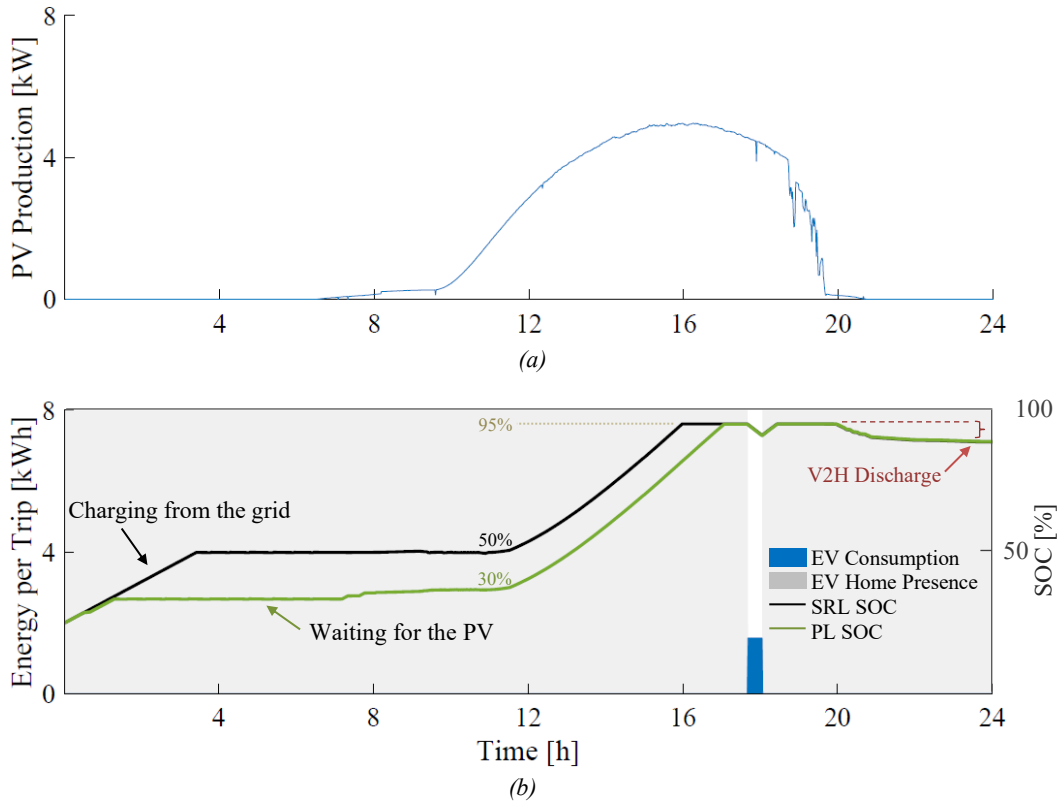


Figure 4.15: Control Algorithms comparison: PV production (a) and SOC evolution (b) - EV#C-Monday of the July week

From Figure 4.15-*b*, it is visible that at the beginning of the day, since the initial SOC is less than 30%, the SRL operates a charging from the grid until the energy spent in the last absence from home is recovered. On the contrary, the Proposed Logic, due to the expected future PV availability, limits the charge from the grid to the energy necessary to bring the battery at $SOC_{min,tot}$ (30% plus SOC_{TOLL}). In this latest case, the battery will be fully charged some hours later directly from the PV.

It should be noted that during the sunlight hours, the battery controlled with the Proposed Logic is able to intercept a greater PV production with respect to the battery controlled by SRL. In fact, once the PV availability exists, the PL controlled battery charges from 30% to 95% (upper boundary), thus 65% of the

total battery capacity. Meanwhile, the SRL controlled battery charges from around 50% to 95%, thus 45% of the total battery capacity.

At 5:40 P.M., EV#C starts a trip consuming 1,5 kWh, thus around 4% of the battery capacity. At 6:02 P.M., EV#C is back at home and some PV production is still available. At 8:45 P.M. there is no more PV production and the EV battery is used to feed the Domestic Load (V2H discharge).

Figure 4.16 shows the entire of the week of July. The State of Charge decreases in correspondence with EV#C trips and increases in correspondence with PV availability. Moreover, SOC decreases are observed during dark hours for the discharging intervals toward the house. For sake of graphic clarity only the V2H discharge occurring in the night between Monday and Tuesday is highlighted in Figure 4.16-*b*.

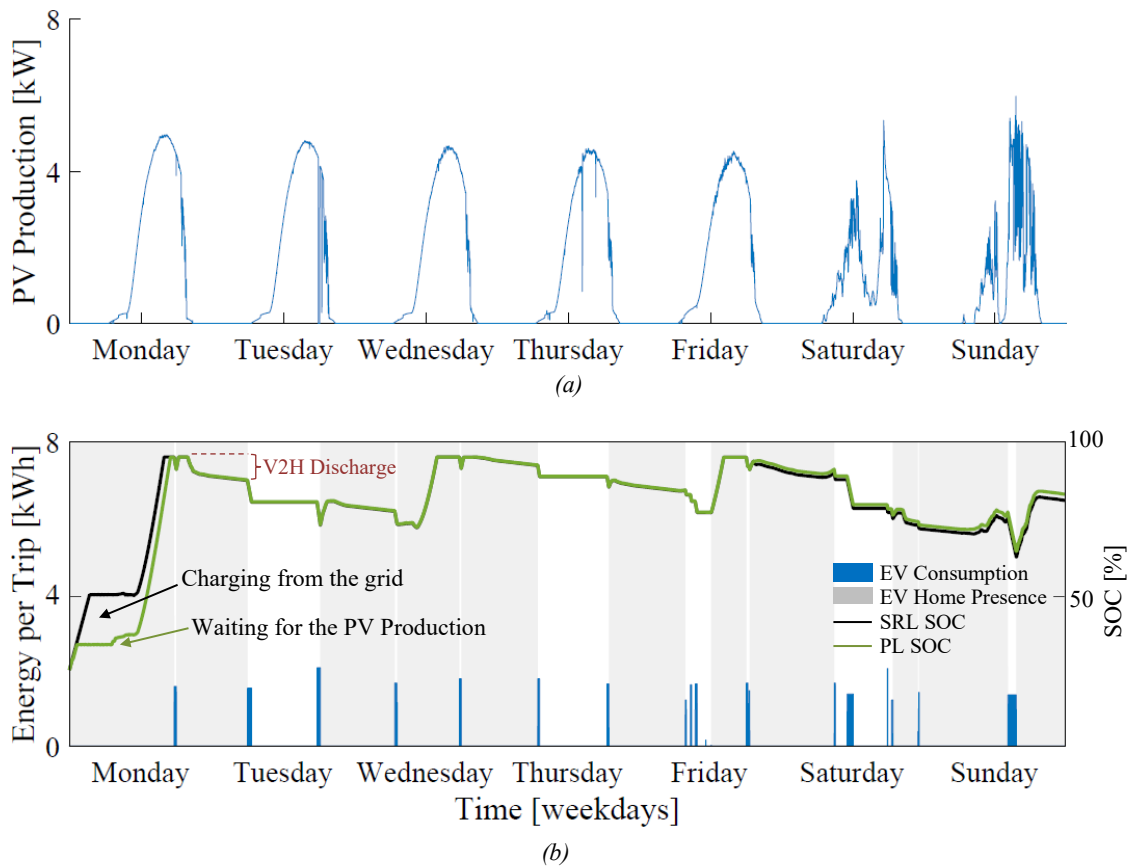


Figure 4.16 Control Algorithms comparison: PV production (a) and SOC evolution (b) - EV#C-week of July

Table 4.8 and Table 4.9 report the results of Proposed and Reference Logic (i.e., SRL), in terms of self-consumption and self-sufficiency respectively. As expected, due to the highest presence at home, EV#C reports the best results. In particular, in the week of May and July, it overcomes the 100% self-sufficiency. This is explicable with the fact that the PV production was able not only to satisfy the energy demand but also some energy was stored into the EV battery. The worst case is instead represented by EV#A which is characterized by high EV consumption and low presence at home.

Table 4.8 Self Consumption: Proposed and Reference Logic

	Proposed Logic			Reference Logic		
	EV#A %	EV#B %	EV#C %	EV#A %	EV#B %	EV#C %
Jan	54	41	88	54	41	89
May	35	43	43	35	40	42
Jul	58	38	43	57	35	40
Oct	45	22	69	45	22	69

Table 4.9 Self Sufficiency: Proposed and Reference Logic

	Proposed Logic			Reference Logic		
	EV#A %	EV#B %	EV#C %	EV#A %	EV#B %	EV#C %
Jan	24	36	70	24	35	69
May	54	95	119	53	87	113
Jul	104	119	121	100	109	111
Oct	22	18	46	22	18	44

Table 4.10 highlights the percentage deviation achieved from the proposed logic with respect to the reference one for both self-consumption and self-sufficiency indexes. From the comparison it results evident that the proposed logic creates some improvements in the warm seasons. On the contrary, no tangible differences are observed in the cold seasons.

More in detail, the proposed logic guarantees performance effects if the PV energy generated while the car is at home, thus the maximum obtainable PV energy in charge (E_{PV-EV}), is similar or higher with respect to the EV consumption ($E_{PV-EV}/E_{EV\ week} \geq 1$).

This behaviour is easy to explain with the fact that if the PV availability is very low with respect to the car needs or the car is never at home, the grid charging time positioning does not have any impact in energetic terms. To make more visible this dependence, Table 4.11 reports the obtainable PV energy in charge with respect to the EV consumption ($E_{PV-EV}/E_{EV\ week}$), confirming that the logic performance for both indexes is strongly dependent on this rate. However, in terms of self-sufficiency, little improvement becomes visible even with lower PV availability thanks to a wiser exploitation of the battery capacity (e.g., the logic temporarily disables V2H operations in order to preserve the energy for an imminent trip).

Moreover, in one case (EVC January week), a slight under-performance with respect to the reference logic is obtained. This is due to the imprecise forecasting that has left to a not optimal battery management. This aspect will be fully investigated in the next Section 4.3.1.

Table 4.10 Proposed Logic percentage deviation from Reference

	S_{cons}			S_{suff}		
	EV#A %	EV#B %	EV#C %	EV#A %	EV#B %	EV#C %
Jan	-	-	-1	-	-	+1
May	-	+7,5	+2	+2	+7,5	+5
Jul	+3,5	+9	+7,5	+4	+9	+9
Oct	-	-	-	-	-	+5

Table 4.11 EV consumption under PV energy in charge

	$E_{PV-EV}/E_{EV\ week}$		
	EV#A %	EV#B %	EV#C %
Jan	26	44	146
May	64	191	723
Jul	155	745	470
Oct	28	20	83

Finally, for a matter of comparison, Table 4.12 reports the energy indicators calculated for the four weeks without any EV. It can be noticed S_{cons} is lower than when EV#A, EV#B or EV#C are considered. On the other hand, in some cases, especially in the seasons with lower solar radiation, S_{suff} can result higher without the EV. This occurs because the absence of the EV brings to a reduced total electric load, easier satisfied by the PV generator.

Table 4.12 Case without EV: energy indexes

	S_{cons} %	S_{suff} %
Jan	26	44
May	15	63
Jul	8	52
Oct	14	23

4.3.1 Further Results

From the above analysis it follows that the performance of the Proposed Logic depends on two factors: quality of the forecasts and PV availability. These two parameters are fully investigated in the next two paragraphs. Moreover, in the analysis until now addressed it has been assumed as reference the SRL with a $SOC_{ch\ grid}$ equal to SOC_{min} . In the following, a third paragraph compares the Proposed Logic with a different EV user Charging behaviour.

Effect of the Forecasts Error in the PL Performance

The proposed logic is dependent on the quality of the forecasts. With the aim to investigate the full potential of the methodology, the logic was tested with real data as inputs of the optimization in STEP # β (exact predictions).

Table 4.13 shows the percentage deviation of the results obtained with exact predictions (a posteriori) with respect to the reference logic. The results, in this latest case, are clearly higher with respect to the proposed logic with forecasts. In particular, improvements in self-consumption and self-sufficiency of 17% and 19% respectively have been recorded for EV#C in the week of May, when the theoretical PV energy in charge is seven times higher than the car energy need. Moreover, exact prediction leads to a visible improvement in self-consumption even for the week of May of EV#A characterized by a relatively low theoretical PV energy in charge (64% of the car energy need). Furthermore, no underperformance has been obtained in the specific case of EV#C January week.

Table 4.13 Exact Prediction percentage deviation from Reference

	S_{cons}			S_{suff}		
	EV#A %	EV#B %	EV#C %	EV#A %	EV#B %	EV#C %
Jan	-	-	-	-	+3	+1
May	+3	+8	+17	+2	+9	+19
Jul	+9	+14	+10	+10	+15	+9
Oct	-	-	-	-	-	+5

As last consideration, it is worth to notice that an analysis conducted by using the Infra-day forecasts described in Section 0 (not addressed in this research), would lead to results lying between the ones related to the day ahead forecasts of Table 4.10 and the results obtained with the exact predictions in Table 4.13.

Effect of the PV Availability in the PL Performance

As shown from the above results in Section 4.3, the PV availability also effects the Proposed Logic performance. With the aim to investigate this effect, the logic was tested for different PV plant sizes.

Figure 4.17 and Figure 4.18 show the behaviour of the proposed logic both with forecasts and exact predictions (a posteriori) for the worst case of EV#C January week. In particular, Figure 4.17 shows in a histogram the self-consumption indexes while Figure 4.18 provides the self-sufficiency indexes.

The results show that already with 12 kWp plant the proposed logic does not anymore underperform the reference, while a potential 13% increment in self-consumption is obtainable with exact predictions (Figure 4.17).

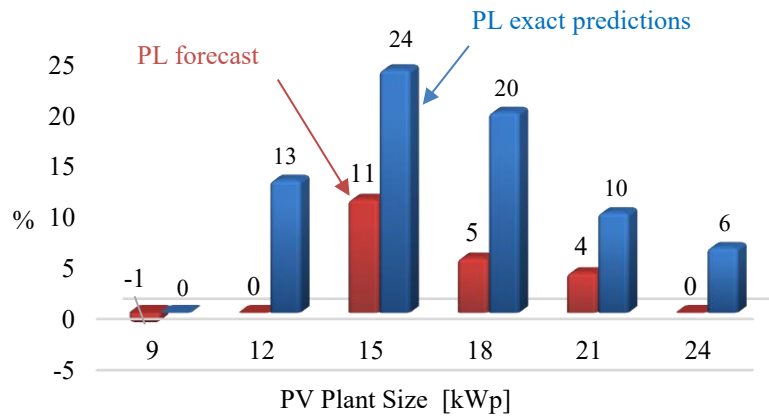


Figure 4.17 Self-consumptions for different PV plant sizes: PL and PL with exact predictions - EV#C week of January

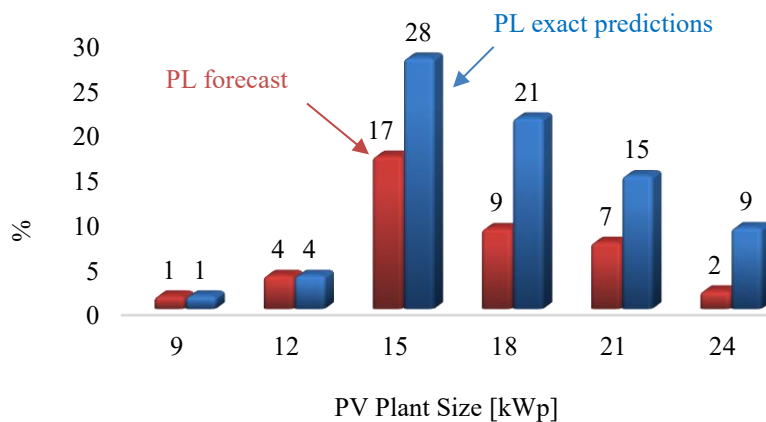


Figure 4.18 Self-sufficiencies for different PV plant sizes: PL and PL with exact predictions - EV#C week of January

For the considered case (i.e., EV#C January week) and with the EV battery capacity considered (40 kWh), the best result is achieved with the 15 kWp plant. In particular, the improvements of the Proposed Logic reach 10% and 20% for Self-consumption and Self-sufficiency, respectively. On the other hand, the potential improvements of exact predictions are in the order of 25% and 30% respectively. Higher PV plant sizes lead to an earlier battery capacity filling reducing the possibility of the logic to operate, thus reducing the benefits.

Different EV User Behaviour: Effect on Reference Logic

In the analysis until now addressed the Simple Rule-based Logic has been used as reference. The SRL consists of the Self-consumption Logic and the Charge once Home Logic. This latest Logic aims to simulate the EV user charging behaviour. As explained in Section 4.2.1, the Charge once Home Logic represents already a virtuous behaviour of the user if $SOC_{ch\ grid}$ is chosen equal or close to SOC_{min} . In this case, in fact the EV user makes available for the PV production most of the battery capacity.

This paragraph aims to show the effect in self-consumption and self-sufficiency if $SOC_{ch\ grid}$ is chosen to be equal to 50%. In this case, the EV user starts charging the EV from the grid if once at home the State of Charge is less or equal to 50%. Thus, in the facts, making available for the PV production and V2H operations just half of the total battery capacity.

Table 4.14 reports the absolute S_{cons} and S_{suff} for the considered case respectively. Meanwhile, Table 4.15 reports the percentage deviations of the Proposed logic with respect to this new reference. From the results it can be seen that improvements are now present in the majority of the cases. In particular, the deviations lie around 10%; maximum values are found for the week of May of EV#C with 19% and 22% for Self-consumption and Self-sufficiency, respectively.

Table 4.14 Energy Indexes: SRL-Reference Logic with $SOC_{ch\ grid}=50\%$

	S_{cons}			S_{suff}		
	EV#A %	EV#B %	EV#C %	EV#A %	EV#B %	EV#C %
Jan	54	41	76	24	35	56
May	32	36	39	48	78	103
Jul	56	33	37	96	100	102
Oct	43	22	66	21	17	41

Table 4.15 PL Percentage Deviation from SRL with $SOC_{ch\ grid}=50\%$

	S_{cons}			S_{suff}		
	EV#A %	EV#B %	EV#C %	EV#A %	EV#B %	EV#C %
Jan	-	-	+16	-	-	+25
May	+9	+19	+10	+13	+22	+16
Jul	+4	+15	+16	+8	+19	+19
Oct	+5	-	+4	+5	-	+12

4.4 Future Works on EV and PV integrations

This Chapter has discussed the methodology proposed in order to manage the charge/discharge pattern of an EV battery connected to a household provided of a PV plant. The methodology is hybrid and uses historical data and complete forecasting for all the variables of the system (EV consumption, PV generation, and loads), in order to optimize the battery management over a defined time window (one week). The aim of the optimization is the reduction of power exchanges with the grid, thus the improving of self-consumption and self-sufficiency indexes. On the other hand, a rule-based logic ensures the real time management.

The proposed logic was compared with a pure hierarchical approach (simple rule-based logic). The results have shown tangible improvement in self-consumption and self-sufficiency with respect to the pure hierarchical approach (up to 9%_{rel}), if the PV availability is not too low compared with the EV energy need.

Future works could test the same approach also in application different from households, such as offices, industrial or commercial buildings provided with PV plants. In these latest cases, in fact, the proposed hybrid approach may lead to better performance due to the higher availability of EVs for charging/discharging operations during sunlight hours. Others possible improvements may regard the optimization time window (in this work one week), which can be enlarged or shortened in order to find the best compromise between quality of the results and computational time.

Finally, in order to reduce the errors due to the EV miss-forecasts, future works could consider the use of the infra-day EV forecast logic.

Chapter 5

EVs Grid Integration: A Vehicle to Grid Case Study

As discussed in Section 2.1, the EVs batteries have the potential, if opportunely controlled, to provide grid services with the ultimate purpose of ensuring safety, reliability, and efficiency of the power grid operations. In order to provide such services and assure adequate charge levels, a new entity called Aggregator must intercept the role of control and optimization of the power exchange between the EVs and the power system [34]. As already seen in Section 2.3, different Architectures are possible (centralized and decentralized architectures), and different optimal management approaches have been proposed in literature such as deterministic, stochastic and forecast based optimization.

This Chapter proposes a methodology to integrate EVs and the power system aiming to maximize the economic benefit achievable by an appropriate exploiting of the V2G operations. The architecture used has the form of a centralized architecture and applied to a fleet of 214 EVs. Meanwhile, the approach is hybrid, thus it coordinates a forecast based optimization with a real-time management. The EVs usage future estimations are obtained through the Day-ahead EV forecast logic described in Section 3.2, thus are in the form of vehicle by vehicle future behaviors. The methodology here proposed does not make use of direct travel information provided by the EV users and an economic analysis is provided in order to measure the potential of the solution. The entire following model, simulations and results are developed in Matlab.

In the following, Section 5.1 describes the physical and the electricity market participation models. Section 5.2 discusses the proposed hybrid methodology used to assess the EV fleet management while enabling the electricity market participation. Section 5.3 presents the simulation results. Finally, Section 5.4 concludes the chapter and discusses future possible improvements on the methodology.

5.1 Model Formulation

The model presented in this Chapter refers to the Centralized Architecture already discussed in Section 2.3.1 and elucidated in Figure 2.3. The Aggregator handles the power of all the EVs under its region and allows the participation of in the EVs at the day-ahead electricity market. More in details, the electricity market can be divided in the energy market and in the reserve market. In the electricity market the Aggregator provides energy offers in order to define the power profile for the next day, thus accomplish at its energy needs. Meanwhile, in the reserve market the Aggregator provides offers in order to express its availability to provide ancillary services, thus it performs the role of a Balancing Service Provider (BSP). The services considered in this work are Replacement Reserve [28] and Secondary Regulation [29]. Finally, at the day of dispatch the Transmission System Operator (TSO) can require the activation of such ancillary services.

Figure 5.1 shows the considered model and highlights the information flows from and toward the Aggregator. The principal hypotheses in which the model is based on are:

- The aggregator has the possibility to control all the chargers where the EVs are connected.
- EVs are always connected when parked, thus vehicles are always connected if not in traveling.
- EVs are able to collect data regarding their usages and the aggregator (or an on-board logic) uses these data to forecasts the next day EVs behaviour.

In the following, Section 5.1.1 and Section 5.1.2 deeply describe the physical and the electricity market participation models, respectively.

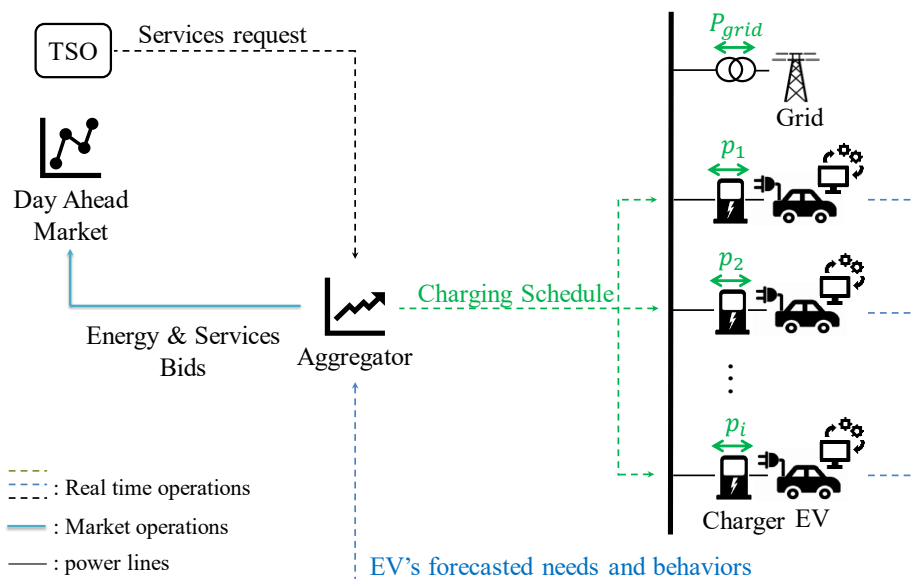


Figure 5.1 Scheme of the EVs-grid integration model

5.1.1 Physical Model

This section describes how the EVs, their travels and the chargers interact in the model formulated in the Matlab environment. First, the representation of EVs and chargers and the relative hypotheses are discussed. Secondly, how the EVs are allocated in the respective chargers is explained. Finally, the principal quantities of the model, both in terms of individual and aggregated powers and SOCs, are defined.

EVs and Chargers Definitions

The EVs behaviours during a day are modelled with the vehicle usage profiles described in Section 3.1. Moreover, it is assumed that a single vehicle is always connected in a bidirectional charger point when not in travel. Finally, it is assumed that at the end of a simulated day the car is always connected to the same charger in which it has been at the beginning of the day (assumed as home).

Figure 5.2 shows, as an example, the last Monday of the first vehicle in the dataset. In the following it is referred to this vehicle with EV#1. At midnight, EV#1 is parked near EV#1 user's home through a bidirectional power charger (i.e., CH-home). At 5:54 A.M., the first trip occurs. This trip lasts 44 min, thus at 6:38 A.M. it arrives to another place (e.g., workplace). Under the made assumption EV#1 has the possibility to be connected through a bidirectional power charger also in this place (i.e., CH-work). At 04:05 P.M. another trip occurs, since it is the last trip of the day, it is assumed that it is addressed to home. This last trip lasts 54 min, thus at 04:59 P.M., EV#1 is again parked close to the EV#1 user's home through a bidirectional power charger.

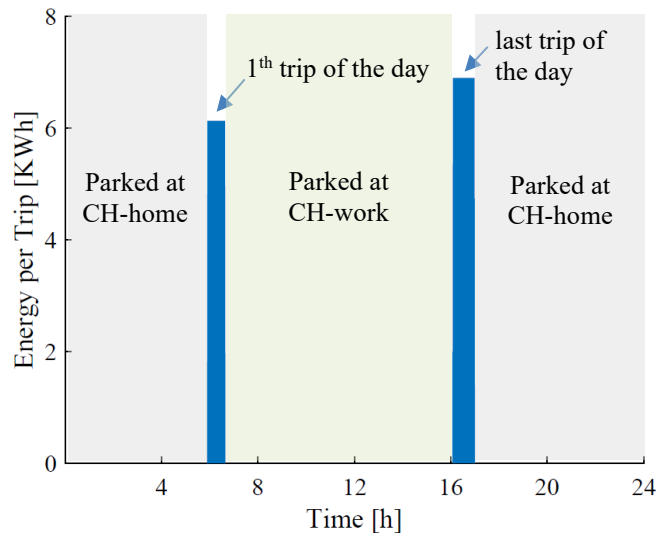


Figure 5.2 EV-to-charger connections: battery availability hypothesis

The chargers are modelled with N vectors \mathbf{Ch} corresponding to the N numbers of chargers considered (i.e., $\mathbf{Ch}_1, \mathbf{Ch}_2, \mathbf{Ch}_3 \dots \mathbf{Ch}_N$). A generic charger is indicated with i . Each vector \mathbf{Ch}_i assumes value 0 when no car is connected to the i^{th} charger, while it assumes value 1 when a car is connected to the i^{th} charger.

$$Ch_i = \begin{cases} 1, & \text{if charger } i \text{ has an EV connected} \\ 0, & \text{if charger } i \text{ has not an EV connected} \end{cases} \quad (5.1)$$

In the example of Figure 5.2, CH#1 is occupied from midnight to 5:54 A.M. and from 04:59 P.M. to midnight by EV#1, thus in this periods Ch_1 assumes the value of 1. Meanwhile, CH#1 is available for other vehicles between the 6:38 A.M. to the 4:05 P.M. On the contrary, the charger at the workplace is occupied by EV#1 from 6:38 A.M. to 4:05 P.M., while it is available for other vehicles in the early morning and in the evening.

EVs Allocation on Chargers

As above described, in the morning and in the evening EV#1 is allocated to CH#1. This operation is done for all the vehicles. Every vehicle is associated with the relative charger assumed as the charger near the home of the user (i.e. EV#1 associated to CH#1, EV#2 associated to CH#2 etc.). Thus, in morning and evening all the EVs are directly associated to the respective chargers. In order to assign at EV#1 also the generic charger i in the rest of the simulated day, a charger Availability Criteria is used. For this scope a Charger Scheduling Algorithm (CSA) is created.

- First, all EVs are allocated to their respective chargers (i.e. EV#1 associated to CH#1, EV#2 associated to CH#2 etc.) for the morning and the evening of the simulated day.
- At the end of the first trip, EV#1 looks for a charger in which has to be allocated for a certain period (e.g. EV#1 looks for a charger in which to be parked for 6 hours).
- Charger Scheduling Algorithm checks if a charger is available for the next 6 hours; thus, if in the required period the charger is not occupied from the vehicle that uses it as home charger or from other vehicles. In general, CSA conducts its research from CH#1 ahead, excludes the charger of origin of the trip, and chooses the first that requires this condition (i.e. for EV#1 finds CH#4).
- EV#1 is allocated to CH#4, thus its state will be changed from available to occupied.
- At the end of the first trip, EV#2 starts looking for a charger and the algorithm is repeated until all the EVs are allocated during the entire simulated day.

Figure 5.3 shows the positioning of the first three vehicles of the dataset in five chargers. The allocation is based on the EV usages discussed in Section 3.2.3 (last Monday in the dataset). EV#1 leaves CH#1 and after its first trip goes to

CH#4, then it goes back to CH#1. EV#2 leaves CH#2 and after its first trip goes to CH#1 for a short period before the next trip with CH#5 as destination, then EV#2 goes back to CH#2. Finally, EV#3 stays parked at CH#3 for almost all day, until the 06:16 P.M. when the first trip occurs. The duration of this trip is 10 min and its destination is CH#4. At 08:38 P.M., with a duration of 12 min, the second and last trip occurs with destination again CH#3. Due to the relative short duration of the trips, especially in this latest case, it is not always easy to distinguish the departure and arrival times with the used scale of the graph.

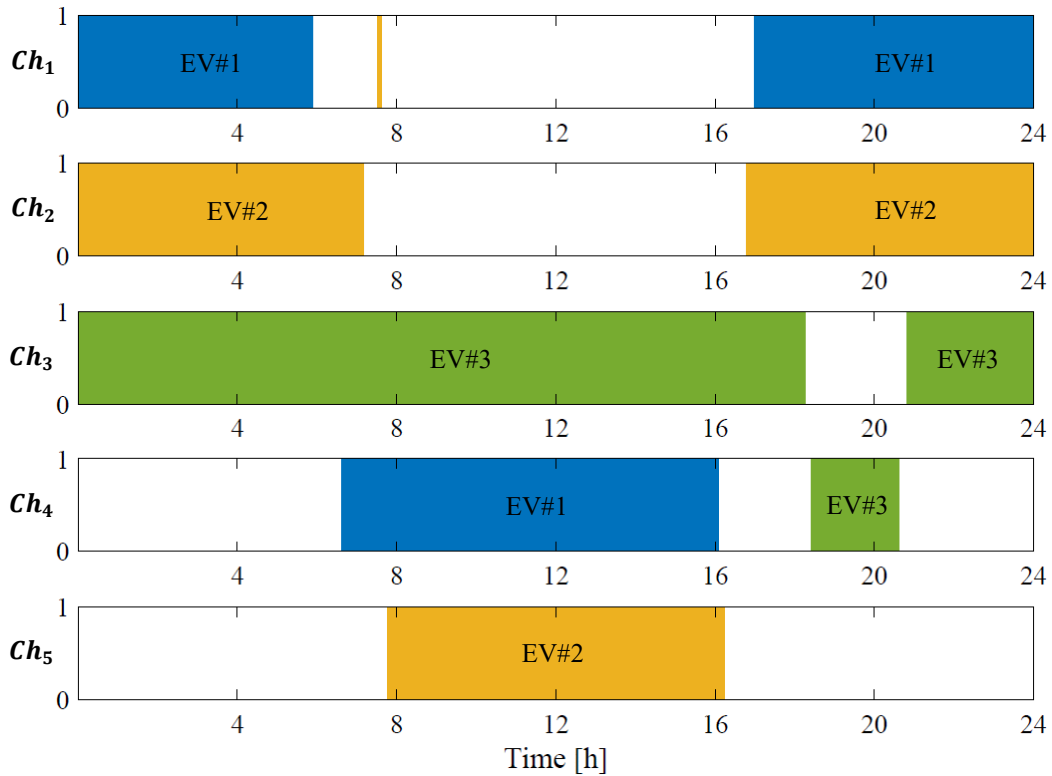


Figure 5.3 EVs allocation in chargers

All the 214 EVs of the Dataset have been allocated with CSA. With the used methodology of allocation, and under the condition that EVs are always parked and connected if not in travel, the number N of needed Chargers results in 225.

Aggregated State of Charge and Power

The State of Charge of the generic vehicle j in a time step t is indicated with $SOC_{j,t}$ and defined as follows:

$$SOC_{j,t} := \begin{cases} SOC_{j,t-1} + 100 \cdot \left(\frac{p_{i,t} \cdot \Delta t}{E_{batt,Tot}} - \frac{E_{EV,t}}{E_{batt,Tot}} \right) & \text{if } p_{i,t} \geq 0 \\ SOC_{j,t-1} + 100 \cdot \left(\eta_{rt} \frac{p_{i,t} \cdot \Delta t}{E_{batt,Tot}} - \frac{E_{EV,t}}{E_{batt,Tot}} \right) & \text{if } p_{i,t} \leq 0 \end{cases} \quad (5.2)$$

Equation (5.3) defines the SOC similarly to Equation (4.10). However, it is indicated with $p_{i,t}$ the power delivered or adsorbed from the charger i to the vehicle therein connected at the time step t . For example, for EV#1 before its first trip, $p_{i,t}$ corresponds to with the power provided by CH#1.

For sake of clarity, here the meanings of the other variables are again listed. The quantity η_{rt} is the round-trip efficiency (fraction of energy put into the storage that can be retrieved). The variable $E_{batt,Tot}$ is the battery capacity of the car. Finally, $E_{EV,t}$ is the energy among the time associated to the EV trips. In particular $E_{EV,t}$ assumes the value of 0 if no trips occur in t , while the energy used for a certain trip z ($E_{trip z}$) is instantaneously absorbed at the trip starting time $t_{start z}$. Thus, the SOC is subtracted of the respective trip energy percentage portion at each trip starting minutes.

However, the State of Charge of a vehicle is not always available for the Aggregator. Actually, when a car is in travel (not connected), the capacity of its battery cannot participate in the aggregated capacity. To consider this issue, it is useful introduce the SOC of the Charger as $SOCH_i$. This variable indicates the evolution of the States of Charge that the Charger i can read during the day. The variable $SOCH_i$ is defined in Equation (5.3) where with j^\wedge is indicating the generic vehicle connected in the charger i at t .

$$SOCH_{i,t} := \begin{cases} SOC_{j^\wedge,t} & | \text{if EV } j^\wedge \text{ connected in } i \text{ at } t \\ 0 & | \text{else} \end{cases} \quad (5.3)$$

In the example of Figure 5.3 CH#1 assumes the State of Charge of EV#1 until its first trip. Later, for a short period it assumes the SOC of EV#2 (after its first trip and before its second trip). Finally, in the evening CH#1 assumes again the SOC of EV#1. In all the other moments, $SOCH_1$ is equal to 0. It should be noted that every time a car is connected to a charger, the SOC of the car is already updated considering the subtraction of energy due to the trip. In fact, Equation (5.3) ensures this operation through the variable $E_{EV,t}$.

The Aggregated State of Charge $SOC_{BSP,t}$ is defined as the sum of the $SOCH_{i,t}$ of the Chargers under the control of the Aggregator (or in general BSP), divided by the total number of vehicles NV . Thus, it represents the amount of energy stored into the EVs with respect to the aggregated battery capacity. The total battery capacity of a car is assumed 40 kWh and the number of vehicles is 214, thus the aggregated battery capacity is 8,5 MWh.

$$SOC_{BSP,t} := \sum_i^N \frac{SOCH_{i,t}}{NV} \quad (5.4)$$

Finally, the Aggregated Power is defined as the sum of the powers $p_{i,t}$ delivered or adsorbed from the charger i .

$$P_{BSP,t} := \sum_i^N p_{i,t} \quad (5.5)$$

5.1.2 Participation in the Electricity Market

The first objective of the Aggregator is guaranteeing the amount of energy required from the vehicles during a day of usage. This amount of energy must be provided punctually to the different vehicles and at the most appropriate time in manner to satisfy all the EV user's mobility needs.

However, as Balancing Service Provider the Aggregator, needs also to reserve part of its capacity in order to provide grid services in case they are required from the TSO. Assuming D as the current day in real-time, the fleet energy needs (thus the Power Profile at D), must be defined in the electricity market at the day $D-1$. This Power profile will be defined considering also the reserve for the grid services in the eventuality they will be required the next day (activation). More in details, two grid services are considered: Replacement Reserve and Secondary Reserve.

Figure 5.4 shows a simple Market Model. At the day $D-1$ Power Profile for the next day is defined in the Day-Ahead Energy Market. Contemporarily in the Reserve Market the availability to address ancillary services such as the Replacement or Secondary regulation, is defined. At the day D , the Power Profile defined the previous day is effectively dispatched. Moreover, the reservation of capacity can be activated by providing the grid services if they are required.

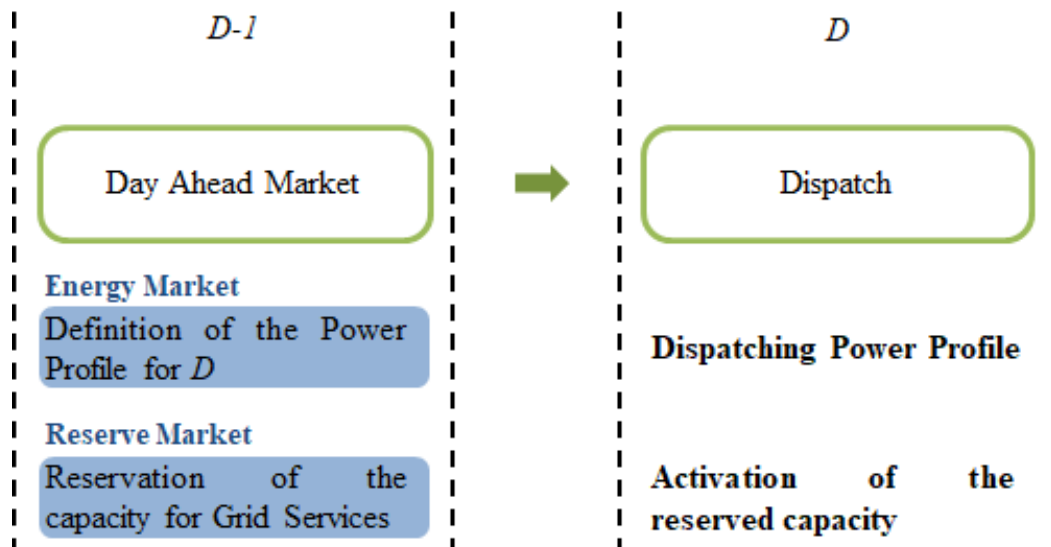


Figure 5.4 Market model and services activation

In this work the 6th of April 2020, a Monday, is chosen as day of dispatch D . This choice is motivated by the fact that the first days of the April 2020 have been characterized by a low national electricity load in Italy due to the Covid-19 pandemic. Thus, the electricity price has been affected. This scenario with low electricity absorption and high renewables penetration, can be consistent with a next future electricity grid scenario. Therefore, the choice of the 6th of April as day D , has the ambition to provide a future perspective to this work.

In the following, firstly the participation in both energy and reserve day ahead market is discussed, and the relative ancillary services are deeper described. Then, the cost or economic benefit achievable by the EV fleet is defined.

Day Ahead Energy Market: Energy Arbitrage Criterion

In the Day Ahead Market, the Aggregator needs to define the Power Profile of the next day in order to buy the energy that it needs if he directly. This means having the knowledge of the energy that it is necessary for the vehicles and how it is distributed during the day. However, the Aggregator it is not just an energy consumer. Indeed, under the made assumptions, all the vehicles are enabled for bidirectional power exchanges. It follows that during the Day Ahead Market, the aggregator can, not only buy, but also offer some energy to the market.

In this work it is assumed that the Aggregator participates in the Day Ahead Energy Market aiming to obtain a Power Profile P_{base} able to guarantee the EV user's mobility needs with the minimum cost. At this purpose the aggregator makes use of an Energy Arbitrage Strategy. As Energy Arbitrage revenue, it is intended the difference between the revenue received during the energy sales (discharges) and the charging cost which includes also the additional energy due to losses [106]. Thus, the Energy Arbitrage Strategy is the set of operations that the Aggregator needs to do in order to maximize this revenue, thus minimize the charging cost.

Figure 5.5 shows the Energy Arbitrage criterion. At the top of the figure an example of daily Electricity Price profile is shown. Meanwhile at the bottom of the figure, the Power Profile obtained according with the Energy Arbitrage Strategy is presented. In the first part of the day, the Electricity Price is low, thus it is convenient to purchase energy, thus charge (positive profile). In the second part of the day, the price of electricity becomes higher, thus it is convenient to stop buying and start selling energy, thus discharge (negative profile). Exploiting this criterion, at the end of the day the Aggregator can acquire the energy it needs for the EVs trips with a remarkable cost reduction.

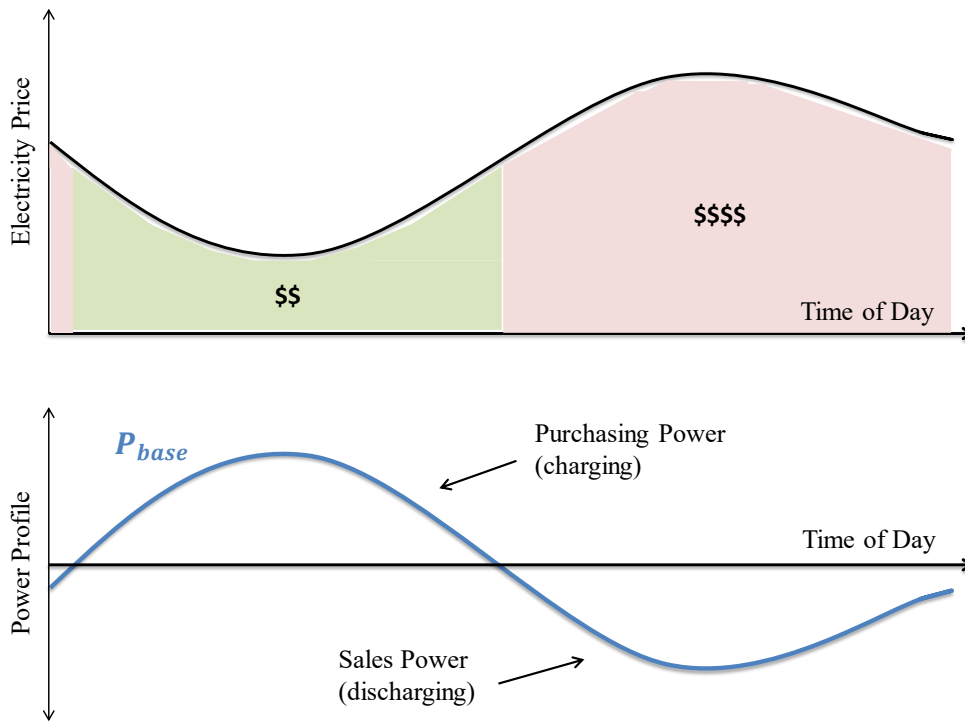


Figure 5.5 Energy arbitrage criterion

For the sake of simplicity, in Figure 5.5 the Electricity Price is shown as an unique profile which valorises equally the energy purchases and the energy sales. However, in the reality a slight difference is present. Figure 5.6 shows the real Electricity prices for the considered day D (April 6th, 2020). The grey profile is the cost of the energy purchases (charges), while the orange profile is the price at which the energy sales (discharges) are valorised during the day. The two profiles are almost completely overlapped.

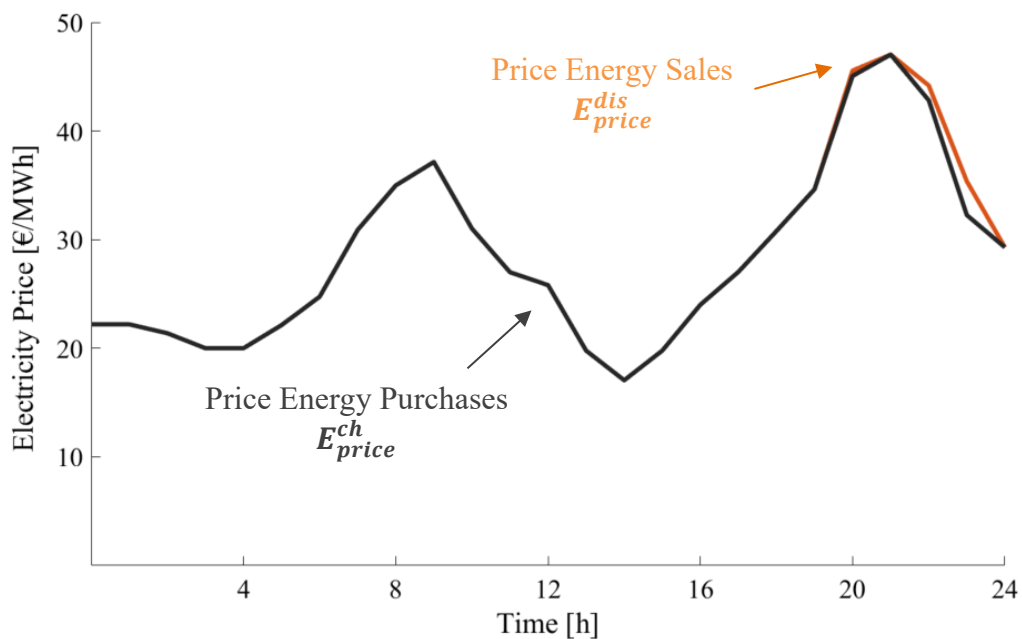


Figure 5.6 Electricity cost/price: Italy - April 6th 2020

In the following it is referred to the electricity cost profile for charging as E_{price}^{ch} , while to the electricity price paid for the discharges as E_{price}^{dis} . Finally, the variable E_{price} synthesizes both cases as in Equation (5.6).

$$E_{price} := \begin{cases} E_{price}^{ch} & |if P_{base} \geq 0 \\ E_{price}^{dis} & |if P_{base} \leq 0 \end{cases} \quad (5.6)$$

Finally, as above mentioned, the Power Profile P_{base} cannot be defined exclusively basing on the Energy Arbitrage Strategy. In fact, the power of the next day needs to be defined also in manner to maintain available part of the Aggregated Capacity in order to satisfy the grid services. This operation is deeper discussed in the following.

Reserve Market: Replacement Reserve Availability

If an Aggregator is proposed to provide Grid Services, it becomes a Balancing Services Provider (BSP). At this scope in the Day Ahead Market, the BSP must reserve part of its capacity in the eventuality that at the day D the TSO requires the activation of some Grid Service.

The model here proposed is based on the recent regulatory development on the Italian ancillary services market discussed in Section 1.2.2. From the 2017 (directive 300/2017) at the Reserve Market participation not only Relevant Production Units are enabled but also Aggregators. However, some conditions are required to this last's subjects. The specific requirements used to define the economic model of this work are listed below.

- The Aggregator must be able to change its Power Profile by reducing its power adsorption (or discharging) at least of 1 MW. In other words, the Control Power must be at the minimum 1 MW.
- The Aggregator must be able to change its Power Profile within 15 min from the reception the command.
- The Aggregator must be able to maintain the Power Profile variation for at least two consecutive hours. Considering the minimum Control Power of 1 MW, this means to guarantee at least 2 MWh of available energy. More in details, the BSP must guarantee always this availability within the 2:00 P.M. and the 8:00 P.M. of each day.

From the above discussion, it follows that the Aggregator in the Day Ahead Market, needs to define a Power Profile considering its possible modification during 2 h within the 2:00 P.M. and the 8:00 P.M. In particular, this variation must result in a reduction of power adsorption. However, since the Vehicles are enabled for bidirectional power exchanges, if at the reception of the command the Power Profile is less than 1 MW, the reduction results in an injection of power

toward the grid. For example, if at the moment of the reception of the reduction command, the absorption is 0.5 MW, a reduction of 1 MW results in an injection of 0.5 MW.

Figure 5.7 shows the evolution during the day of the Aggregated State of Charge defined in Equation (5.4). Within the 2:00 P.M. and the 8:00 P.M., the State of Charge must be higher than a certain level which ensures at least 2MWh of Energy to discharge without effecting the EV user's mobility needs.

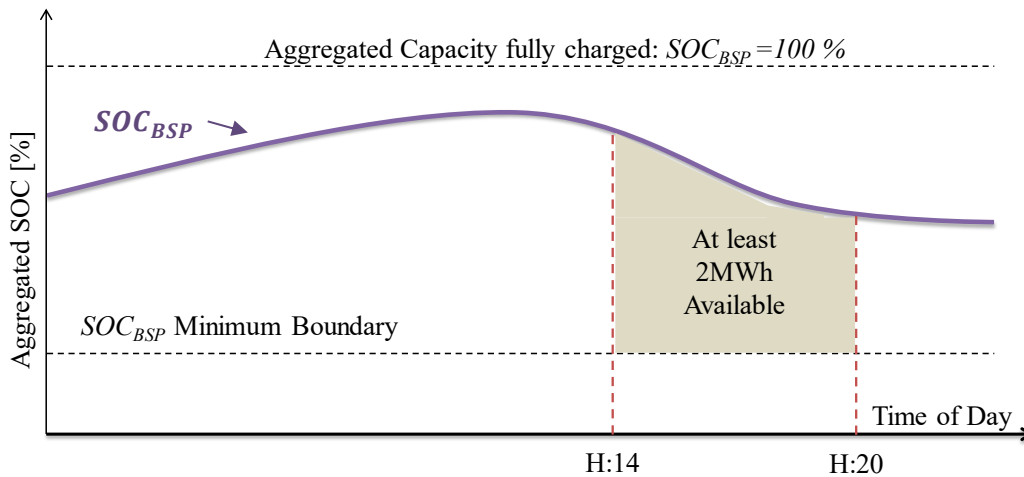


Figure 5.7 Replacement service energy reservation

At the Day of dispatch D , the TSO can require or not the reserved availability to the Aggregator. If the reserve is activated the Aggregator will be paid for the service delivered. The price paid to the aggregator depends on the trend of demand and offer of the market, thus it is not related to the electricity price shown in Figure 5.6.

In this work it is assumed that the Replacement reserve service is paid at the average price of the offers occurred in the simulated day, and it is indicated with R_{price} . More in details the R_{price} differs taking into account the type of variation: for reductions of the absorbed power (with respect to the P_{base}) it assumes R_{price}^- , for increases of the absorbed power R_{price}^+ . The case of power reduction can be assimilated to an energy sale; thus, the price must be intended as a revenue (upward regulation from the point of view of the TSO). Meanwhile, the case of power increase is in the facts an energy purchase; thus, the price is a cost (downward regulation from the point of view of the TSO).

Figure 5.8 shows the Replacement service prices for the considered day D (April 6th, 2020). The orange profile is the price at which the electricity is paid in case of power reduction (energy sale-upward regulation). On the contrary, the grey profile is the cost of energy in case the TSO requires an increase of consumption (energy purchase-downward regulation). However, this work only considers availability in power reduction for the Replacement Reserve; thus, only the orange profile must be considered in the following.

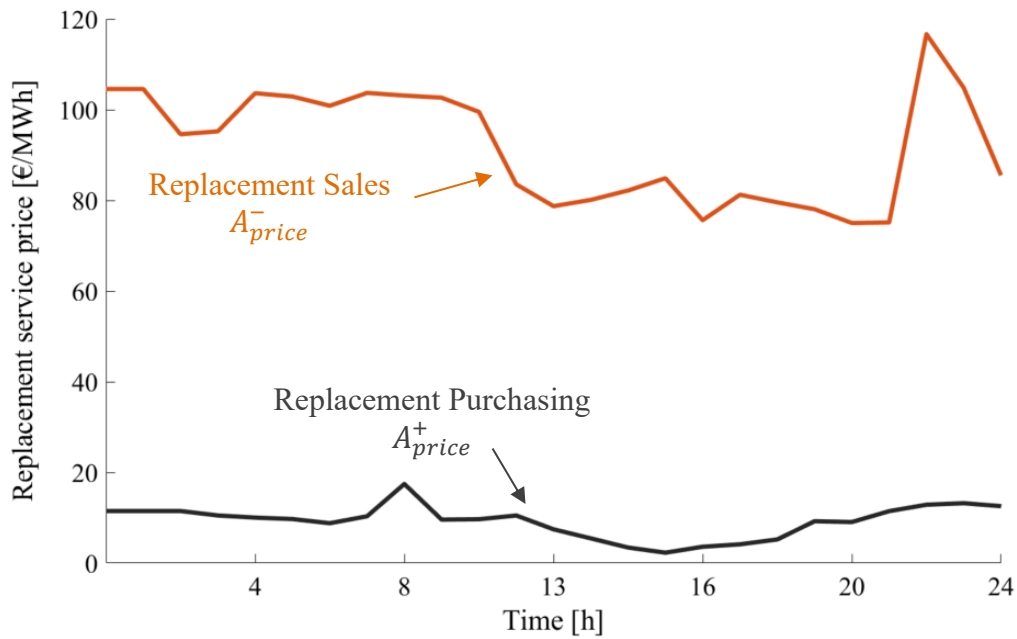


Figure 5.8 Replacement service energy cost/price: Italy – April 6th 2020

At the end of the day, the Aggregator can have a revenue due to the way exploiting of the Energy Arbitrage and the Ancillary Service provided. Then, this revenue can be partially redistributed between the EV users as reward for their battery usage. For Example, the Aggregator could stipulate with the EV users a bilateral contract that attributes a percentage of the net revenue or guarantee them free charges. This kind of agreement must be done in order to make possible the EV users' participation in the bidirectional power exchanges.

However, the conditions of this bilateral contract are out of the scope of this work. In the following, it is referred to the revenues as the net economic benefit that is possible to obtain from a single car or from the Aggregator as whole under the proposed model.

Reserve Market: Secondary Reserve Availability

In this work also the possibility that the Aggregator participates in the Secondary reserve is considered. In this case the TSO provides a Regulation Signal with the instantaneous deviation from the Power Profile. The deviation request, in this case can take place in both directions: reducing power adsorption (upward deviation) or increasing power adoption (downward deviation). Thus, the regulation Signal is here represented in the form of a percentage level, variable between -100% and 100%. The maximum entity of the deviation is instead agreed with the TSO.

Figure 5.9 shows an example of Regulation signal (top of figure) and the relative power deviation with respect to the P_{base} (bottom of figure). Even in this case the Aggregator will be paid for the provided service to the grid. The price depends on the trend of demand and offer of the market and it is indicated with S_{price} .

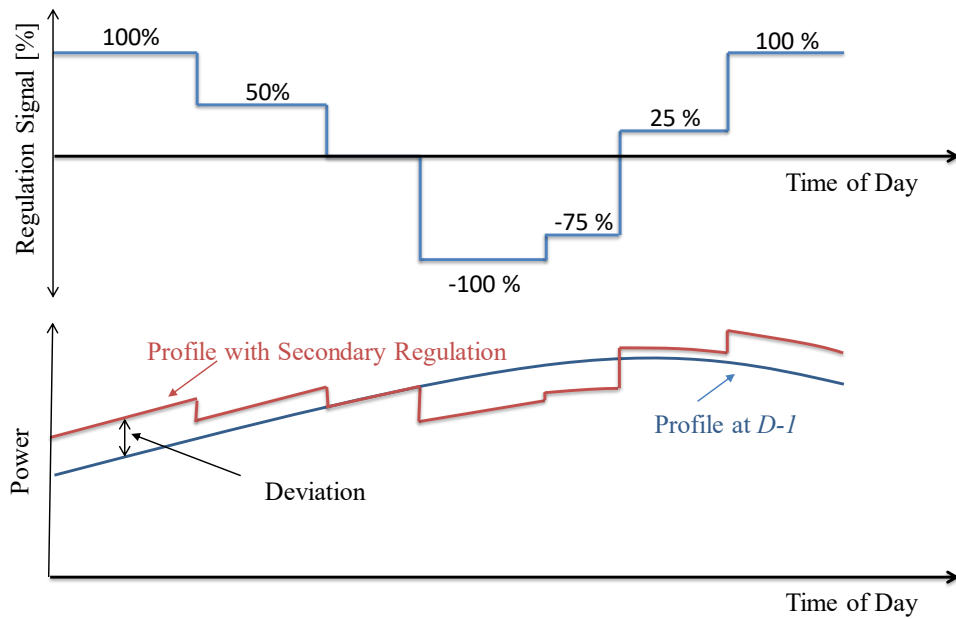


Figure 5.9 Secondary regulation: control signal and activation

More in details, S_{price} assumes different values taking into account the direction of the power deviation. The case of power reduction can be assimilated to an energy sale; thus, the price S_{price}^- must be intended as a revenue. Meanwhile, the case of power increase is in the facts an energy purchase; thus, the price S_{price}^+ is a cost. However, since the purchasing is required from the TSO, this cost is much lower than the negative deviation revenue. Thus, a net gain is possible. Figure 5.10 shows the considered Secondary Reserve prices for the simulated day D (April 6th, 2020).

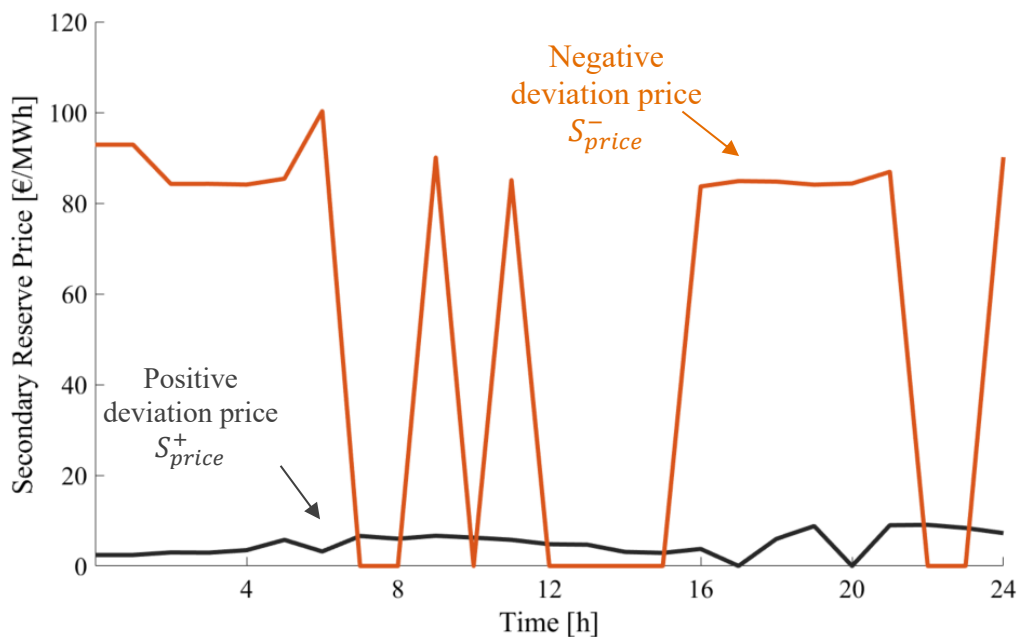


Figure 5.10 Secondary regulation energy cost/price: Italy – April 6th 2020

Finally, the revenue due to the Secondary Reserve activation can be partially redistributed between the EV users. However, this work considers the revenues as the net economic benefit that is possible to obtain from a single car or from the Aggregator as whole.

Definition of Aggregated Cost and Economic Benefit

At the day $D-1$, the BSP defines the Power Profile \mathbf{P}_{base} (i.e. the power profile of the next day if no Replacement or Secondary reserve is activated). Follows that the Aggregated Power at D already defined in Equation (5.5), is the sum of \mathbf{P}_{base} with the powers due to the activation of the grid services (i.e. Replacement and Secondary Reserve). Qualifying \mathbf{P}_R as the power variation due to the Replacement activation and \mathbf{P}_{sec} as the power deviation due to the secondary reserve activation, the Aggregated Power at D , \mathbf{P}_{BSP} can be expressed by Equation (5.7).

$$\mathbf{P}_{BSP} = \mathbf{P}_{base} + \mathbf{P}_R + \mathbf{P}_{sec} \quad (5.7)$$

In Equation (5.7), all the variables are written in form of vectors, thus they have to be intended as power Profiles defined during all the simulated day. In particular, \mathbf{P}_R assumes values different from 0 only in the hours in which the Replacement service is activated (2 hours). On the contrary, \mathbf{P}_{sec} if activated, represents the power deviation with respect to \mathbf{P}_{base} among all the simulated day. Finally, in order to indicate the value of the profiles in a specific time-step t the variables $P_{base,t}$, $P_{Anc,t}$, and $P_{sec,t}$ are used respectively.

From the above follows that the Aggregated economic cost/revenue C_{TOT} can be expressed by Equation (5.8).

$$C_{TOT} = (\mathbf{P}_{base} \cdot \mathbf{E}_{price}) + (\mathbf{P}_{Anc} \cdot \mathbf{A}_{price}) + (\mathbf{P}_{sec} \cdot \mathbf{S}_{price}) \quad (5.8)$$

In Equation (5.8), \mathbf{E}_{price} represents the Electricity Price profile during the simulated day, while \mathbf{A}_{price} and \mathbf{S}_{price} are the price paid to the BSP for the grid services provided; as defined in the previous paragraphs. It worth to notice that in Equation (5.8), all the prices are positive values while the power can assume negative values (selling energy to the market). Thus if C_{TOT} presents a negative value, this must be intended as a net economic benefit or a gain. Moreover, since the Aggregated cost/gain is obtained exploiting the power of each vehicle, it can be expressed also as the sum of the cost/revenue c_j of each j vehicle:

$$C_{TOT} = \sum_j^{NV} c_j \quad (5.9)$$

For sake of clarity, in the following, the case with negative values of C_{TOT} will be distinguished with the Gain G_{TOT} .

Despite the grid services provision, the Aggregator every day has a net energy consumption due to the fleet energy requirement for travels. Moreover, depending on the final occurred power profile P_{BSP} , the Aggregator at the end of the day, can have stored in the Aggregated Battery (AB) more, or less energy with respect to the beginning of the day. Thus, the Net Energy Purchased (NEP) can be defined as in Equation (5.10).

$$NEP = E_{fleet} + (SOC_{BSP,0} - SOC_{BSP,T}) \cdot \frac{E_{batt,Tot}^{AB}}{100} \quad (5.10)$$

In Equation (5.10), E_{fleet} is the fleet energy requirement for travels during the day. Meanwhile, $SOC_{BSP,0}$ and $SOC_{BSP,T}$ represent the State of Charge at the beginning and at the end of the day respectively. Finally, $E_{batt,Tot}^{AB}$ is the total capacity of the Aggregated Battery equal to 8,5 MWh.

Finally, the Cost of the Net Energy Purchased is indicated with $CNEP$. This variable is defined in order to have a comparison between the Aggregated cost/gain and the value of the net energy acquired from the Aggregator. In fact, the $CNEP$ can be considered as the cost that the Aggregator would have incurred if no V2G operations were allowed. $CNEP$ is calculate by multiplying the Net energy purchased with the Electricity price average among the day $\overline{E_{price}}$, Equation (5.11).

$$CNEP = NEP \cdot \overline{E_{price}} \quad (5.11)$$

5.2 Aggregator Management: Proposed Methodology

Congruently with the methodology of Chapter 4, here is proposed a methodology which permits to the Aggregator to manage the EVs fleet. The proposed methodology aims to provides the grid services maximizing the obtainable economic benefit and contextually satisfy the EV users' mobility needs. Moreover, as it is structured the methodology is fully automatic, thus do not require for its working any further travel information provided directly from the users. In fact, an EV user can be discouraged to make available his car for V2G operations if he must constantly adduce his forthcoming travels. In addition, it is not guaranteed that the EV user provided information will correspond with his next real behaviour. However, in future application, any further EV user's information can be used to improve the performance of the proposed logic.

Figure 5.11 shows the flowchart of the proposed methodology for the scheduling and powers control the of the EV fleet.

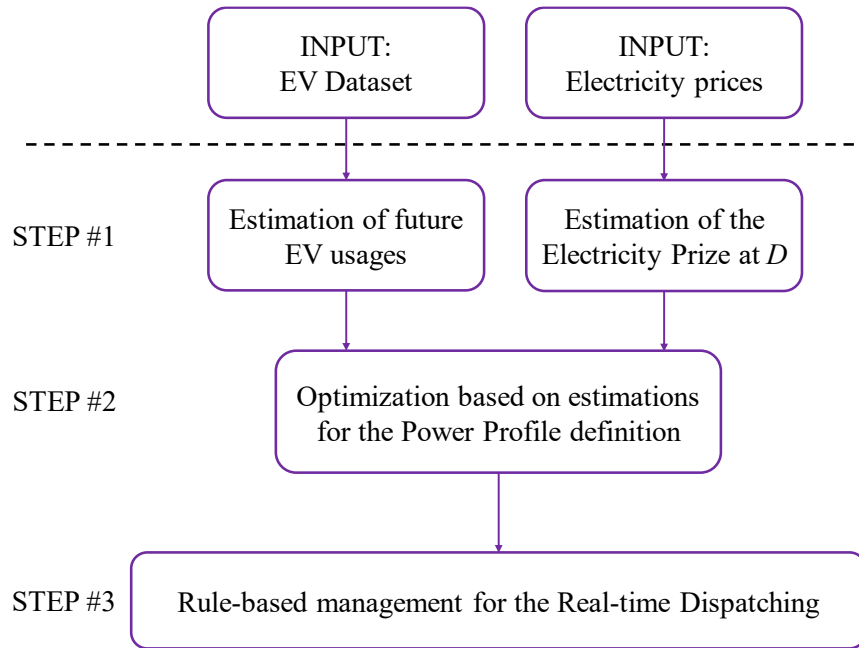


Figure 5.11 Proposed procedure flowchart (EV fleet)

The inputs of the Control Algorithm are the historical data related to the EVs usage (dataset in Section 3.1), and the historical daily profiles of the electricity price. Starting from these inputs the algorithm is then articulated in three steps indicated with numbers (i.e., STEP #1, STEP #2 and STEP #3).

- In STEP #1, each dataset is elaborated to estimate the next day profiles. Regarding the EVs, the historical data of each vehicle of the dataset (214 EVs) are elaborated. The Day ahead forecast procedure discussed in Section 3.2.1 is used at this purpose. Meanwhile, for the electricity price forecast, an Autoregressive Moving Average based Algorithms (ARMA) is used. The future estimated profiles are provided in a daily base with a time-step of 10 minutes.
- In STEP #2, the next day estimated profiles are used to run an optimization problem which aim to define the Power Profile \mathbf{P}_{base} of the next day (i.e. the Power Profile in absence of Replacement or Secondary Reserves activation). However, the optimization problem needs to consider the possible activation of the grid services. Thus, the base power profile is defined in manner to maintain available the needed reserve.
- In STEP #3, a Rule-based logic implements the real time power dispatch. It will force the Power Profile \mathbf{P}_{base} defined in STEP #2 and will activate the eventual grid services considered (i.e. Replacement Service, Secondary regulation).

STEP #1, STEP #2 and STEP #3 are detailed presented in the next paragraphs.

STEP #1: Forecast of Electric Vehicle Usage Profiles

In order to estimate next day behaviour of the EVs fleet, it is used the procedure described in Section 3.2.1. The procedure refers to a Day Ahead Forecast routine. In particular, the routine is able to individuate eventual systematic usage of a certain vehicle from its historical data. Thus, it returns the most probable EV future behaviour. Moreover, in order to capture as much as possible systematic behaviours, the logic operates a differentiation between the weekdays (e.g. treats separately Mondays from Tuesdays from Wednesday etc.).

As above mentioned, the considered day of dispatch D (April 6th 2020) is a Monday. Thus, for all the vehicles in the dataset (214) it calculated the most probable usage for the next Monday as shown in Section 3.2.3. Furthermore, an average error of the forecast has been calculated. This is done in order to have an idea on the possible deviation of the forecast with respect to the real next day behaviour. This average error has been calculated similarly to that defined in Section 3.2.2. However, for the case in Chapter 3, the errors have been calculated comparing the forecast of a certain vehicle with the last Monday usage. Meanwhile, now the forecast is compared with all the Mondays in the dataset of that vehicle. Results an average error proper of each vehicle and each weekday that returns the reliability of a specific forecast. In the following it is referred to this error with the symbol \overline{TE}_j^{all} . It will be used in the next paragraphs in order to define the boundary minimum SOC of each charger.

Finally, in order to define when it is expected that a certain car is connected to a bidirectional charger a similar approach to that in Section 5.1.1 is used. It is considered that the EVs are always connected to a bidirectional charger if in the time step t no travel is forecasted. Thus, the forecasted Charger are defined and indicated with \widehat{Ch}_t .

STEP #1: Forecast of Electricity Price

In order to estimate the next day Electricity Price, it is used an Autoregressive Moving Average based approach, congruently with what has been discussed in Section 4.2.2.

The estimated electricity price for the day D (April 6th, 2020) is calculated as the hour by hour average of the previous four Monday's prices. In the specific case the electricity price profiles of March 9, March 16, March 30 of 2020 are used. Due to the similarity between the charging cost E_{price}^{ch} and the discharging price E_{price}^{dis} , the electricity price forecast is based only on the charging cost data.

Figure 5.12 shows the estimated Electricity Price \widehat{E}_{price} (in red) and the real Italian Electricity Price E_{price}^{ch} occurred April 6th, 2020.

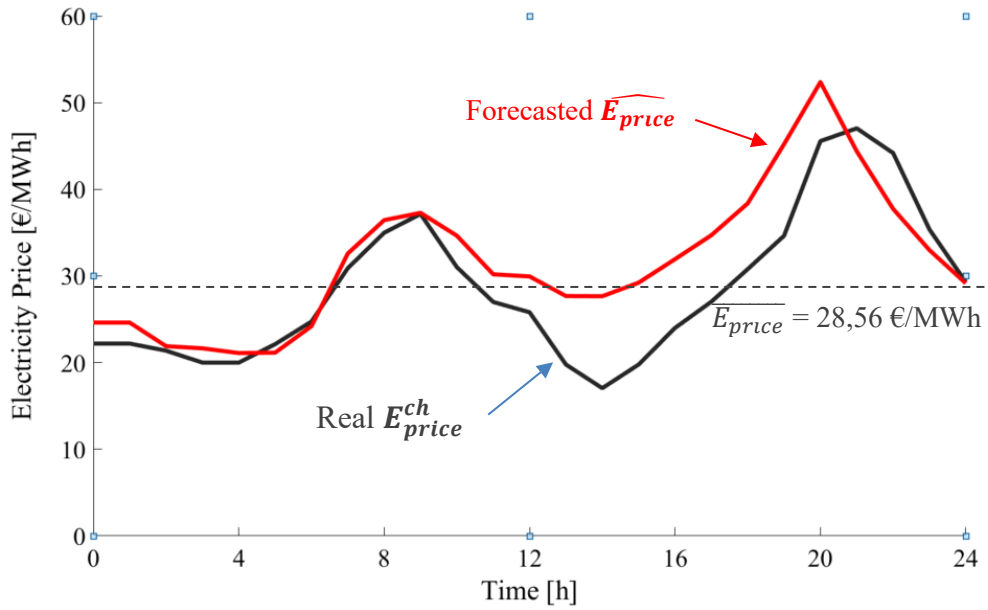


Figure 5.12 Forecasted and real electricity price: Italy – April 6th 2020

STEP #2: Optimization of the Power Profile Based on Forecasts

The aim of STEP #2, is define a Power Profile for the next day which ensure the EV user's mobility needs with the minimum cost. To do this, the Energy Arbitrage Strategy is used. However, at the day of dispatch D , there is the eventuality of grid services activation. Thus, the Power Profile must be defined also in manner to maintain the Aggregated State of Charge to a level which guarantee a certain availability in charge and a certain availability in discharge. In order to achieve this goal STEP #2 is formulated as a multi-objective optimization problem and performed through "Yalmip" Matlab tool.

The optimization consists of the multi-objective function defined in (5.12). The objective function is the sum in t of three different objectives.

- The first objective is related to the Energy Arbitrage Strategy. The variable $P_{base,t}$ is the variable that need to be found, thus the output of the optimization. Meanwhile, similarly to what defined in Section 5.1.2, \widehat{E}_{price_t} is the forecasted Electricity Price at t . Thus, in this first objective, it is asked to find the Power Profile which minimize the product between power and the forecasted price of electricity.
- The second objective aims to maximize the availability in power reduction (energy sales - upward reserve). The variable AED_t indicates the Available Energy in Discharge at t . Thus, it is proportional to the difference between the level of the Aggregated State of Charge $SOC_{BSP,t}$ and its minimum boundary. Meanwhile, the variable AED_{price} is the economic price at which the energy sales are valorised. The price AED_{price} consider both the ancillary services

prices in discharge (i.e., R_{price}^- and S_{price}^- .) In this work it is obtained from historical data and assumed 105 €/MWh. The product between AED_t and AED_{price} is under fraction because the problem is formulated as a minimization, while this quantity must be maximized. Therefore, this second objective has the final effect to orient the Aggregated State of Charge close to 100%, thus guarantee a certain availability in discharge.

- The third objective aims to maximize the availability power adsorption increase (energy purchases - downward reserve). The variable AEC_t indicates the Available Energy in Charge at t . Thus, it is proportional to the difference between the level of the Aggregated State of Charge $SOC_{BSP,t}$ and its maximum value (100%). Meanwhile, the variable AEC_{price} is the economic price at which the energy purchases for grid services are valorised. In this work, AEC_{price} is obtained from historical data and it is assumed 8 €/MWh. Contrarily to the second objective, this third objective has the final effect to orient the Aggregated State of Charge close to the minimum boundary, thus guarantee a certain availability in charge. Finally, the product between the variables is under fraction because the problem is formulated as minimization, while this quantity must be maximized.

In the multi-objective function, the three objectives are considered equally important, thus no weighted factors are considerate. The formulation will compromise between the three objectives returning the power profile that better satisfy the requests. However, due to computational reasons (it takes 20 min with 10 vehicles, 1h with 15 vehicles and diverge with more than 20 vehicles) the optimization is solved on a sample of 10 vehicles, then the output is scaled in order to achieve the profile \mathbf{P}_{base} for the 214 EVs.

$$\min_{P_{base,t}} \sum_t^T \left[\left(P_{base,t} \cdot \widehat{E}_{price,t} \right) + \left(\frac{1}{AED_t \cdot AED_{price}} \right) + \left(\frac{1}{AEC_t \cdot AEC_{price}} \right) \right] \quad (5.12)$$

s.t.

$$0 \leq \widehat{p}_{i,t} \leq \widehat{C}h_{i,t} \cdot p_{i,max} \quad | \text{if } \widehat{SOCH}_{i,t} \leq \widehat{SOCH}_{i,t}^{min} \quad \forall t, \forall i \quad (5.13)$$

$$-\widehat{C}h_{i,t} \cdot p_{i,max} \leq \widehat{p}_{i,t} \leq \widehat{C}h_{i,t} \cdot p_{i,max} \quad | \text{if } \widehat{SOCH}_{i,t} \geq \widehat{SOCH}_{i,t}^{min} \quad \forall t, \forall i \quad (5.14)$$

$$0 \leq \widehat{SOCH}_{i,t} \leq 100 \quad \forall t, \forall i \quad (5.15)$$

$$\widehat{SOC}_{BSP,t} \geq \widehat{SOCH}_{BSP,t}^{min} + SOC_{2MWh} \quad h: 14 \leq t \leq h: 20 \quad (5.16)$$

The constraints of the optimization are defined as follows.

- The constraint in (5.13) imposes that if the forecasted State of Charge ($\widehat{SOCH}_{i,t}$) of the generic charger i , is in t under a minimum value, chosen as boundary, only charging is permitted. The variable $\hat{p}_{i,t}$ is the power estimated for the charger i . The variable $\widehat{Ch}_{i,t}$ indicates if at the time step t is estimated a car connected in the charger i . The variable $p_{i,max}$ is the maximum power that a single charger can inject or receive from the EV. In this work is assumed as maximum the power level that ensures a full charge of a battery in three hours, i.e. 13,3 kW. Finally, $\widehat{SOCH}_{i,t}^{min}$ is the charger SOC boundary, better defined in the following. Therefore, if $\widehat{Ch}_{i,t}$ is 0 in t (no vehicles are connected to the charger) the delivered power is zero. Meanwhile, if $\widehat{Ch}_{i,t}$ is 1 in t , only positive powers (charging) are permitted.
- The constraint in (5.14) imposes that the injected or received power at the charger i , does not overcome the power limits neither in charge or discharge. In this case if $\widehat{Ch}_{i,t}$ is 0 (no vehicles connected) the power is forced to be 0. Meanwhile if $\widehat{Ch}_{i,t}$ is 1, the power of the charger is forced between $-p_{i,max}$ and $p_{i,max}$.
- The constraint in (5.15) ensures that the forecasted charger SOC lies between the boundaries: 0% and 100%.
- The constraint in (5.16) guarantees the discharging availability for the ancillary service in the time window within the 2:00 P.M. and the 8:00 P.M. (requirements in Section 5.1.2). The variable $\widehat{SOCH}_{BSP,t}$ is the estimated Aggregated State of Charge. The variable $\widehat{SOCH}_{BSP,t}^{min}$ is the estimated Aggregated boundary State of Charge, better defined in the following. Meanwhile, SOC_{2MWh} is the State of charge level which corresponds with the minimum requested discharge availability (2MWh). In the case under analysis (with a total aggregated battery capacity of 8,5 MWh), the SOC_{2MWh} corresponds to 23%.

The boundary SOC of a charger in a certain time step $\widehat{SOCH}_{i,t}^{min}$, is defined in Equation (5.17). The SOC_{min} is a minimum value fixed in order to not stress the chemistry of the EV battery, here equal to 30%. Considering a certain time step t , the variable $\widehat{E}_{EV_{j^{\wedge}},next}$ is the energy consumption estimated for the next trip of the vehicle j^{\wedge} connected in i at t . Meanwhile, $SOC_{Toll,j^{\wedge}}$ is an added value which aims to mitigate the EV forecast error. This variable presents different values for different vehicles. More in details, $SOC_{Toll,j^{\wedge}}$ is defined in Equation (5.18) as the product between the error $\overline{TE_j^{all}}$ (defined in the previous paragraphs) and the

average trip energy consumption ($\overline{E_{EVj^\wedge}}$) of the vehicle j^\wedge . The error $\overline{TE_{j^\wedge}^{all}}$ is a measure of the reliability of the forecast for the vehicle j^\wedge . It is calculated by comparing the forecast with all the Mondays in the dataset of the vehicle j^\wedge . Moreover, $\overline{TE_{j^\wedge}^{all}}$ lies between 0 and 100%, thus the tolerance value SOC_{Toll,j^\wedge} is defined as a portion of the average trip energy consumption of the vehicle j^\wedge . From above follows, that the minimum boundary SOC of a charger changes in time basing on the car that is therein connected. Moreover, it represents the amount of energy that a vehicle needs in order to approach the next trip with an appropriate level of tolerance.

$$\widehat{SOCH}_{i,t}^{min} := SOC_{min} + \widehat{E}_{EVj^\wedge,next} + SOC_{Toll,j^\wedge} \quad (5.17)$$

$$SOC_{Toll,j^\wedge} := \overline{TE_{j^\wedge}^{all}} \cdot \overline{E_{EVj^\wedge}} \quad (5.18)$$

Finally, the estimated aggregated boundary $\widehat{SOC}_{BSP,t}^{min}$ is given by the sum of all chargers minimum boundary as in Equation (5.19).

$$\widehat{SOC}_{BSP,t}^{min} := \sum_i^N \frac{\widehat{SOCH}_{i,t}^{min}}{NV} \quad (5.19)$$

STEP #3: Rule-based Management for the real-time Dispatching

The Rule-based logic finally applies minute by minute the effective charging/discharging profile to each charger. During the day of dispatch D , the logic must be able to applies the Power Profile P_{base} (output of STEP #2) to the EVs fleet. This needs to be done in the real-time scenario, thus with an EVs behaviour in general different from the forecasts. Moreover, the Rule based logic also has the role of implementing the eventual request of grid services activation.

In order to achieve these objectives, the Rule-based logic bases on a priority criterion. In case of absence of grid services activation, the logic will apply the optimized power profile by splitting minute by minute the power $P_{base,t}$ among the different chargers, thus among the different vehicles. This operation is possible thanks to a definition of different Priority indexes proper of each vehicle and varying among the day accordingly with the EV energy need. The symbol j^\wedge , indicates the generic vehicle connected in the charger i , while t^* indicates the real time instant. The Priority, is a value between 0 and 1 which represents the portion of the $P_{base,t}$ that must be handled by the charger i according with the forecasted charging urgency or discharging disposal of the connected vehicle j^\wedge .

Therefore, in case of absence of grid services activation the charging/discharging power of each charger is provided accordingly to Equation (5.20) and the Conditions in (5.21).

$$p_{i,t^*} = \begin{cases} P_{base,t^*} \cdot PC_{j^{\wedge},t^*} & | \text{if } P_{base,t^*} > 0 \\ P_{base,t^*} \cdot PD_{j^{\wedge},t^*} & | \text{if } P_{base,t^*} < 0 \end{cases} \quad (5.20)$$

Where:

$$\sum_i PC_{j^{\wedge},t^*}=1 \quad | \quad \sum_i PD_{j^{\wedge},t^*}=1 \quad | \quad \text{with } j^{\wedge} \text{ in } i \text{ at } t^* \quad (5.21)$$

In Equation (5.20), PC_{j^{\wedge},t^*} is the Charging Priority of the vehicle j^{\wedge} at t^* ; while PD_{j^{\wedge},t^*} represent its Priority in Discharge. The Condition in (5.22) imposes that the sum of all the priority indexes in the N chargers is equal to unity. Due to this condition, in absence of grid services activation, the real-time aggregated power $P_{BSP,t}$ is equal to $P_{base,t}$ – see Equation (5.5) –, while each car will support a portion of the aggregated power.

The Charging and Discharging Priorities PC_{j^{\wedge},t^*} and PD_{j^{\wedge},t^*} are defined in Equation (5.22) and Equation (5.23) respectively. These definitions are based on the estimated EVs usage. As discussed in the previous paragraph, Equation (5.17), the variable $\widehat{SOCH}_{i,t}^{min}$ represents the estimated amount of energy that a vehicle needs in order to approach the next trip with an appropriate level of tolerance. Thus, it is the minimum State of Charge that the vehicle needs before to leave the charger i for a trip.

However, during the correct functioning of the real-time operations, the SOC of the Charger can be below $\widehat{SOCH}_{i,t}^{min}$. In this case, the rule-based logic has the role of restore the amount $\widehat{SOCH}_{i,t}^{min}$ before the next trip occurs. With this purpose is defined the Charging Priority as the rate between the current $SOCH_{i,t}$ and the forecasted minimum State of Charge $\widehat{SOCH}_{i,t}^{min}$. Then, this rate is normalized with respect to the sum of the rates for all the other chargers (in order to obtain a value between 0 and 1). In this way, the chargers, thus the vehicles, with a lower SOC will charge with a higher power (i.e. higher portion of P_{base,t^*} if positive).

Finally, the PC_{j^{\wedge},t^*} is defined until the SOC of the charger is inferior to the maximum value 99%. In fact, once reached this level, the vehicle j^{\wedge} is disabled to the charge and other vehicles will take its power portion.

$$PC_{j^{\wedge},t^*} = \frac{SOCH_{i,t^*}}{\widehat{SOCH}_{i,t^*}^{min}} \cdot \sum_i^N \frac{\widehat{SOCH}_{i,t^*}^{min}}{SOCH_{i,t^*}} \quad | \text{if } SOCH_{i,t^*} \leq 99\% \quad (5.22)$$

On the contrary, the Discharging Priority is obtained as the rate between the forecasted SOC required for the next trip $\widehat{SOCH}_{i,t}^{min}$ and the current $SOCH_{i,t}$ (inverse of the prior rate). In fact, if the SOC of a charger, thus a vehicle, is close to the full charge, it will discharge a higher power (i.e. higher portion of P_{base,t^*} if negative). Finally, the PD_{j^{\wedge},t^*} is defined until the SOC of the charger is higher than the SOC_{min} (fixed in order to not stress the chemistry of the battery). In fact, once

this boundary is passed, the vehicle j^{\wedge} is disabled to the discharge and other vehicles will take its power portion.

$$PD_{j^{\wedge},t^*} = \frac{\widehat{SOCH}_{i,t}^{min}}{SOCH_{i,t^*}} \cdot \sum_i^N \frac{SOCH_{i,t^*}}{\widehat{SOCH}_{i,t}^{min}} \quad |if\ SOCH_{i,t^*} \geq SOC_{min} \quad (5.23)$$

Figure 5.13 aims to clarify the working principle of the rule-based logic. The Charging urgency and the Discharging disposability in figure are proportional to the Charging and Discharging Priority Indexes respectively. However, they do not correspond exactly with the quantities defined in Equation (5.22) and Equation (5.23).

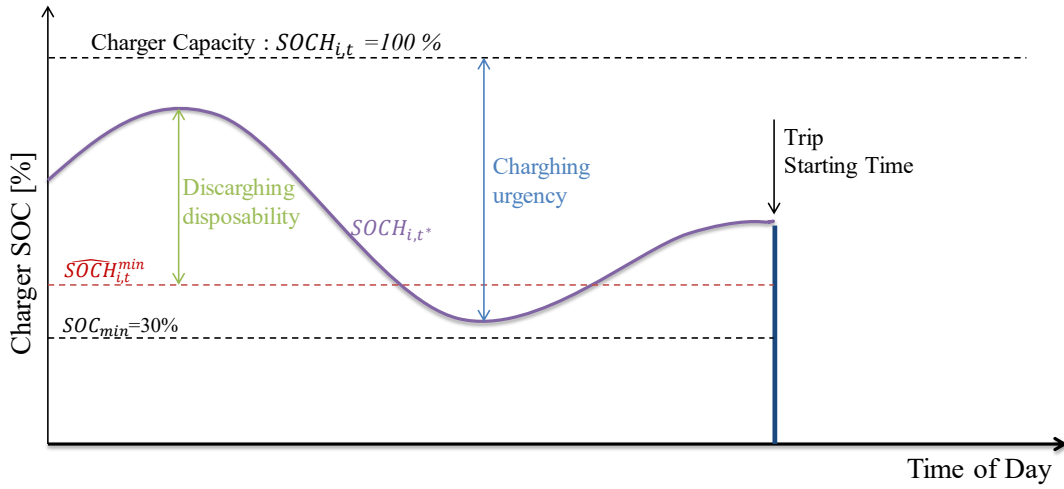


Figure 5.13 EV fleet real time management working principle

Equation (5.20) expresses the dispatched power to each charger in the case of absence of grid services activation. However, during D , the Replacement Reserve or the secondary reserve can be activated. Thus, the Aggregated Power P_{BSP} is given by the sum of the optimized power profile P_{base} with the powers due to the grid services, as already determinate in Equation (5.7). For sake of completeness, Equation (5.24) rewrites this equality using the respective time depending variables.

$$P_{BSP,t^*} = P_{base,t^*} + P_{Anc,t^*} + P_{sec,t^*} \quad (5.24)$$

Finally, the dispatched power to each charger in its general form can be expressed as in Equation (5.25).

$$p_{i,t^*} = \begin{cases} P_{BSP,t^*} \cdot PC_{j^{\wedge},t^*} & |if\ P_{BSP,t^*} > 0 \\ P_{BSP,t^*} \cdot PD_{j^{\wedge},t^*} & |if\ P_{BSP,t^*} < 0 \end{cases} \quad (5.25)$$

5.3 Simulations and Results

The proposed methodology is tested by the model based on 214 EVs described in Section 5.1.1. The entire cost analysis refers to the real prices occurred in Italy on April 6th, 2020. The initial State of Charge is different for each vehicle and it is assumed equal to the sum of $SOC_{min}=30\%$ and the tolerance defined for each EV as in Equation (5.18). The Aggregated Battery capacity is 8,56 MWh obtained considering the battery capacity of each EV equal to 40 kWh. Finally, the maximum charge/discharge power for each vehicle is 13,3 kW (full charge in three hours).

The proposed logic uses the definitions of priority in charge and discharge based on the EVs forecasts as in Equation (5.22) and Equation (5.23). Here, is proposed a comparison with the alternative scenario without priorities. In this latest case the Aggregated power profile is equally shared between the EVs. Finally, in order to fully investigate the potential of the proposed logic, priorities based on real data (exact priorities) are also considered.

In the following, the results for three cases are reported. The first case reports the output of the real time management on STEP #3 and the relative cost analysis, if any grid service is activated at the day of dispatch D . Meanwhile, the other two cases report the result for the Replacement service activation and for the Secondary Reserve activation, respectively.

5.3.1 Case with No Grid Services Activation

Figure 5.14 shows the SOC evolution during the simulated day of the first three vehicles for the case without grid services activation. The vehicles are allocated in five chargers as already discussed in Section 5.1.1. Thus, the different colours represent the different EVs State of Charges. It worth to notice that the state of charge of a car is correctly subtracted at the trip starting time. For example, once the EV#1 arrives at the CH#4 after the first trip, its SOC is appropriately reduced according with the trip energy consumption.

The dashed red lines represent the minimum SOC that the car needs in order to approach the next real trip without never going below the 30 %. Thus, similarly to what defined in Equation (5.17), it is indicated with $SOCH_{i,t}^{min}$. It is calculated as the sum of $SOC_{min}=25\%$ and the real consumption of the next real trip. it follows that the State of Charge of a vehicle should be higher of this boundary when a trip starts. In the specific case in figure, is possible to observe that for all the trip starting times the SOC of the cars is always higher than the relative boundary.

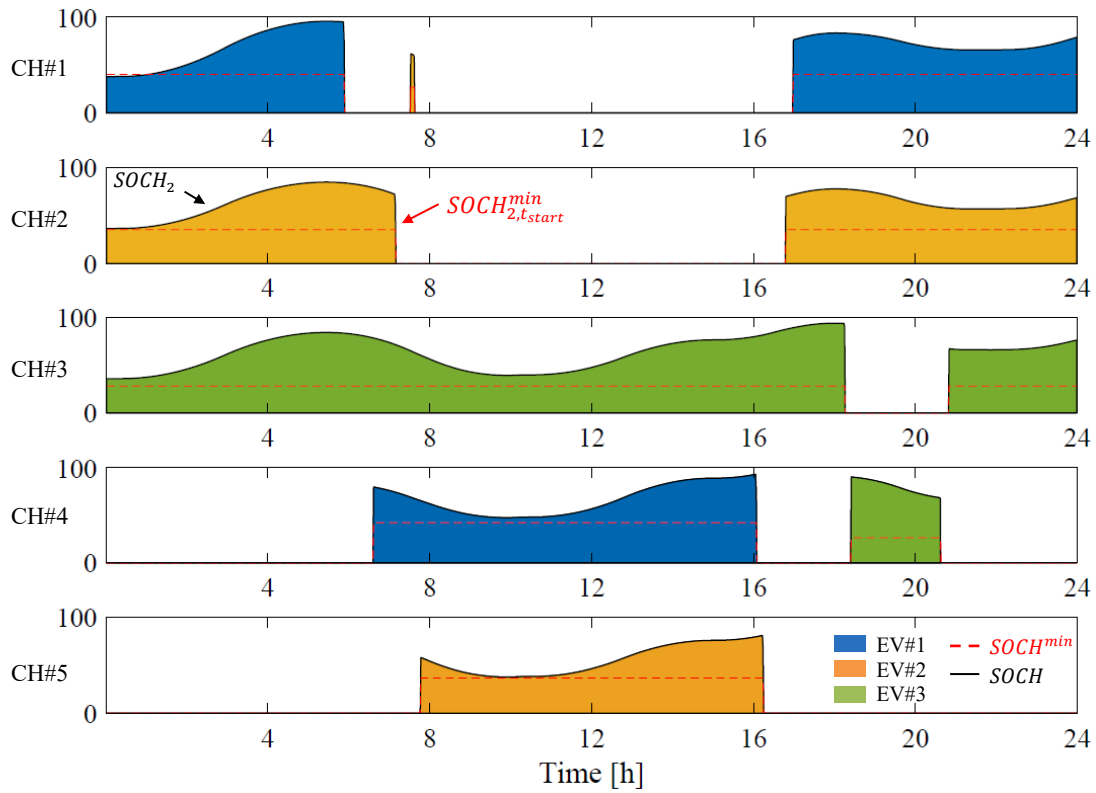


Figure 5.14 EV SOC evolutions by charger: no services activation

Figure 5.14, as above mentioned, shows only the first three vehicles of the dataset and their allocation in the first five chargers. However, these chargers are used during the day also from other vehicles. Figure 5.15 shows the CH#1 allocation when the simulation considers 214 EVs. The first vehicle EV#1 (in blue) is still connected in the morning and evening, as well as EV#2 is connected for a short period after its first trip (orange). However, other vehicles during the simulated day occupy CH#1 (in grey). The boundary $SOCH_1^{min}$, is represented by the dashed red line and changes value with each vehicle.

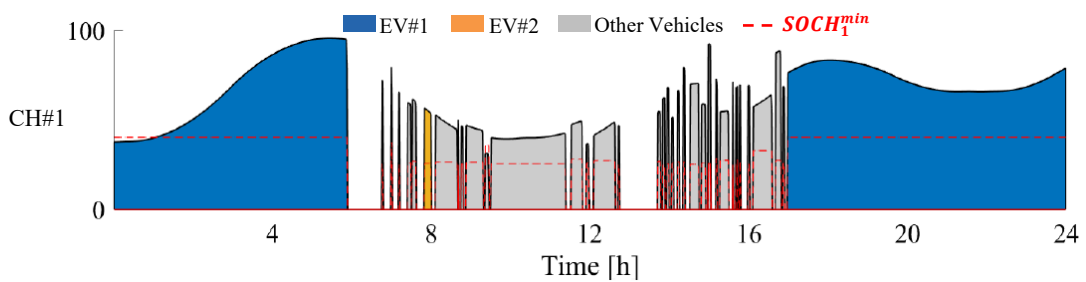


Figure 5.15 CH#1 occupation during the simulated day

Figure 5.16 shows the Aggregated Power Profile P_{BSP} at the day of simulation D , and the relative Aggregated State of Charge SOC_{BSP} . In this case, with no grid services activation, the Power profile is perfectly overlapped with the base power profile P_{base} defined as output of the optimization.

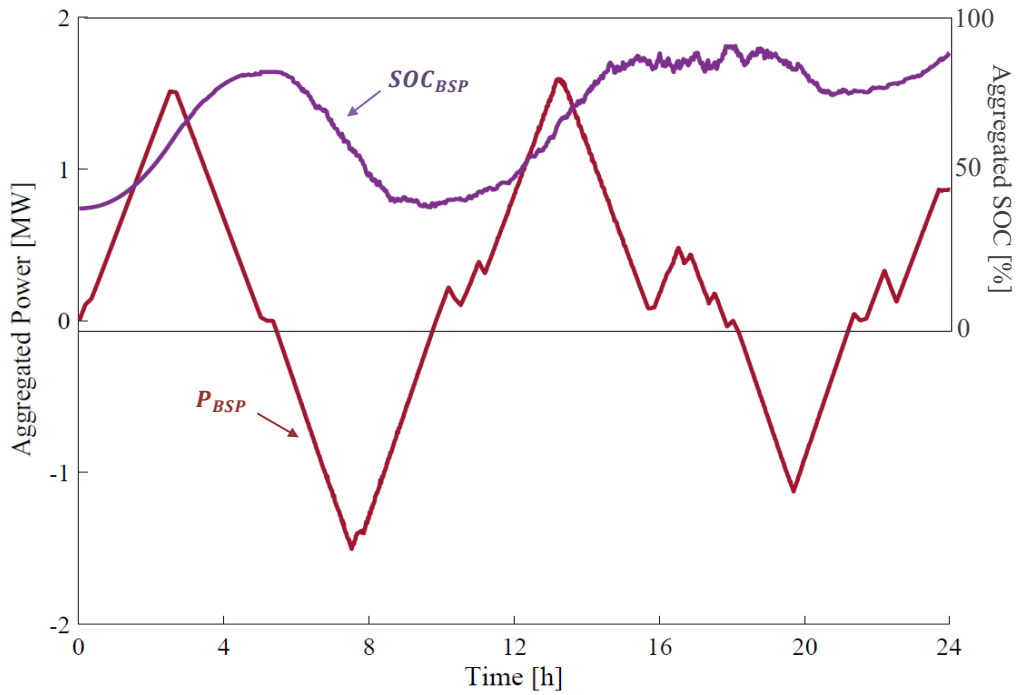


Figure 5.16 Aggregated Power and SOC: no services activation

When P_{BSP} is negative means that the Aggregator is injecting power to the grid. Meanwhile, when it is positive the Aggregator is purchasing power, thus charging the Aggregated battery. This is observable also from the Aggregated state of charge profile which increase when the power is positive, while decrease when the power profile is negative. Moreover, if this figure is compared with the Electricity Price Profile in Figure 5.6, it is possible to notice that the defined power profile follows the Energy Arbitrage Strategy.

Table 5.1 lists the cost analysis of the case under study. In particular, the total cost C_{TOT} of the fleet management at the end of the simulated day results in 77 € (0,36 € per car per day). This cost is due to the Electricity Price applied at the Power profile of Figure 5.16. However, the value of the Net Energy Purchased from the fleet, given by Equation (5.11), amounts to 124€. This means that in absence of Energy Arbitrage Strategy, in order to acquire the same amount of energy at the end of the day the expense would have been 124€. Thus, an economic saving of 38% is achieved.

Table 5.1 lists also the cases in which the State of Charge of a car result below the boundary $SOCH_{i,t}^{min}$ at the time-step t before a trip. This condition occurs 29 times during the day. However, the total number of trips made during the simulated day by the 214 EVs is 895. Therefore, the boundary results passed in the 3% of the cases. This means that during their trips same vehicles reach a SOC inferior to 30%. In particular, the minimum SOC has been reached from EV#62 at 9:27 A.M. (during one of its trips), and it amount to 20%.

Table 5.1 Technical-economic performance: no services activation

C_{TOT}	$CNEP$	Economic Saving	Average Cost per car per day	Boundary Exceedances	Boundary Exceedances
[€]	[€]	[%]	[€]	[#]	[%]
77	124	38	0,36	29	3

Table 5.2 lists the results, in terms of boundary “exceedances” (excesses), also for the two other cases: when priorities are not considered and when exact priorities are considered. If priorities are not considered, the rule-based logic imposes the power profile by equally sharing the power among the 214 EVs. Meanwhile, if exact priorities are considered, the indexes in Equation (5.22) and Equation (5.23) are calculated not anymore basing on the forecasted boundary $\widehat{SOCH}_{i,t}^{min}$, but with the actual boundary $SOCH_{i,t}^{min}$.

The results show that without priorities the number of boundary exceedances are 36. Thus, the proposed logic shows a relative improvement of 19%. Meanwhile, with exact priorities the exceedances fall to 18, with a relative improvement of 50% with respect to the case without priorities. The reason why also in this latest case exceedances are present, is because some vehicle does not stay parked for a period long enough to be charged (at the maximum power considered) or because they connect while the power profile is not in charging. In future application, this can be improved by admitting higher level of power in charge and enabling Vehicle to Vehicle operations (V2V), here not considered.

Table 5.2 Different priorities adoptions comparison: no services activation

Boundary Exceedances	With No priorities	With Priority Indexes	With Exact Priorities
[#]	36	29	18
[% _{rel}]	-	-19	-50

As last consideration, it is worth to notice that an analysis conducted by using the Infra-day forecasts described in Section 0 (not addressed in this research), would lead to a more precise definition of the priorities. Thus, the relative results would lead to a number of boundary exceedances between the ones obtained with the used priorities and the ones obtained with exact prediction.

5.3.2 Case with Replacement Reserve Activation

Figure 5.17 shows the SOC evolution during the simulated day of the first three vehicles for the case with the Replacement Service activation. Also in this figure, the State of Charge of the cars is always higher than the boundary at the trip starting times. However, it is visible for EV#1 and EV#2 (around 10:00 P.M.) the SOC goes below the boundary for a short time while connected. This is part of the normal functioning of the logic. In fact, by the end of the day (before midnight) the missing energy is fully recovered and the EV users can approach the next trip in safety.

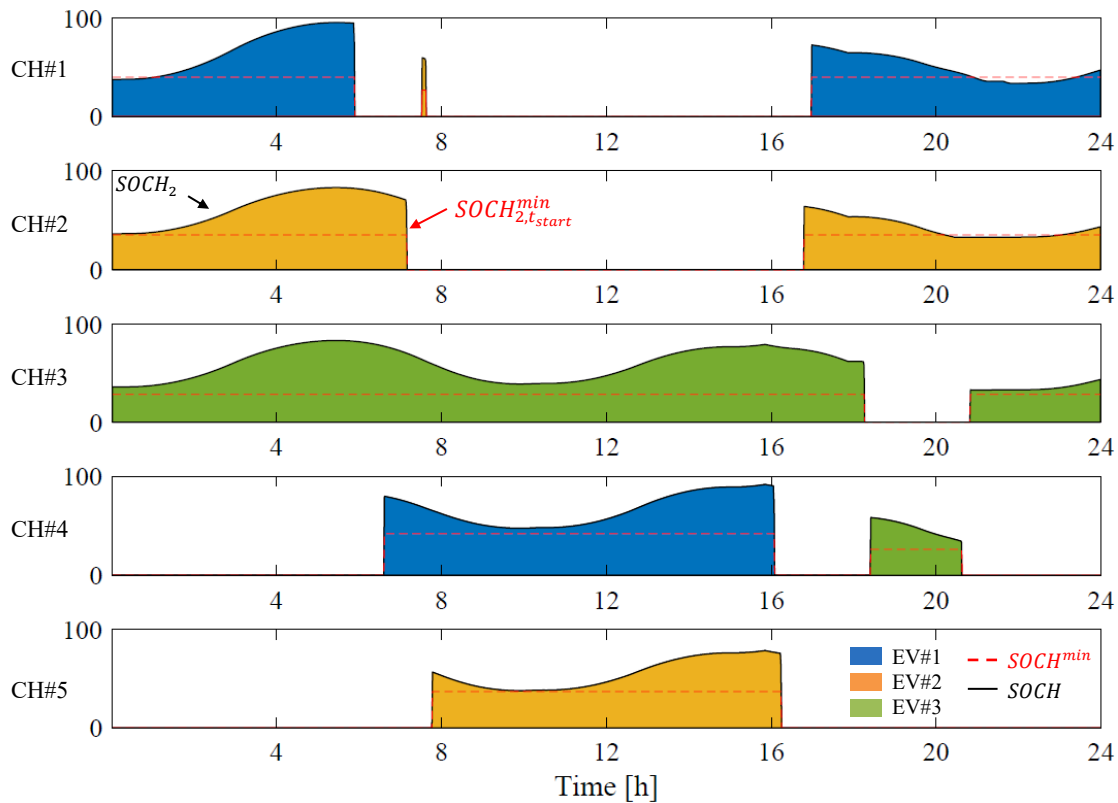


Figure 5.17 EV SOC evolutions by charger: Replacement reserve activation

Figure 5.18 shows the Aggregated Power Profile P_{BSP} at the day of simulation D , and the relative Aggregated State of Charge $SOCH_{BSP}$. In this case, with the Replacement reserve activation, the Power Profile is overlapped with P_{base} until the 3:51 P.M., when the ancillary service is activated. This ancillary service remains activated for two hours until the 5:51 P.M, then the Power profile again follows P_{base} .

During these 2 h, a reduction of power adsorption of 1,1 MW is operated, thus resulting in a total energy for the Replacement of about 2,2 MWh (27% of the Aggregated Battery Capacity). This amount of variation is the maximum that the fleet under analysis can operate as Replacement being able to always follow the profile defined the previous day P_{base} . With higher variation in power, thus in energy, the State of Charge of some vehicles reaches the ultimate boundary ($SOCH_{min}=30\%$). Then, these vehicles are disabled for the discharging operations.

As a result, they do not anymore participate at the Aggregated Power Profile dispatching and the other vehicles take charge of this gap. If a noticeable number of vehicles are in this condition it is not anymore possible to follow P_{base} until it become positive, thus charging is required. If a Balancing Service Provider is unable to respect the defined profile it will incur in penalties from the TSO.

Finally, Figure 5.18 also shows the State of Charge which increases when the power is positive (charge) while decrease if the power is negative (discharge).

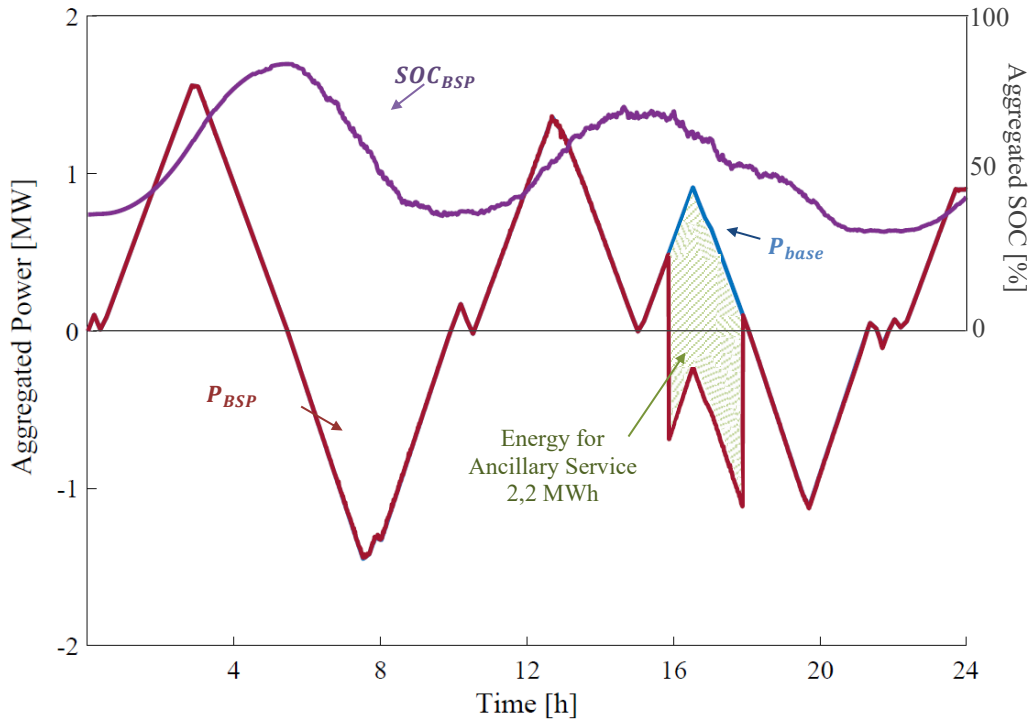


Figure 5.18 Aggregated Power and SOC: Replacement reserve activation

The energy for the Replacement is paid through the sales price R_{price}^- in Figure 5.8. Table 5.3 lists the cost analysis of the case under study. Due to both the Energy Arbitrage Strategy and the grid service provided, at the end of the day a net gain of 109€ is present. Meanwhile, the value of the Net Energy Purchased from the fleet amounts to 48€. This means that in absence of Energy Arbitrage and Ancillary Service, in order to acquire the same amount of energy, an expense of 48€ would have been occurred. Thus, an economic benefit of 327% is achieved. In this case, on average, every car has gained 0,5€. Meanwhile, 45 boundary exceedances have been recorded with an effect of the 5% on the total. Finally, the minimum SOC has been reached by EV#175 at 7:57 P.M. (during one of its trips), and it amount to 16%.

Table 5.3 Technical-economic performance: Replacement reserve activation

G_{TOT}	$CNEP$	Economic benefit	Average Gain per car per day	Boundary Exceedances	Boundary Exceedances
[€]	[€]	[%]	[€]	[#]	[%]
109	48	327	0,51	45	5

Table 5.4 lists the results of the comparison with no priorities and with exact priorities. With no priorities the number of exceedances goes to 67. Thus, the proposed logic shows a relative improvement of 33%. Meanwhile, with exact priorities the exceedances are 35, with a relative improvement of 48% with respect to the case without priorities.

Table 5.4 Different priorities adoptions comparison: Replacement reserve activation

Boundary Exceedances	With No priorities	With Priority Indexes	With Exact Priorities
[#]	67	45	35
[% _{rel}]	-	33	48

5.3.3 Case with Secondary Reserve Activation

Figure 5.19 shows the SOC evolution during the simulated day of the first three vehicles for the case with the Secondary Reserve activation. The State of Charge of the cars in figure is always higher than the boundary at the trip starting times. For the vehicles EV#1 and EV#2 (around 11:00 A.M. and 10:00 P.M.) the SOC goes below the boundary for a short time, but by the next trip starts the missing energy is fully recovered.

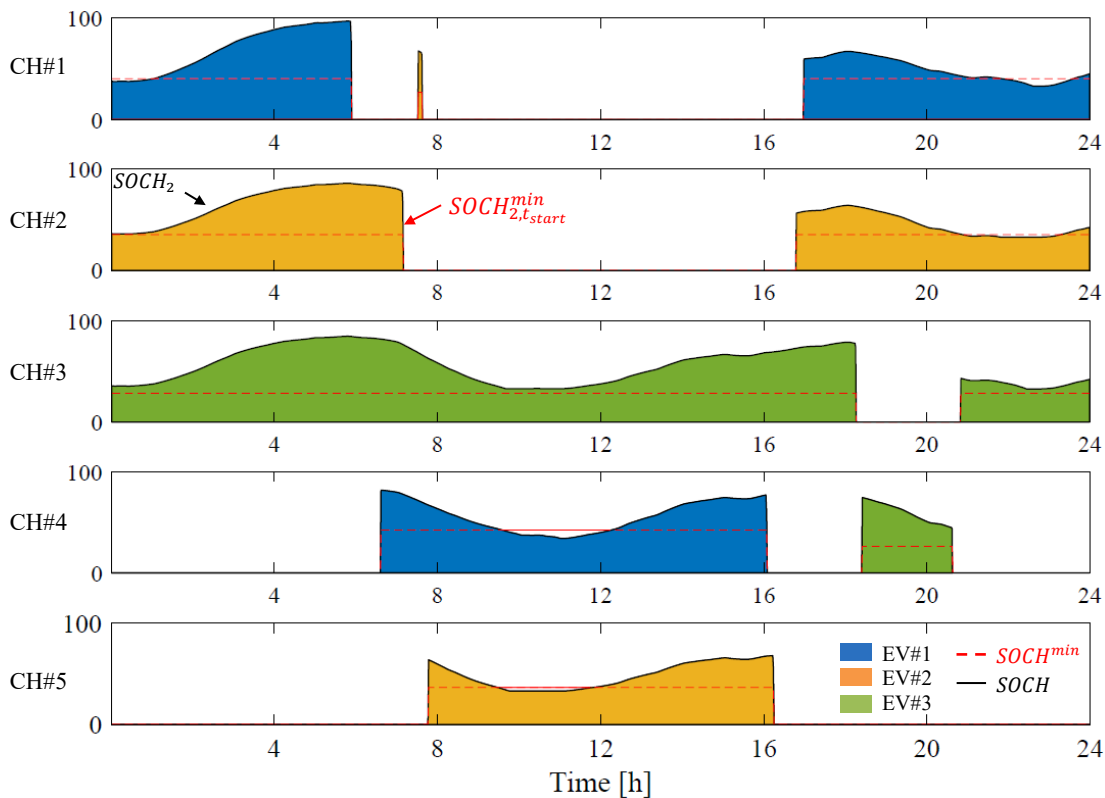


Figure 5.19 EV SOC evolutions by charger: Secondary reserve activation

Figure 5.20 shows the Aggregated Power Profile P_{BSP} at the day of simulation D , and the relative Aggregated State of Charge SOC_{BSP} . In this case, with the Secondary Reserve activation, the Power Profile orbits around P_{base} with a maximum deviation chosen equal to 13% of the maximum power (thus 370 kW). This deviation is the maximum that the fleet under analysis can operate as Secondary Reserve being able to always follow the profile defined the previous day P_{base} . The regulation Signal used for the analysis is provided by the Italian TSO (Terna.S.p.A) and refers to a real signal occurred in the North of Italy on

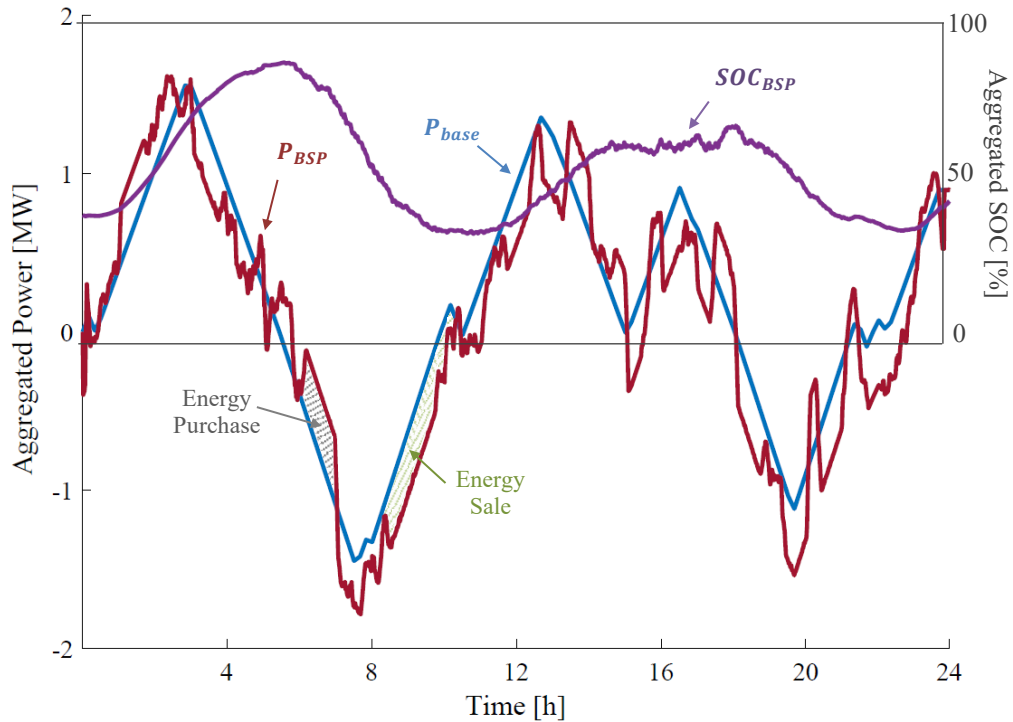


Figure 5.20 Aggregated Power and SOC: Secondary reserve activation

April 6th, 2020. Finally, the State of Charge increases when the power is positive (charge) while decreases if the power is negative (discharge).

When the Power Profile is below P_{base} (negative deviation), the corresponding energy is in the fact a sale. Thus, it is paid with the Negative deviation price S_{price}^- in Figure 5.10. Meanwhile, when the deviation is positive, this must be considered as a purchasing, thus it is bought at the Positive deviation price S_{price}^+ in Figure 5.10. However, since the purchasing is required from the TSO, this cost is much lower than the negative deviation revenue. Thus, a net gain is possible.

The case with Secondary Reserve activation is the case that shows the highest economical gain. Table 5.5 lists the cost analysis of the case under study. Due to both the Energy Arbitrage Strategy and the Secondary Reserve activation, at the end of the day a net gain of 243€ is present. Meanwhile, the value of the Net Energy Purchased from the fleet amounts to 53€. This means that in absence of Energy Arbitrage and Secondary reserve activation, in order to acquire the same amount of energy, an expense of 53€ would have been occurred. Thus, an economic benefit of 558% is achieved. In this case, in average every car has gained 1,15€. Meanwhile, 56 boundary exceedances have been recorded with an effect of the 6% of the total. Finally, the minimum SOC has been reached from EV#170 at 7:57 P.M. (during one of its trips), and it amount to 14%.

Table 5.5 Technical-economic performance: Secondary reserve activation

G_{TOT}	$CNEP$	Economic Saving	Average Gain per car per day	Boundary Exceedances	Boundary Exceedances
[€]	[€]	[%]	[€]	[#]	[%]
243	53	558	1,15	56	6

Table 5.6 lists the results of the comparison with no priorities and with exact priorities. With no priorities the number of exceedances goes to 77. Thus, the proposed logic shows a relative improvement of 27%. Meanwhile, with exact priorities the exceedances are 47, with a relative improvement of 39% with respect to the case without priorities.

Table 5.6 Different priorities adoptions comparison: Secondary reserve activation

Boundary Exceedances	With No priorities	With Priority Indexes	With Exact Priorities
[#]	77	56	47
[% _{rel}]	-	27	39

As above mentioned, the average car as gained a value of 1,15€. Figure 5.21 shows, as an example, the cost profile during the day c_j , Equation (5.9), occurred for EV#3. The cost is reported in Euro millesimal and, as it can be seen, is almost always below zero, thus it is a revenue. The sum of the profile returns the final cost for EV#3 at the end of the simulated day. In this case, the final cost is negative, thus equal to a net gain of 1,3€.

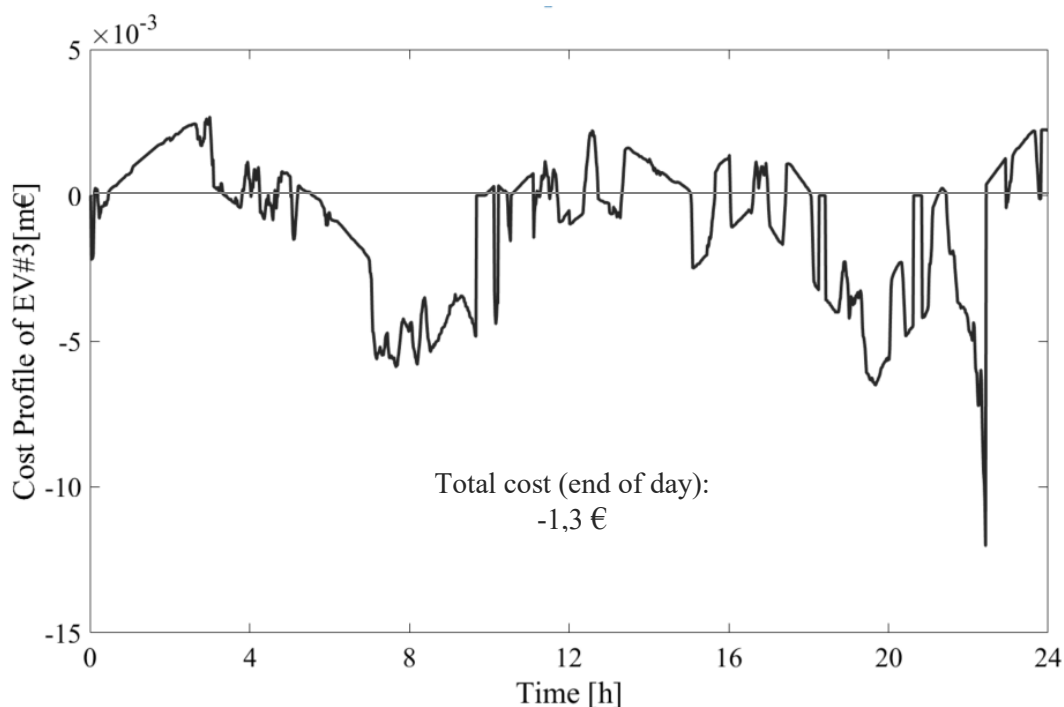


Figure 5.21 EV daily cost/revenue profile: EV#3

Finally, Figure 5.22 shows the final cost at the end of the day of all the vehicles. As it can be seen, practically all the vehicles present a net gain which lies around the average value of 1,15€.

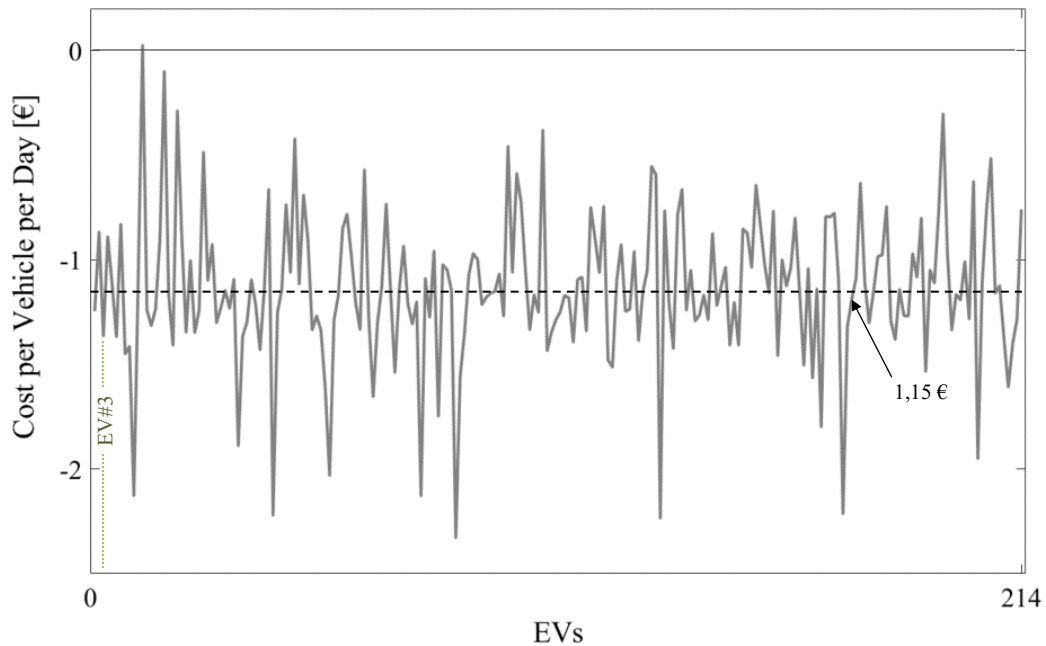


Figure 5.22 Final net cost/revenue per EVs

Sensitivity to Variation of Available Chargers

The analysis until now addressed is based on the hypothesis that each car is always connected when not in travel. This condition is obtained if 225 chargers are available for the 214 EVs (i.e. the chargers are the 105% of the EVs). Figure 5.23 shows (in blue) the number of connected cars among the day under this hypothesis, thus it returns the visible effect of the incidence of travels. In particular, the average number of connected vehicles results 204, thus the 95% of the entire fleet, as showed from the dashed black line.

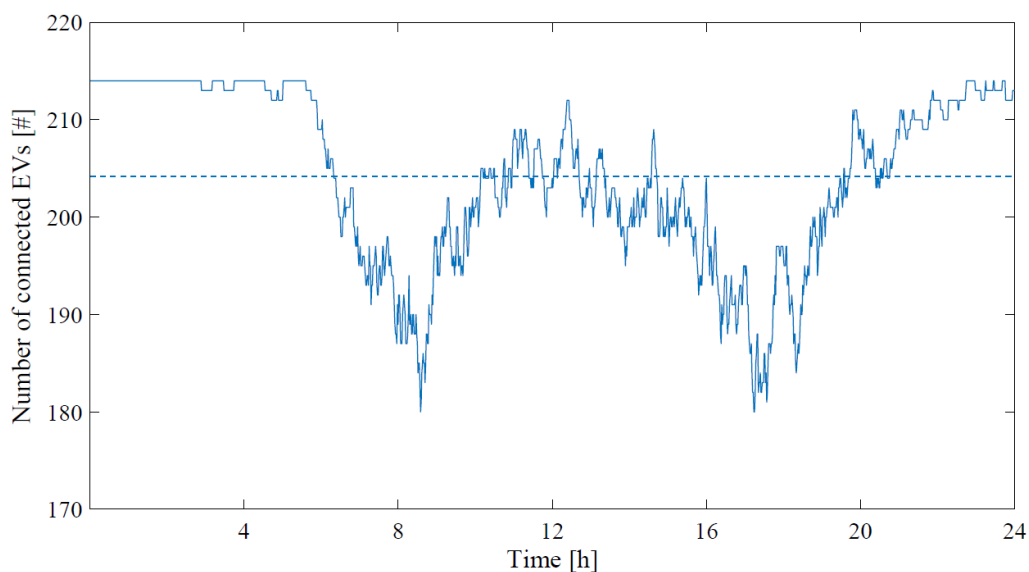


Figure 5.23 Number of connected EVs among the day: 225 available chargers

This hypothesis considers not only the presence of the public charging infrastructure but also the possibility to plug the electric vehicle at the workplaces, homes, and points of interest such as commercial centers. However, it may result a strong assumption if compared to the current scenario characterized by a low density of the charging network. At this purpose is here presented a further analysis which aims to investigate the impact of a progressive reduction of the available charging points.

Figure 5.24 shows the variation of the number of connected vehicles among the day when the number of available chargers is reduced by 30%, 60%, and 90% respectively. Table 5.7 lists the associated numerical results of the analysis.

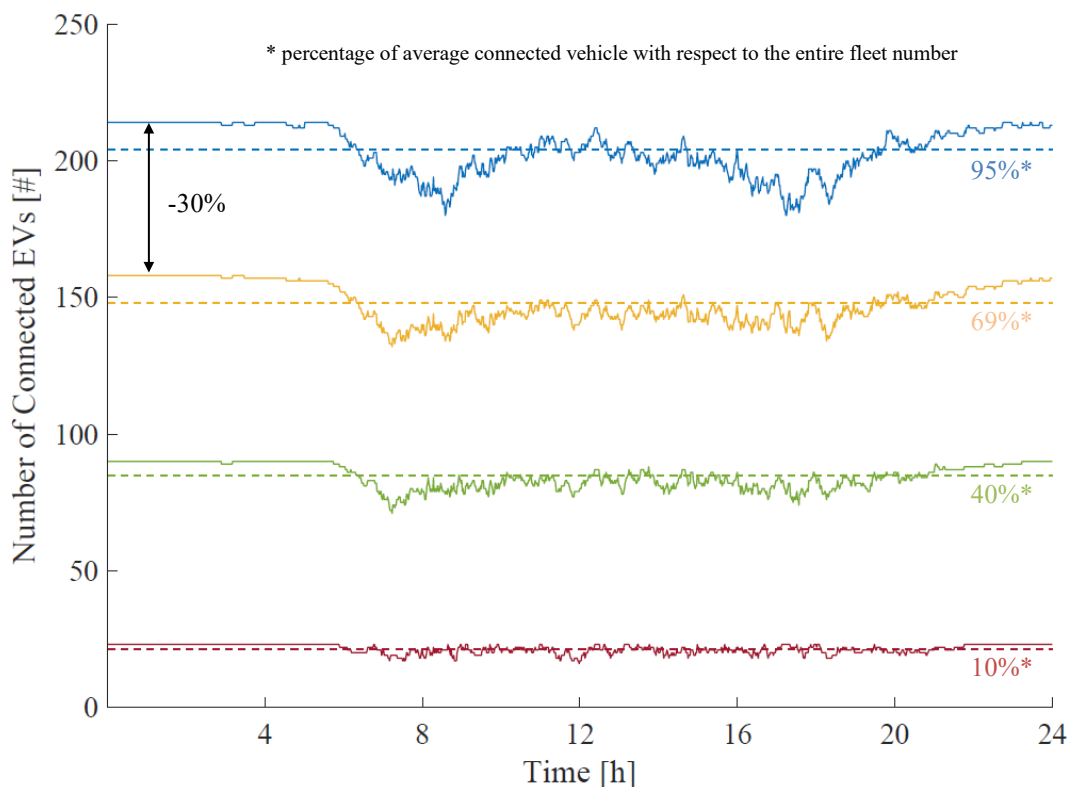


Figure 5.24 Number of connected EVs by varying the chargers availability

From the results it can be seen that a reduction of 30% of the charger number results in a number of averagely connected vehicles of 148 (69% of the total fleet), thus in a reduction with respect to the previous scenario of 26%. Similarly, a reduction of 60% in the charger number results in 55% averagely less connected car and a reduction of 90% brings to a reduction in the vehicle availability of 85%. This last percentages reduction represents the sensitivity of the proposed model at the variation of number of chargers.

To investigate the economic impact of the charging availability reduction it is necessary to scale down the power requests (both P_{base} and Secondary Reserve) in order to take into account, the reduced vehicles availability.

Table 5.7 Effect on averagely connected EVs for different number of available chargers

No. of available charger [#]	Available charger reduction [%]	Available charger with respect to EVs* [%]	No. of EVs averagely connected [#]	Averagely connected EVs with respect to the total* [%]	No. of averagely connected EVs reduction [%]
225	-	105	204	95	-
158	30	74	148	69	26
90	60	42	85	40	55
23	90	10	21	10	85

*Total number of EVs:214

Table 5.8 compares the cost analysis obtained for the different number of available chargers for the case with the Secondary Reserve activation. It worth to notice that with the Secondary Reserve activation a net gain is always present even in the worst case with only 23 available for the fleet. However, the value of this economic benefit suffers a drastically reduction from the original value of 243 € achieved with 225 charges to just 34€ with 23 chargers. Similarly, the average gain per car per day goes from 1,15 € to 0,16 €. Finally, the boundary exceedances effect (partially mitigated by the considered tolerances) rise from the 6% observed with 225 chargers up to 25% if 23 chargers are available.

Table 5.8 Technical-economic performance: different number of available chargers

Available charger [#]	G_{TOT} [€]	$CNEP$ [€]	Average Gain per car per day [€]	Boundary Exceedances [#]	Boundary Exceedances [%]
225	243	53	1,15	56	6
158	168	36	0,78	111	12
90	101	21	0,47	168	19
23	34	3	0,16	220	25

5.4 Future Works on EVs and Grid Integration

This chapter has discussed the methodology proposed in order to integrate EVs with the power system, thus maximize the economic benefit achievable by an opportune exploiting of the V2G operations. The used centralized architecture was applied to a fleet of 214 EVs. Meanwhile, the approach is hybrid, thus coordinate a forecast based optimization with a real time management.

Two grid services have been considered: Replacement Reserve and Secondary Reserve. Thus, three case studies have been addressed by the simulations: case with no grid services activation (only energy arbitrage), case with Replacement Reserve activation, and case with Secondary Reserve activation. The highest economic benefit is achieved for the case with Secondary Reserve activation with a net gain in the simulated day of 243€ for the entire fleet (1,15 € per car per day) to be compared with an avoided cost for energy purchased of 53€. However,

minimum SOC exceedances occur in the 6% of the cases among all the trips travelled during the day by the fleet

Future works need to consider a more consistent sample of vehicles and extend the analysis to more than a single day, in order to make possible a generalization of the results. In fact, if a wider analysis will be conducted, the relative results could provide a support also in the optic of the normative definition process (e.g., requirements and constraints on the contractual control power level depending on the number of vehicles controlled from the Aggregator). Moreover, a wider analysis could enable a more accurate setting of the aggregated SOC range that is possible to exploit for grid services. Thus, leading to a more reliable operations toward both EV's users and the power system perspectives.

Purely regarding the proposed logic, a more sophisticated definition of the Priorities (used to proportionally dispatching the available power among the EVs) could be implemented in next works. In fact, in this work priorities only considers the forecasted SOC needed for the next trip; while better results (thus less minimum SOC exceedances) may be achieved if also remaining hours before the next trip are considered from priorities. In the same direction, also the enabling of Vehicle to Vehicle exchanges between cars, may have the effect to reduce the minimum SOC exceedances, thus ensure a more reliable management. Finally, in order the reduce the errors due to the EV miss-forecasts, future works could make use of the infra-day EV forecast logic.

Conclusion

This Dissertation has presented a novel approach to control the EV batteries power of network integrated vehicles using individual EV forecasts. The approach is based on a bilevel programming where the real-time management is integrated by a preliminary optimization phase. On the other hand, the EV forecasts rely on statistical elaborations of the real EVs usages historical data provided by [96]. Moreover, the proposed approach has been declined in two different case studies with different purposes. The first case study has provided an application of the battery energy management for the integration of an EV with a PV powered household. The second case study has considered an entire fleet of 214 EVs connected to the power system and able to supply grid services.

In Chapter 3 the proposed methodology of individual EV forecasts has been defined. In particular, two different forecast logics have been presented: Day-ahead and Infra-day forecasts. Proper errors have been defined and calculated in order to measure the proposed methodologies performance; thus, the forecasts have been compared with specific days of usage among the dataset assumed as real scenarios. Considering the defined errors, the results showed a global reliability around 50% for the day-ahead forecast logic. Moreover, it was shown that by infra-day updates, able to read the last few hours of the EV behaviour, improvements of the forecasts up to around 60% are possible (compared to the Day-ahead results).

Chapter 4 has presented the application of an EV integrated in a PV powered household. Different scenarios have been provided by an accurate choice of the three most representative EVs among the available dataset of 214 vehicles. For each scenario, four weeks (one for each season) have been chosen for the analysis. Moreover, the proposed approach was compared with a pure hierarchical approach (simple rule-based logic) in order to evaluate the quality of the results.

The comparison shows that tangible improvements in PV self-consumption are achieved (up to 9%_{rel}) if the PV availability is not too low with respect to the EV energy need. In addition, in order to investigate the full potential of the methodology, different PV plant sizes and the use of exact predictions have been also considered. In this context, maximum improvements were found for a PV plant size of 15kWp (11%_{rel} for the proposed logic with forecasts, and 24%_{rel} if exact predictions are used) - week of January of EV#A. Finally, higher improvements in PV self-consumption (up to 19%_{rel}) have been proved if the proposed logic is compared with less virtuous EV user charging behaviour.

In Chapter 5 the integration of an entire fleet of 214 EVs into the power system has been discussed. The real time management makes use of priority indexes to better dispatch the power among the vehicles and considers the possible activation of two grid services: Replacement Reserve and Secondary Reserve. Thus, three cases have been addressed: case with no grid services activation (only energy arbitrage), case with only Replacement Reserve activation, and case with only Secondary Reserve activation (Secondary Regulation).

The highest economic benefit is achieved for the case with Secondary Reserve activation with 243€ net gain in the simulated day for the entire fleet (1,15 € per car per day) to be compared with an avoided cost for energy purchased of 53€. However, minimum SOC exceedances (excesses) occur in the 6% of the cases among all the trips travelled during the day by the fleet. Moreover, a comparison which does not make use of priority indexes was provided. In this latest case the minimum SOC exceedances among the total rise till overcome the 8%.

The case with the Replacement Reserve activation showed as well a net but lower gain of 109€ (0,51 € per car per day) to be compared with an avoided cost for energy purchased of 48€ and a 5% of minimum SOC exceedances. On the contrary, the case with no services activation resulted in 77€ net cost (0,36 € per car per day). However, thanks to the exploiting of energy arbitrage an economic savings of around 40% is still achieved. In fact, a quantity of energy for a value of 124 € was purchased during the simulated day.

Finally, at the end of each chapter the main possible future improvements are traced in detail. Regarding the individual EV forecasts it is highlighted the possibility to make the logic able to adjust itself basing on error or quality indexes check (being retroactive), and integrating information from different sources such as internet. Considering the EV and PV integration, is suggested for future works, to test the proposed approach also in applications different from households such as offices, industrial or commercial buildings characterized by an higher presence of EVs during sunlight hours. In conclusion, for the EVs integration with the power system analysis, an extension in time and number of vehicles could enable more generalizable consideration, thus it might provide support in the normative definition process.

References

- [1] IEA, *Tracking Transport 2020*. Paris, 2020.
- [2] V. Masson-Delmotte *et al.*, *IPCC Special Report 1.5 - Summary for Policymakers*. 2018.
- [3] G. Bundestag, *Smart Charging System for Electric Vehicles*. 2019.
- [4] I. R. E. Agency, *Renewable Power Generation Costs in 2019*. 2020.
- [5] W. Kempton and S. E. Letendre, “Electric vehicles as a new power source for electric utilities,” *Transp. Res. Part D Transp. Environ.*, vol. 2, no. 3, pp. 157–175, 1997, doi: 10.1016/S1361-9209(97)00001-1.
- [6] F. M. Camilo, R. Castro, M. E. Almeida, and V. F. Pires, “Self-consumption and storage as a way to facilitate the integration of renewable energy in low voltage distribution networks,” *IET Gener. Transm. Distrib.*, vol. 10, no. 7, pp. 1741–1748, 2016, doi: 10.1049/iet-gtd.2015.0431.
- [7] O. R. Christer Tryggestad, Namit Sharma, “Global Energy Perspective 2019 : Reference Case,” *Energy Insights by McKinsey Co.*, no. January, p. 31, 2019.
- [8] European Environmental Agency, *Trends and projections in Europe 2020 - Tracking progress towards Europe’s climate and energy targets*, no. 13/2020. 2020.
- [9] Ministero dello Sviluppo Economico, Ministero dell’Ambiente e della Tutela del Territorio e del Mare, and Ministero delle Infrastrutture e dei Trasporti., “PNIEC - Piano Nazionale Integrato per l’Energia e il Clima,” 2019, [Online]. Available: <https://www.mise.gov.it/index.php/it/2040668>.
- [10] IEA, *Renewables 2020- Analysis and forecast to 2025*. 2020.
- [11] International Energy Agency, “Status of Power System Transformation 2019: Power system flexibility,” *OECD Publ.*, pp. 1–26, 2019, [Online]. Available: https://www.oecd-ilibrary.org/energy/status-of-power-system-transformation-2019_7c49400a-en.
- [12] E. Taibi *et al.*, *Power system flexibility for the energy transition: Part 1, Overview for policy makers*, no. November. 2018.
- [13] IRENA, *Demand-side flexibility for power sector transformation*. 2019.
- [14] Politecnico di Milano, *Electricity Market Report*. 2020.
- [15] BloombergNEF, “2019 Battery Price Survey,” 2019. <https://about.bnef.com/blog/behind-scenes-take-lithium-ion-battery-prices/>.

- [16] IEA, *Global EV Outlook 2020*. 2020.
- [17] Politecnico di Milano, *Smart Mobility Report*. 2020.
- [18] Deloitte insight, *Electric vehicles*. .
- [19] W. Kempton and J. Tomić, “Vehicle-to-grid power fundamentals: Calculating capacity and net revenue,” *J. Power Sources*, vol. 144, no. 1, pp. 268–279, 2005, doi: 10.1016/j.jpowsour.2004.12.025.
- [20] F. Giordano, A. Ciocia, P. Di Leo, F. Spertino, A. Tenconi, and S. Vaschetto, “Self-Consumption Improvement for a Nanogrid with Photovoltaic and Vehicle-to-Home Technologies,” 2018, doi: 10.1109/EEEIC.2018.8493708.
- [21] D. B. Richardson, “Electric vehicles and the electric grid: A review of modeling approaches, Impacts, and renewable energy integration,” *Renew. Sustain. Energy Rev.*, vol. 19, pp. 247–254, 2013, doi: 10.1016/j.rser.2012.11.042.
- [22] L. Liu, F. Kong, X. Liu, Y. Peng, and Q. Wang, “A review on electric vehicles interacting with renewable energy in smart grid,” *Renew. Sustain. Energy Rev.*, vol. 51, pp. 648–661, 2015, doi: 10.1016/j.rser.2015.06.036.
- [23] A. R. Bhatti, Z. Salam, M. J. B. A. Aziz, K. P. Yee, and R. H. Ashique, “Electric vehicles charging using photovoltaic: Status and technological review,” *Renew. Sustain. Energy Rev.*, vol. 54, pp. 34–47, 2016, doi: 10.1016/j.rser.2015.09.091.
- [24] B. C. Liu, M. Ieee, K. T. Chau, F. Ieee, D. Wu, and S. M. Ieee, “Opportunities and Challenges of Vehicle-to-Home , Vehicle-to-Grid Technologies,” pp. 1–19, 2013.
- [25] R. Luthander, J. Widén, D. Nilsson, and J. Palm, “Photovoltaic self-consumption in buildings: A review,” *Appl. Energy*, vol. 142, pp. 80–94, 2015, doi: 10.1016/j.apenergy.2014.12.028.
- [26] Q. Hoarau and Y. Perez, “Interactions between electric mobility and photovoltaic generation: A review,” *Renew. Sustain. Energy Rev.*, vol. 94, no. February, pp. 510–522, 2018, doi: 10.1016/j.rser.2018.06.039.
- [27] E. Sortomme and M. A. El-Sharkawi, “Optimal charging strategies for unidirectional vehicle-to-grid,” *IEEE Trans. Smart Grid*, vol. 2, no. 1, pp. 131–138, 2011, doi: 10.1109/TSG.2010.2090910.
- [28] D. K. ; G. Strbac, *Fundamentals of power system economics*. 2004.
- [29] I. Pavić, T. Capuder, and I. Kuzle, “Value of flexible electric vehicles in providing spinning reserve services,” *Appl. Energy*, vol. 157, pp. 60–74, 2015, doi: 10.1016/j.apenergy.2015.07.070.
- [30] P. J. M. Manual, A. Services, M. Operations, E. Date, and F. M. Operations, “PJM Manual 11 : Energy & Ancillary Services Market Operations Revision : 60 Effective Date : June 1 , 2013 Prepared by Forward Market Operations Table of Contents,” 2013.
- [31] V. Pandurangan, H. Zareipour, and O. Malik, “Frequency regulation services: A comparative study of select North American and European reserve markets,” *2012 North Am. Power Symp. NAPS 2012*, no. September, 2012, doi: 10.1109/NAPS.2012.6336376.
- [32] F. Mwasilu; J.J. Justo; E. Kim; T.D. Do; J. Jung, “Electric vehicles and smart grid interaction:A review on vehicle to grid and renewable energy sources integration,” *Renew. Sustain. Energy Rev.*, vol. 34, pp. 501–516, 2014, [Online]. Available: <https://doi.org/10.1016/j.rser.2014.03.031>.
- [33] K. M. Tan, V. K. Ramachandaramurthy, and J. Y. Yong, “Integration of electric vehicles in smart grid: A review on vehicle to grid technologies and

- optimization techniques,” *Renew. Sustain. Energy Rev.*, vol. 53, pp. 720–732, 2016, doi: 10.1016/j.rser.2015.09.012.
- [34] Q. Wang, X. Liu, J. Du, and F. Kong, “Smart Charging for Electric Vehicles: A Survey from the Algorithmic Perspective,” *IEEE Commun. Surv. Tutorials*, vol. 18, no. 2, pp. 1500–1517, 2016, doi: 10.1109/COMST.2016.2518628.
- [35] J. García-Villalobos, I. Zamora, J. I. San Martín, F. J. Asensio, and V. Aperribay, “Plug-in electric vehicles in electric distribution networks: A review of smart charging approaches,” *Renew. Sustain. Energy Rev.*, vol. 38, pp. 717–731, 2014, doi: 10.1016/j.rser.2014.07.040.
- [36] A. Foley, B. Tyther, P. Calnan, and B. Ó Gallachóir, “Impacts of Electric Vehicle charging under electricity market operations,” *Appl. Energy*, vol. 101, no. 2013, pp. 93–102, 2013, doi: 10.1016/j.apenergy.2012.06.052.
- [37] L. Jian, Y. Zheng, and Z. Shao, “High efficient valley-filling strategy for centralized coordinated charging of large-scale electric vehicles,” *Appl. Energy*, vol. 186, pp. 46–55, 2017, doi: 10.1016/j.apenergy.2016.10.117.
- [38] H. Liang, Y. Liu, F. Li, and Y. Shen, “Dynamic Economic/Emission Dispatch Including PEVs for Peak Shaving and Valley Filling,” *IEEE Trans. Ind. Electron.*, vol. 66, no. 4, pp. 2880–2890, 2019, doi: 10.1109/TIE.2018.2850030.
- [39] M. Coffman, P. Bernstein, and S. Wee, “Integrating electric vehicles and residential solar PV,” *Transp. Policy*, vol. 53, pp. 30–38, 2017, doi: 10.1016/j.tranpol.2016.08.008.
- [40] A. T. Al-Awami and E. Sortomme, “Coordinating vehicle-to-grid services with energy trading,” *IEEE Trans. Smart Grid*, vol. 3, no. 1, pp. 453–462, 2012, doi: 10.1109/TSG.2011.2167992.
- [41] M. van der Kam and W. van Sark, “Smart charging of electric vehicles with photovoltaic power and vehicle-to-grid technology in a microgrid; a case study,” *Appl. Energy*, vol. 152, pp. 20–30, 2015, doi: 10.1016/j.apenergy.2015.04.092.
- [42] C. Diaz-Londono, L. Colangelo, F. Ruiz, D. Patino, C. Novara, and G. Chicco, “Optimal strategy to exploit the flexibility of an electric vehicle charging station,” *Energies*, vol. 12, no. 20, pp. 1–29, 2019, doi: 10.3390/en12203834.
- [43] M. Broussely *et al.*, “Main aging mechanisms in Li ion batteries,” *J. Power Sources*, vol. 146, no. 1–2, pp. 90–96, 2005, doi: 10.1016/j.jpowsour.2005.03.172.
- [44] S. B. Peterson, J. Apt, and J. F. Whitacre, “Lithium-ion battery cell degradation resulting from realistic vehicle and vehicle-to-grid utilization,” *J. Power Sources*, vol. 195, no. 8, pp. 2385–2392, 2010, doi: 10.1016/j.jpowsour.2009.10.010.
- [45] M. Dubarry, G. Baure, and A. Devie, “Durability and Reliability of EV Batteries under Electric Utility Grid Operations: Path Dependence of Battery Degradation,” *J. Electrochem. Soc.*, vol. 165, no. 5, pp. A773–A783, 2018, doi: 10.1149/2.0421805jes.
- [46] K. Uddin, T. Jackson, W. D. Widanage, G. Chouchelamane, P. A. Jennings, and J. Marco, “On the possibility of extending the lifetime of lithium-ion batteries through optimal V2G facilitated by an integrated vehicle and smart-grid system,” *Energy*, vol. 133, pp. 710–722, 2017, doi: 10.1016/j.energy.2017.04.116.
- [47] K. Uddin, M. Dubarry, and M. B. Glick, “The viability of vehicle-to-grid

- operations from a battery technology and policy perspective,” *Energy Policy*, vol. 113, no. August 2017, pp. 342–347, 2018, doi: 10.1016/j.enpol.2017.11.015.
- [48] J. Wang, Y. Shao, Y. Ge, and R. Yu, “A survey of vehicle to everything (V2X) testing,” *Sensors (Switzerland)*, vol. 19, no. 2, pp. 1–20, 2019, doi: 10.3390/s19020334.
- [49] Y. M. Wi, J. U. Lee, and S. K. Joo, “Electric vehicle charging method for smart homes/buildings with a photovoltaic system,” *IEEE Trans. Consum. Electron.*, vol. 59, no. 2, pp. 323–328, 2013, doi: 10.1109/TCE.2013.6531113.
- [50] T. Zhang, C. C. Chu, and R. Gadh, “A two-tier energy management system for smart electric vehicle charging in UCLA: A Solar-To-Vehicle (S2V) case study,” *IEEE PES Innov. Smart Grid Technol. Conf. Eur.*, pp. 288–293, 2016, doi: 10.1109/ISGT-Asia.2016.7796400.
- [51] R. Lasseter, A. Akhil, C. Marnay, and J. Ste, “Consortium for Electric Reliability Technology Solutions White Paper on Integration of Distributed Energy Resources The MicroGrid Concept,” no. April, 2002.
- [52] P. J. Tulpule, V. Marano, S. Yurkovich, and G. Rizzoni, “Economic and environmental impacts of a PV powered workplace parking garage charging station,” *Appl. Energy*, vol. 108, pp. 323–332, 2013, doi: 10.1016/j.apenergy.2013.02.068.
- [53] D. Van Der Meer, G. R. C. Mouli, G. M. E. Mouli, L. R. Elizondo, and P. Bauer, “Energy Management System with PV Power Forecast to Optimally Charge EVs at the Workplace,” *IEEE Trans. Ind. Informatics*, vol. 14, no. 1, pp. 311–320, 2018, doi: 10.1109/TII.2016.2634624.
- [54] K. S. P. Jochem, W. Fichtner, “Integrating renewable energy sources by electric vehicle fleets under uncertainty,” *Energy*, vol. 141, pp. 2145–2153, 2017.
- [55] M. Huber, A. Trippe, P. Kuhn, and T. Hamacher, “Effects of large scale EV and PV integration on power supply systems in the context of Singapore,” *IEEE PES Innov. Smart Grid Technol. Conf. Eur.*, pp. 1–8, 2012, doi: 10.1109/ISGTEurope.2012.6465831.
- [56] J. Munkhammar, P. Grahn, and J. Widén, “Quantifying self-consumption of on-site photovoltaic power generation in households with electric vehicle home charging,” *Sol. Energy*, vol. 97, pp. 208–216, 2013, doi: 10.1016/j.solener.2013.08.015.
- [57] J. Munkhammar, J. D. K. Bishop, J. J. Sarralde, W. Tian, and R. Choudhary, “Household electricity use, electric vehicle home-charging and distributed photovoltaic power production in the city of Westminster,” *Energy Build.*, vol. 86, pp. 439–448, 2015, doi: 10.1016/j.enbuild.2014.10.006.
- [58] C. Roselli and M. Sasso, “Integration between electric vehicle charging and PV system to increase self-consumption of an office application,” *Energy Convers. Manag.*, vol. 130, pp. 130–140, 2016, doi: 10.1016/j.enconman.2016.10.040.
- [59] M. S. Elnozahy and M. M. A. Salama, “Studying the feasibility of charging plug-in hybrid electric vehicles using photovoltaic electricity in residential distribution systems,” *Electr. Power Syst. Res.*, vol. 110, pp. 133–143, 2014, doi: 10.1016/j.epsr.2014.01.012.
- [60] A. Ciocia *et al.*, “Voltage control in low-voltage grids using distributed photovoltaic converters and centralized devices,” *IEEE Trans. Ind. Appl.*,

- vol. 55, no. 1, pp. 225–237, 2019, doi: 10.1109/TIA.2018.2869104.
- [61] F. Spertino, G. Chicco, A. Ciocia, G. Malgaroli, A. Mazza, and A. Russo, “Harmonic distortion and unbalance analysis in multi-inverter photovoltaic systems,” *SPEEDAM 2018 - Proc. Int. Symp. Power Electron. Electr. Drives, Autom. Motion*, pp. 1031–1036, 2018, doi: 10.1109/SPEEDAM.2018.8445358.
- [62] N. Liu *et al.*, “A Heuristic Operation Strategy for Commercial Building Microgrids Containing EVs and PV System,” *IEEE Trans. Ind. Electron.*, vol. 62, no. 4, pp. 2560–2570, 2015, doi: 10.1109/TIE.2014.2364553.
- [63] G. Byeon, T. Yoon, S. Oh, and G. Jang, “Energy management strategy of the DC distribution system in buildings using the EV service model,” *IEEE Trans. Power Electron.*, vol. 28, no. 4, pp. 1544–1554, 2013, doi: 10.1109/TPEL.2012.2210911.
- [64] M. Alirezaei, M. Noori, and O. Tatari, “Getting to net zero energy building: Investigating the role of vehicle to home technology,” *Energy Build.*, vol. 130, pp. 465–476, 2016, doi: 10.1016/j.enbuild.2016.08.044.
- [65] F. Fattori, N. Anglani, and G. Muliere, “Combining photovoltaic energy with electric vehicles, smart charging and vehicle-to-grid,” *Sol. Energy*, vol. 110, pp. 438–451, 2014, doi: 10.1016/j.solener.2014.09.034.
- [66] J. Salpakari, T. Rasku, J. Lindgren, and P. D. Lund, “Flexibility of electric vehicles and space heating in net zero energy houses: an optimal control model with thermal dynamics and battery degradation,” *Appl. Energy*, vol. 190, pp. 800–812, 2017, doi: 10.1016/j.apenergy.2017.01.005.
- [67] E. Parzen, “On the Estimation of Probability Density Functions and Mode,” *Ann. Math. Stat.*, vol. 33, pp. 1065–1076, 1962.
- [68] E. Karan, S. Asadi, and L. Ntaimo, “A stochastic optimization approach to reduce greenhouse gas emissions from buildings and transportation,” *Energy*, vol. 106, pp. 367–377, 2016, doi: 10.1016/j.energy.2016.03.076.
- [69] D. Thomas, O. Deblecker, and C. S. Ioakimidis, “Optimal operation of an energy management system for a grid-connected smart building considering photovoltaics’ uncertainty and stochastic electric vehicles’ driving schedule,” *Appl. Energy*, vol. 210, pp. 1188–1206, 2018, doi: 10.1016/j.apenergy.2017.07.035.
- [70] N. Liu, F. Zou, L. Wang, C. Wang, Z. Chen, and Q. Chen, “Online energy management of PV-assisted charging station under time-of-use pricing,” *Electr. Power Syst. Res.*, vol. 137, pp. 76–85, 2016, doi: 10.1016/j.epsr.2016.04.002.
- [71] A. Ito, A. Kawashima, T. Suzuki, S. Inagaki, T. Yamaguchi, and Z. Zhou, “Model Predictive Charging Control of In-Vehicle Batteries for Home Energy Management Based on Vehicle State Prediction,” *IEEE Trans. Control Syst. Technol.*, vol. 26, no. 1, pp. 51–64, 2018, doi: 10.1109/TCST.2017.2664727.
- [72] S. J. Qin and T. A. Badgwell, “A survey of industrial model predictive control technology,” *Control Eng. Pract.*, vol. 11, pp. 733–764, 2003.
- [73] K. Valentine, W. G. Temple, and K. M. Zhang, “Intelligent electric vehicle charging: Rethinking the valley-fill,” *J. Power Sources*, vol. 196, no. 24, pp. 10717–10726, 2011, doi: 10.1016/j.jpowsour.2011.08.076.
- [74] M. G. Vaya and G. Andersson, “Centralized and decentralized approaches to smart charging of plug-in Vehicles,” *IEEE Power Energy Soc. Gen. Meet.*, pp. 1–8, 2012, doi: 10.1109/PESGM.2012.6344902.
- [75] J. A. P. Lopes, F. J. Soares, and P. M. R. Almeida, “Integration of electric

- vehicles in the electric power system,” *Proc. IEEE*, vol. 99, no. 1, pp. 168–183, 2011, doi: 10.1109/JPROC.2010.2066250.
- [76] D. Q. Oliveira, A. C. Zambroni De Souza, and L. F. N. Delboni, “Optimal plug-in hybrid electric vehicles recharge in distribution power systems,” *Electr. Power Syst. Res.*, vol. 98, pp. 77–85, 2013, doi: 10.1016/j.epsr.2012.12.012.
- [77] A. Di Giorgio, F. Liberati, and S. Canale, “Electric vehicles charging control in a smart grid: A model predictive control approach,” *Control Eng. Pract.*, vol. 22, no. 1, pp. 147–162, 2014, doi: 10.1016/j.conengprac.2013.10.005.
- [78] C. Jin, J. Tang, and P. Ghosh, “Optimizing electric vehicle charging: A customer’s perspective,” *IEEE Trans. Veh. Technol.*, vol. 62, no. 7, pp. 2919–2927, 2013, doi: 10.1109/TVT.2013.2251023.
- [79] L. Gan, U. Topcu, and S. H. Low, “Optimal decentralized protocol for electric vehicle charging,” *IEEE Trans. Power Syst.*, vol. 28, pp. 1–12, 2012.
- [80] A. Sheikhi, S. Bahrami, A. M. Ranjbar, and H. Oraee, “Strategic charging method for plugged in hybrid electric vehicles in smart grids; A game theoretic approach,” *Int. J. Electr. Power Energy Syst.*, vol. 53, no. 1, pp. 499–506, 2013, doi: 10.1016/j.ijepes.2013.04.025.
- [81] K. Zhang *et al.*, “Optimal decentralized valley-filling charging strategy for electric vehicles,” *Energy Convers. Manag.*, vol. 78, pp. 537–550, 2014, doi: 10.1016/j.enconman.2013.11.011.
- [82] J. Hu, H. Morais, T. Sousa, and M. Lind, “Electric vehicle fleet management in smart grids: A review of services, optimization and control aspects,” *Renew. Sustain. Energy Rev.*, vol. 56, pp. 1207–1226, 2016, doi: 10.1016/j.rser.2015.12.014.
- [83] M. Esmaili and A. Goldoust, “Multi-objective optimal charging of plug-in electric vehicles in unbalanced distribution networks,” *Int. J. Electr. Power Energy Syst.*, vol. 73, pp. 644–652, 2015, doi: 10.1016/j.ijepes.2015.06.001.
- [84] B. Škugor and J. Deur, “Dynamic programming-based optimisation of charging an electric vehicle fleet system represented by an aggregate battery model,” *Energy*, vol. 92, pp. 456–465, 2015, doi: 10.1016/j.energy.2015.03.057.
- [85] V. V. Ashok *et al.*, “Using dedicated EV charging areas to resolve grid violations caused by renewable energy generation,” *2016 IEEE Transp. Electrification Conf. Expo, ITEC 2016*, 2016, doi: 10.1109/ITEC.2016.7520231.
- [86] R. Wang, G. Xiao, and P. Wang, “Hybrid Centralized-Decentralized (HCD) Charging Control of Electric Vehicles,” *IEEE Trans. Veh. Technol.*, vol. 66, no. 8, pp. 6728–6741, 2017, doi: 10.1109/TVT.2017.2668443.
- [87] C. Deng, N. Liang, J. Tan, and G. Wang, “Multi-objective scheduling of electric vehicles in smart distribution network,” *Sustain.*, vol. 8, no. 12, 2016, doi: 10.3390/su8121234.
- [88] Federal Highway Administration, “2009 National Household Travel Survey,” p. 82, 2010, [Online]. Available: <http://nhts.ornl.gov/download.shtml%5Cnhttp://scholar.google.com/scholar?hl=en&btnG=Search&q=intitle:2009+National+Household+Travel+Survey#9>.
- [89] C. Diaz, A. Mazza, F. Ruiz, D. Patino, and G. Chicco, “Understanding Model Predictive Control for Electric Vehicle Charging Dispatch,” *Proc.* -

- 2018 53rd Int. Univ. Power Eng. Conf. UPEC 2018, pp. 1–6, 2018, doi: 10.1109/UPEC.2018.8542050.
- [90] C. Diaz, F. Ruiz, and D. Patino, “Smart Charge of an Electric Vehicles Station: A Model Predictive Control Approach,” *2018 IEEE Conf. Control Technol. Appl. CCTA 2018*, pp. 54–59, 2018, doi: 10.1109/CCTA.2018.8511498.
- [91] I. Sengor, O. Erdinc, B. Yener, A. Tascikaraoglu, and J. P. S. Catalao, “Optimal energy management of EV parking lots under peak load reduction based DR programs considering uncertainty,” *IEEE Trans. Sustain. Energy*, vol. 10, no. 3, pp. 1034–1043, 2019, doi: 10.1109/TSTE.2018.2859186.
- [92] Y. Guo, J. Xiong, S. Xu, and W. Su, “Two-Stage Economic Operation of Microgrid-Like Electric Vehicle Parking Deck,” *IEEE Trans. Smart Grid*, vol. 7, no. 3, pp. 1703–1712, 2016, doi: 10.1109/TSG.2015.2424912.
- [93] H. Zhang, Z. Hu, Z. Xu, and Y. Song, “Evaluation of Achievable Vehicle-to-Grid Capacity Using Aggregate PEV Model,” *IEEE Trans. Power Syst.*, vol. 32, no. 1, pp. 784–794, 2017, doi: 10.1109/TPWRS.2016.2561296.
- [94] F. Giordano; A. Ciocia; P.D. Leo; A.Mazza; F. Spertino; A. Tenconi; S. Vaschetto, “Vehicle-to-Home Usage Scenarios for Self-Consumption Improvement of a Residential Prosumer With Photovoltaic Roof,” *IEEE Trans. Ind. Appl.*, vol. 56, no. 3, pp. 2945–2956, 2020, doi: 10.1109/TIA.2020.2978047.
- [95] F. Giordano, F. Arrigo, C. Diaz-Londono, F. Spertino, and F. Ruiz, “Forecast-based V2G aggregation model for day-ahead and real-time operations,” *2020 IEEE Power Energy Soc. Innov. Smart Grid Technol. Conf. ISGT 2020*, 2020, doi: 10.1109/ISGT45199.2020.9087659.
- [96] “My Electric Avenue Data,” 2015, Accessed: Dec. 06, 2018. [Online]. Available: <http://myelectricavenue.info/>.
- [97] L. Kaufman and P. J. Rousseeuw, “Clustering by means of medoids,” *Statistical Data Analysis Based on the L 1-Norm and Related Methods*. pp. 405–416, 1987, doi: 10.1016/j.homp.2013.07.004.
- [98] X. L. Qian Lii, “A K-medoids Clustering Algorithm with Initial Centers Optimized by a P System,” *Lect. Notes Comput. Sci. (including Subser. Lect. Notes Artif. Intell. Lect. Notes Bioinformatics)*, vol. 8944, pp. 488–500, 2015, doi: 10.1007/978-3-319-15554-8.
- [99] IEA PVPS task 1 *et al.*, *Trends in Photovoltaic Applications 2020*. 2020.
- [100] P. J. Rousseeuw, “Silhouettes: a Graphical aid to the interpretation and validation of cluster analysis,” *Simulation*, vol. 20, pp. 53–65, 1987, doi: 10.1177/003754977702900403.
- [101] M. Ghofrani, A. Arabali, and M. Ghayekhloo, “Optimal charging/discharging of grid-enabled electric vehicles for predictability enhancement of PV generation,” *Electr. Power Syst. Res.*, vol. 117, pp. 134–142, 2014, doi: 10.1016/j.epsr.2014.08.007.
- [102] ABB, “ABB eCharger.” <http://www.abb.com/.../ac-charging-station-echarger-en-aug2012.pdf> (accessed Jan. 25, 2019).
- [103] Growatt New Energy Technology, “EVA 11-D.” <http://www.ginverter.com/.../Growatt-EVA-11D.pdf> (accessed Jan. 25, 2019).
- [104] Peterson Scott B., JayApt, and J.F.Whitacre, “Lithium-ion battery cell degradation resulting from realistic vehicle and vehicle-to-grid utilization,” *J. Power Sources*, [Online]. Available: <https://www.sciencedirect.com/science/article/abs/pii/S0378775309017443>

- [105] Ingeteam, “INGEREV City Duo.” http://www.ingeteam.it/en/energy_division/electric_mobility (accessed Jan. 25, 2019).
- [106] R. Walawalkar, J. Apt, and R. Mancini, “Economics of electric energy storage for energy arbitrage and regulation in New York,” *Energy Policy*, vol. 35, no. 4, pp. 2558–2568, 2007, doi: 10.1016/j.enpol.2006.09.005.